WILLIAM CHONG WOEI FONG

DYNAMIC SIMULATION OF PLASTIC COMPONENTS

SCHOOL OF ENGINEERING

MSc in AUTOMOTIVE PRODUCT ENGINEERING

SCHOOL OF ENGINEERING

MSc in AUTOMOTIVE PRODUCT ENGINEERING

Academic Year 2007-2008

WILLIAM CHONG WOEI FONG

DYNAMIC SIMULATION OF PLASTIC COMPONENTS

Supervisor:

MR JASON BROWN

September 2008

This thesis is submitted in partial [45%] fulfilment of the requirements for the degree of MSc in AUTOMOTIVE PRODUCT ENGINEERING

Abstract

The aim of the study was to simulate the dynamic properties of automotive plastic materials for an FE analysis based on the Empirical Method. The study researched into the effects of strain rate and temperature on the stress-strain behavior of the material. The studied plastic material was DYLARK 480P16 produced by NOVA Chemicals.

The stress-strain behavior of plastic materials used in the automotive industry was reviewed. The study included a review of the Eyring equation used to correlate the strain rate and temperature effects of the plastic materials. Lastly, the impact properties of plastic materials were briefly discussed in the study.

Material models commonly used in the industry to represent plastic materials in LS-DYNA were reviewed. The overviews on *Material 24* and *Material 187* were presented in this study. The theory and parameters related to the development of these material models were briefly discussed.

An overview on the physical tests for the study was included. The physical tests included UNIAXIAL Tensile and Drop Weight Impact tests. Drop Weight Impact test results were provided by Jaguar Cars Limited (JCL) for DYLARK 480P16. The Drop Weight Impact tests were conducted for test temperatures at ambient temperature 85^{o}C and -40^{o}C,.

Finite element (FE) models simulating UNIAXIAL Tensile and Drop Weight Impact tests were produced in LS-DYNA. *Material 24* was used to simulate DYLARK 480P16. The stress-strain related parameters for the material model were provided by JCL. The parameter of interest for the material model was the effect of Failure Plastic Strain (FPS) value.

For Drop Weight Impact tests at temperatures -40^{o}C and 85^{o}C, the stress-strain parameters used for the ambient temperature simulation were scaled based on the Eyring equation and an additional correction factor. All simulation results for the Drop Weight Impact tests showed correlation to physical test results provided by JCL.

Keywords:

LS-DYNA, Plastic Material, Strain Rate, Temperature, Material Modelling and Eyring Equation

Acknowledgements

First of all, I would like to acknowledge and extend my heartfelt gratitude to Mr. Jason Brown for his initiative and effort in supervising the research study. The research study is made possible with the support of his vast experience and knowledge on the subject of interest.

I would also like to thank the industrial supervisors for the research study, Mr. Charlie Loh and Dr Bill Feng from Jaguar Cars Limited (JCL). The research study was successfully completed with their technical support and knowledge on the subject of interest. I would also like to show my gratitude to them for spending their precious time in providing essential technical support whenever needed.

Next, I am grateful to be able to gather useful and helpful advice for the research study from Dr James Campbell. I am also very glad to be able to get the assistance of Dr Kevin Hughes in terms of explicit Finite Element (FE) modelling using LS-DYNA whenever required. I would like to acknowledge the support from Mr. Barry Walker in making the experimental process possible.

Last but not least, I would like to thank my family and especially Chin Yin for their support and encouragement when times are difficult for me.

To my beloved family, Chin Yin and friends for their encouragement and support through out the MSc course

Contents

List of Figures

List of Tables

Nomenclature

Latin Symbols

A_o	Cross section area of specimen before any deformation
c	Speed of sound
C	Material constants for Cowper-Symonds equation
d	Damage parameter for *Material 187*
E	Modulus of Elasticity
E_d	Damaged Modulus of Elasticity for *Material 187*
ETAN	Tangent Modulus
FE	Finite element
FPS	Failure Plastic Strain for *Material 24*
G	Shear Modulus
GRP	Glass reinforced plastic
IS	Impact Strength
JCL	Jaguar Cars Limited
l	Gauge length of specimen after deformation
l_o	Gauge length of specimen before any deformation
L_s	Characteristic length of shell elements for LS-DYNA
p	Material constants for Cowper-Symonds equation
P	Load
PC	Polycarbonate
PMMA	Polymethyl-methacrylate
PP	Polypropylene
PS	Polystyrene
PVC	Polyvinylchloride
SAMP1	Semi analytical model for polymers (*Material 187*)
SC	Scaling Coefficient
SLSFAC	Sliding Interface Penalty Factor
SMA	Styrene-Maleic-Anhydride
T	Temperature
T_g	Glass transition temperature
UNIS	Unnotched Impact Strength
v	Activation volume for Eyring equation

Greek Symbols

α-process	1st activation process for Eyring equation
β-process	2nd activation process for Eyring equation
δ	Elongation
ΔH	Activation energy for Eyring equation
Δt	Time step for explicit direct integration method
Δt_{cr}	Critical time step for explicit direct integration method
ε	Strain
$\varepsilon_{elastic}$	Elastic strain
ε_{eng}	Engineering strain
ε_{p}	Plastic strain
ε_{total}	Total strain
ε_{true}	True strain
ε_{y}	Yield strain
$\dot{\varepsilon}$	Strain rate
$\dot{\varepsilon}_{o}$	Material constant for Eyring equation
$\dot{\varepsilon}_{p}$	Plastic strain rate
ν	Poisson's ratio
ρ	Density
σ_c	Compression stress
σ_d	Damaged stress
σ_{eng}	Engineering stress
σ_f	Fracture stress
σ_{pl}	Plastic stress
σ_s	Shear stress
σ_t	Tensile stress
σ_{true}	True stress
σ_u	Ultimate stress
σ_y	Yield stress

1.0. Introduction

1.1. Research Background

The ever-changing and demanding requirements for the safety of vehicle occupants and pedestrians have placed the automotive industry on the verge of a revolution. The plastic industry is poised to play a major role in this revolution.

Plastic materials or commonly known as polymers in engineering term constitute about 20% of a modern vehicle's total weight [1]. These materials are widely used in the automotive industry as a weight reduction measure where a reduced weight of a vehicle helps in optimizing the fuel economy of that particular vehicle design. Thus, contributes to reduced fuel consumption for a vehicle [2].

However, when safety issues are brought forth regarding the crashworthiness of automotive plastics, car manufacturers can only rely on costly dynamic component testing to obtain the real time dynamic response of their design. This is mainly due to the fact that physical lab test characteristics of automotive plastics show little relevance to their dynamic behavior. Hence, this causes the prediction of the material's collision behavior difficult.

Another reason for the difficulty in predicting the dynamic properties of plastic materials during the design stage is the lack of reliable dynamic material models. The commonly used material models for plastic materials are originally generated for metallic material. The material laws for metals do not comply accurately with the dynamic characteristics of plastics. Using these material models without any suitable modifications will only add to the inaccuracy of the material's dynamic properties prediction.

1.2. Aim

The importance of having access to reliable dynamic properties of automotive plastics was highlighted above. Therefore, the aim of the study is to simulate the dynamic properties of a plastic material for an FE analysis. The plastic material used for the study was DYLARK 480P16 produced by NOVA Chemicals. The study was jointly supervised by Cranfield University and JCL.

1.3. Objectives

Based on the definition of the aim, the objectives for the study are:

i. To simulate the dynamic behavior of DYLARK 480P16 for an FE analysis through Empirical Method.
ii. The Empirical Method is carried out using a combination of physical testing, dynamic testing and Finite Element (FE) analysis.
iii. To obtain the coefficients of the Eyring equation for DYLARK 480P16 through UNIAXIAL Tensile tests at various strain rates and temperatures.
iv. To obtain a correlation between the strain rate and temperature effects on the stress-strain behavior of DYLARK 480P16 through the Eyring equation
v. To simulate and validate a Drop Weight Impact test on DYLARK 480P16 for various test temperatures using *Material 24*.

1.4. Research Outline

i. Reviews on stress-strain behavior of plastic materials
ii. Reviews on material models (*Material 24* and *Material 187)* in LS-DYNA
iii. Conduct UNIAXIAL Tensile test on DYLARK 480P16 at various strain rates and temperatures to compute the coefficients for the Eyring equation
iv. Relate the stress-strain behavior of DYLARK 480P16 for various test temperatures based on the Eyring equation
v. Produce an FE model simulating the Drop Weight Impact test on DYLARK 480P16 using the selected material models in LS-DYNA
vi. Validation of the FE model based on the results of the Drop Weight Impact tests for ambient temperature, 85^{o}C and -40^{o}C.

1.5. Research Deliverables

The main deliverables for the study are:

i. Correlation of strain rate and temperature effect on the stress-strain behavior of DYLARK 480P16 based on the Eyring equation
ii. Stress-strain and dynamic behavior of DYLARK 480P16 through experimental test
iii. Validation of FE model through experimental test results for a Drop Weight Impact test on DYLARK 480P16 using LS-DYNA

1.6. Summary

The chapter covered the research background, the aim and objectives for the study. Based on the aim and objectives, the research outline was briefly discussed. Lastly, the research deliverables were also defined. The review on the stress-strain behavior of the plastic materials will be discussed in the next chapter.

2.0. Review of Automotive Plastics

Automotive plastics can be identified in various manners such as [2]

i. Thermoplastics and Thermosets
ii. Chemical structures
iii. Crystalline and amorphous thermoplastics

The most common categorization for automotive plastics is of thermoplastics and thermosets. Due to the ability of being recycled, thermoplastics are the more widely used plastic material in the automotive industry.

DYLARK 480P16 contains Styrene-Maleic-Anhydride (SMA) as the matrix material. SMA is a type of thermoplastic. The material is reinforced by 16% of glass fiber. The material is commonly used for automotive instrument panels and interior trims.

However, before being able to obtain the dynamic properties of DYLARK 480P16, the stress-strain behavior of common plastic materials should first be reviewed. This will help in identifying critical and sensitive parameters which affect the dynamic properties of plastic materials.

2.1. Stress-Strain Behavior

The stress-strain behavior of plastic materials can be obtained through physical tests such as tensile testing, compression testing and also shear testing. Figure 2.1 illustrates a typical stress-strain curve showing various regions under the curve.

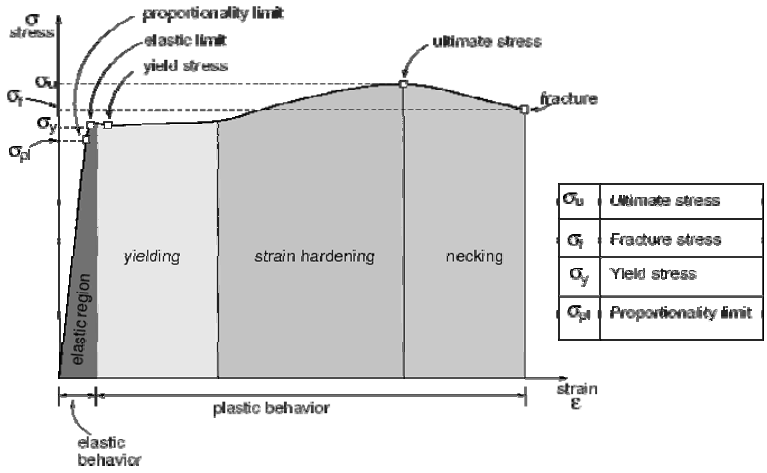

Figure 2.1 Typical Stress - Strain Curve

Physical tests usually provide data regarding the load (P) and the corresponding elongation (δ) of the test piece. To convert the data obtained to stress (σ) and strain (ε), a few considerations have to be taken into account. The stress-strain behavior of a material required must be identified to be either the engineering values or the true values.

The expressions of engineering stress and strain are shown below:

$$\sigma_{eng} = \frac{P}{A_o} \quad ; \quad \varepsilon_{eng} = \frac{\delta}{l_o}$$

Where

A_o = Cross section area of specimen before any deformation

l_o = Gauge length of specimen before any deformation

σ_{eng} = Engineering stress

ε_{eng} = Engineering strain

The engineering stress (σ_{eng}) and engineering strain (ε_{eng}) can be obtained easily as the expressions for the stress and strain involve data which are readily available.

However, in reality, the cross section area of the test piece decreases as load (P) increases. Therefore, the engineering stress computed using the expression above does not represent the actual stress of the specimen. The actual stress is known as the true stress (σ_{true}). The main difference between the two stresses is the behavior during the necking phase of the stress-strain curve [3].

To be able to obtain true stress and the corresponding true strain, a conversion can be made based on the tabulated engineering values of the stress and strain. As stated in ASTM D638M, the conversion expressions are [4]:

$$\sigma_{true} = \sigma_{eng} \cdot (\varepsilon_{eng} + 1) \quad ; \quad \varepsilon_{true} = \ln (\varepsilon_{eng} + 1)$$

Where

σ_{true} = True stress

ε_{true} = True strain

The strain can be divided into elastic strain and plastic strain based on the stress-strain curve. Elastic strain refers to the strain at the elastic range where strain is recoverable. The plastic strain increases as the material is actively yielding whenever the state of stress is on the yield surface. The relationship between the total strain with the elastic and plastic strain is as below [5].

$$\varepsilon_{total} = \varepsilon_{elastic} + \varepsilon_{p}$$

Where

ε_{total} = Total strain
$\varepsilon_{elastic}$ = Elastic strain
ε_{p} = Plastic strain

The expression shown above is valid for both the engineering and true parameters for the stress and strain.

The parameters which affect the stress-strain behavior of a plastic material are:

i. Tensile and Compression
ii. Strain rate effect
iii. Temperature effect
iv. Yield Behavior

2.2. Tensile and Compression of Plastic Materials

Through physical tests, it can be observed that the modulus of elasticity and yield point of plastics are not a constant value under tensile and compression test [6-8]. The modulus of elasticity and yield point obtained from a compression test tend to be higher than the ones obtained through a tensile test.

The stress-strain behavior of Polystyrene (PS) under tension and compression can be observed in Figure 2.2. It can be seen that in tension, PS fails in a brittle manner. When the material is in compression, it shows failure in a ductile manner with a yield point and plastic deformation to fracture [7].

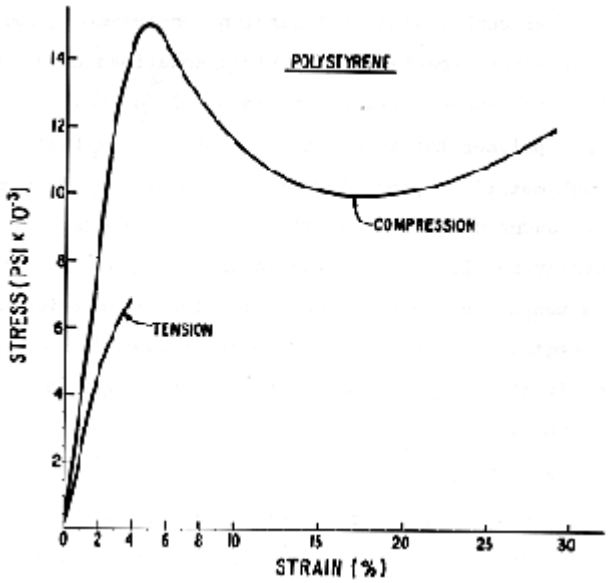

Figure 2.2 Stress-Strain Behavior of PS under tension and compression [7]

The variation of the tensile and compression behavior discussed above is very significant in brittle plastic materials. The tensile properties of brittle plastics are hugely affected by the flaws and cracks. The cracks and flaws will induce stress concentrations which will vastly weaken the material.

However, the cracks do not have a huge effect on the compression properties as the compression stress tends to close the cracks up rather than opening them. Consequently, the compression tests reflect the actual characteristic of a polymer or plastic material rather than the tensile tests [9].

2.3. Strain Rate Effect on Plastic Materials

The mechanical properties of most materials vary depending on the loading rate [10]. This effect is very significant in the context of plastic materials. The loading rate mentioned is quantified as the strain rate. As the strain rate is increased, it can be observed that the modulus of elasticity and the yield point of the plastic material increased as well [9].

The strain rate effect on plastic materials has been widely studied by researchers. Arruda, Boyce and Jayachandran [11] studied on the effects of strain rate and temperature on the deformation of glassy polymers. A compression test was done on Polymethyl-Methacrylate (PMMA) under different strain rates.

Based on their test results, they concluded that the yield point of polymers or plastics is strain rate dependent. In their research, they also found out that plastic materials are also temperature dependent. The temperature effect will be reviewed in the next section. Figure 2.3 illustrates the stress-strain plot for PMMA under strain rates ranging from 0.001/s to 0.1/s.

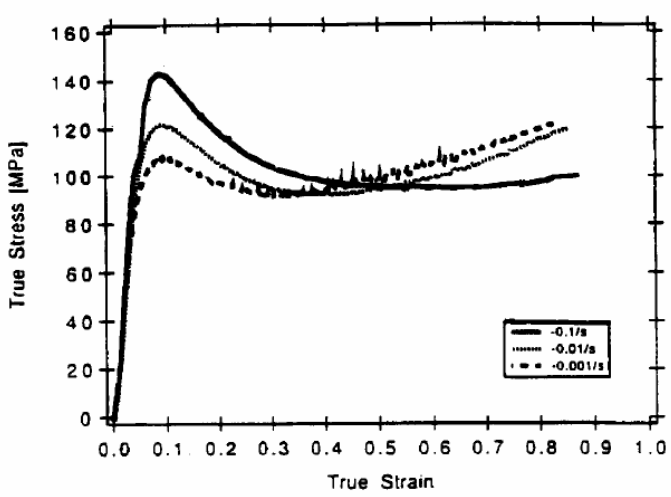

Figure 2.3 Stress-Strain curves of PMMA for various strain rates [11]

Based on the research by Baselmans [12], PS showed an increment or a shift in the yield point as the strain rate was increased. The stress-strain curve for PS under various strain rates are shown in Figure 2.4. The results obtained also reflect the dependency on strain rate of the plastic material.

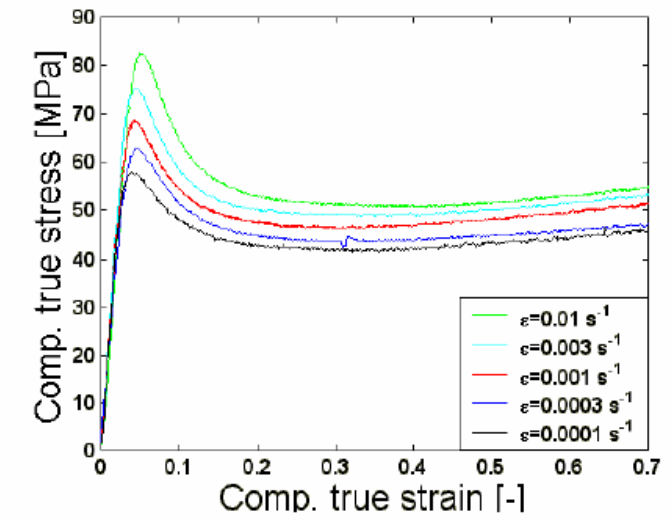

Figure 2.4 Compression True Stress- Compression True Strain Curves of PS for various strain rates [12]

However, the strain rate dependency hugely affects only rigid ductile plastic materials. The effect is less significant if the plastic material is of a brittle behavior [9].

2.4. Temperature Effect on Plastic Materials

Stress-strain properties of most materials are affected by the material temperature itself. This effect is more evident in plastic materials due to its temperature sensitive nature. According to Nielsen [9], plastic material's stress-strain behavior is influenced by its glass transition temperature, T_g. At low temperatures, plastic materials might show brittle behavior where fracture occurs without any yielding. However, at higher temperatures, the material exhibits a ductile behavior.

As published in Arruda, Boyce and Jayachandran's research paper [11], the compression test done on PMMA specimen at temperatures varying from 25°C to 75°C showed the behavior as discussed by Nielsen [9]. The yield point of PMMA decreased as the temperature of the test piece was increased. The effect of temperature on PMMA is reflected in Figure 2.5.

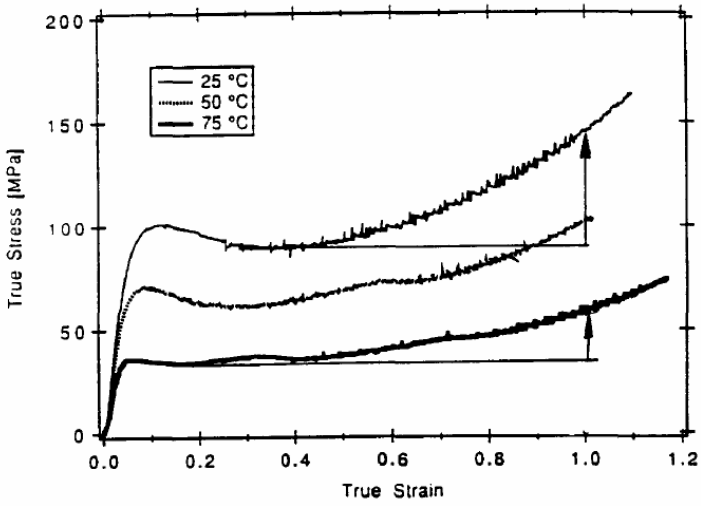

Figure 2.5 Stress-strain curves of PMMA for various test temperatures [11]

The same characteristic was also being observed by Baselmans [12]. Baselmans conducted a compression test on PS with a varied test temperature. The results from the compression test for PS are illustrated in Figure 2.6.

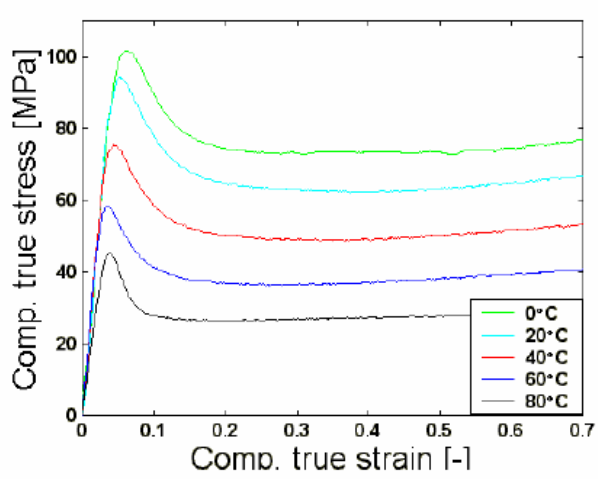

Figure 2.6 Compression True Stress- Compression True Strain Curves of PS for various specimen temperatures [12]

2.5. Yield Behavior of Plastic Materials - Eyring Equation

Eyring equation is used to describe the deformation of a polymer or plastic material at a strain rate as a thermally activated process which depends on the activation energy, ΔH and activation volume, v [10]. The activation volume, v represents the volume of the plastic material segment which has to move as a whole in order for plastic deformation to occur [13].

The equation of a single process of activation for the Eyring equation is shown below [13]:

$$\frac{\sigma_y}{T} = \frac{R}{v}\left[\frac{\Delta H}{RT} + \ln\frac{2\,\dot{\varepsilon}}{\dot{\varepsilon}_o}\right]$$

Where

R	=	Universal gas constant [8.314 J/ (K.mol)]
v	=	Activation volume
ΔH	=	Activation energy
T	=	Temperature
$\dot{\varepsilon}_o$	=	Material constant
$\dot{\varepsilon}$	=	Strain rate
σ_y	=	Yield stress

The equation is found to be able to comply with a wide range of plastic materials over a wide range of strain rates and temperatures. This equation relates the yield behavior of a plastic material to the strain rate and temperature of the material.

2.6. Eyring Equation - Relating Strain Rate and Temperature Effect

Researchers noticed that it might be useful to relate the strain rate and the temperature effect on plastic materials. Constitutive models and theories have been developed and researched to further understand the correlation between these two effects on a plastic material. The most commonly used correlation is the Eyring equation.

In the year 1965, Roetling [14] conducted a tensile test on PMMA over a fairly wide range of strain rates and temperatures. He applied the Eyring viscosity theory to obtain the yield stress behavior of PMMA. In his research, he used the Eyring equation to derive an expression relating the yield stress of PMMA to the strain rate and temperature of the material. The experimental results are shown in Figure 2.7.

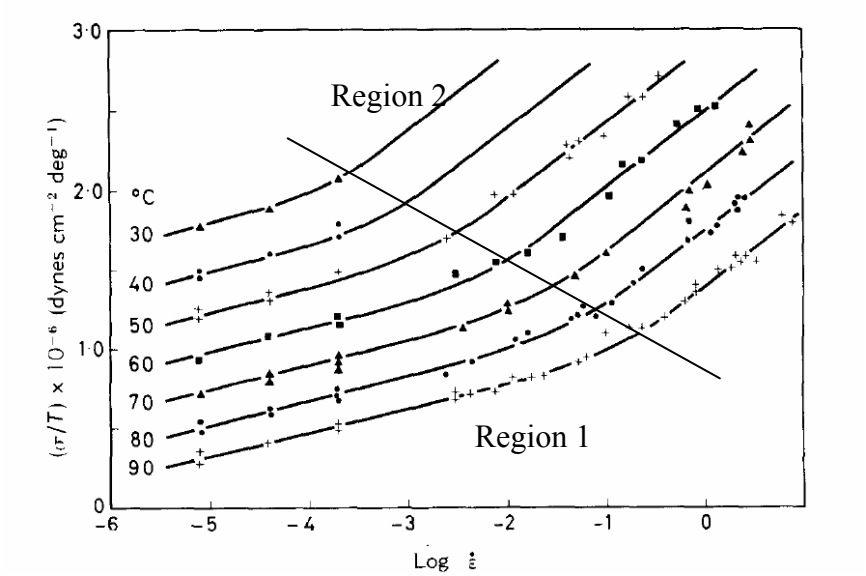

Figure 2.7 Plot of σ_y/T against log $\dot{\varepsilon}$ for PMMA [14]

As shown in Figure 2.7, Roetling described the behavior of material at low strain rates and high temperatures which is at Region 1 using the α-process. The α-process can be expressed using the single process of activation for the Eyring Equation as discussed earlier.

However for Region 2, Roetling used the β-process to express the correlation between the yield stress to the strain rate and temperature. The β-process can be put into an expression where a second process of activation of the Eyring Equation is included. It can also be observed that the slope of the plot at Region 2 is larger than the one of Region 1 which reflects the higher strain rate dependency at Region 2.

In a separate research, Bauwens-Crowet, Bauwens and Homes [6,15] also used the Eyring equation to relate the yield stress of plastic materials to the strain rate and temperature. They conducted a study on PMMA to obtain an expression to correlate the yield stress of the material to the strain rate and temperature [15]. The results from their study agreed with the outcome obtained by Roetling as shown in Figure 2.7.

In a later research, Bauwens-Crowet, Bauwens and Homes experimented on the tensile and compression behavior of polycarbonate (PC) by taking into consideration the temperature and strain rate effect [6]. They came to the same conclusion as Roetling [14] where a second process of activation should be included into the Eyring Equation for materials at low temperatures and high strain rates.

The plot of σ_y/T against log $\dot{\varepsilon}$ for PC illustrated in Figure 2.8 obtained by [6] also showed a change in the slope of the curve at low temperature and high strain conditions. Bauwens-Crowet, Bauwens and Homes divided the plot into 2 regions similar to what Roetling did.

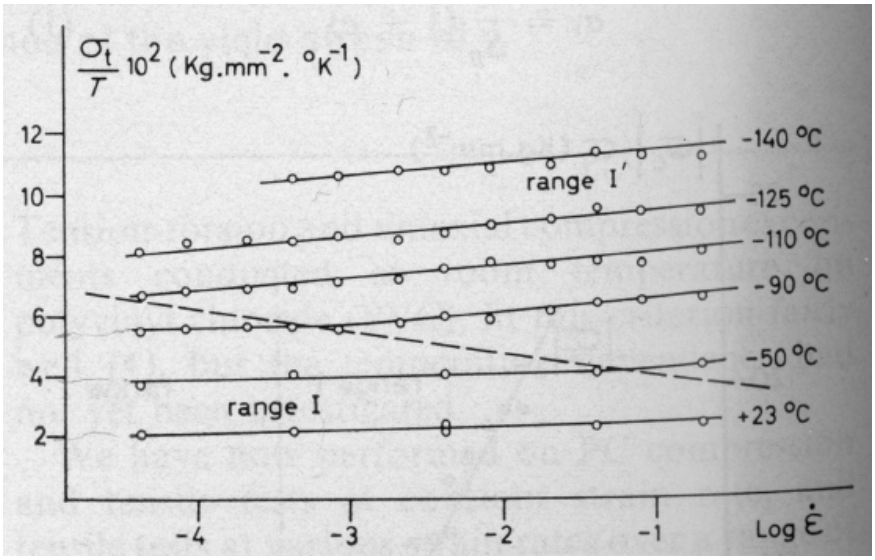

Figure 2.8 Plot of σ_y/T against log $\dot{\varepsilon}$ for PC [6]

Based on the findings discussed above, it can be seen that the yield stress of plastic materials increase more rapidly with an increasing strain rate and a decreasing temperature than at a high temperature and low strain rates. Therefore, the Eyring equation is proposed to be extended to more than one activated process.

The equivalent equation is as follows [13]:

$$\frac{\sigma_y}{T} = \underbrace{\frac{R}{v_1}\left[\frac{\Delta H_1}{RT} + \ln\frac{2\dot{\varepsilon}}{\dot{\varepsilon}_{01}}\right]}_{\alpha\text{-process}} + \underbrace{\frac{R}{v_2}\sinh^{-1}\left[\frac{\dot{\varepsilon}}{\dot{\varepsilon}_{02}}\exp\frac{\Delta H_2}{RT}\right]}_{\beta\text{-process}}$$

Where

α-process	=	1st activation process
β-process	=	2nd activation process
v_1	=	Activation volume for α-process
v_2	=	Activation volume for β-process
$\dot{\varepsilon}_{01}$	=	Material constant for α-process
$\dot{\varepsilon}_{02}$	=	Material constant for β-process
ΔH_1	=	Activation energy for α-process
ΔH_2	=	Activation energy for β-process

The first activation process predominates when the material is subjected to high temperatures and low strain rates. The second activation process becomes important when the material is at low temperature and high strain rate conditions. The 2-stage Eyring equation was used by Bauwens-Crowet, Bauwens and Homes [15] to curve fit the plot of ratio of yield stress to temperature against the logarithmic of the strain rate for Polyvinylchloride (PVC). The equation provided a good curve fit as shown in Figure 2.9.

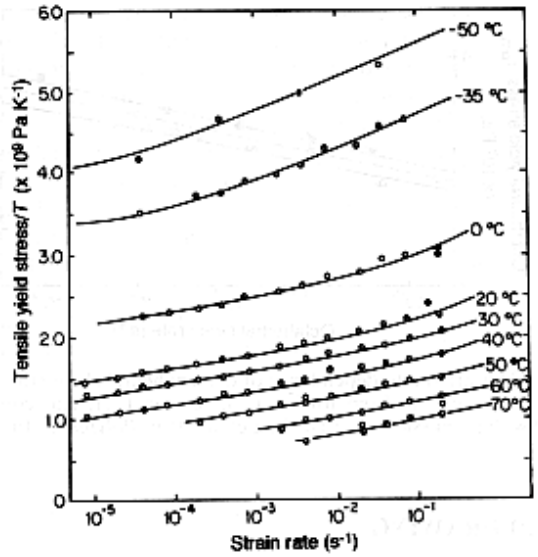

Figure 2.9 Parallel curves calculated using the 2-stage Eyring equation for the plot of σ_y/T against log $\dot{\varepsilon}$ for PVC [15]

The Eyring equation was also used to curve fit the stress-strain curve of PS as done by Baselmans [12]. Baselmans integrated the Eyring equation into an existing polymer model, which is the compression Leonov model to curve fit the stress-strain curve of a PS. The curve-fitting of the stress-strain curve of PS is shown in Figure 2.10.

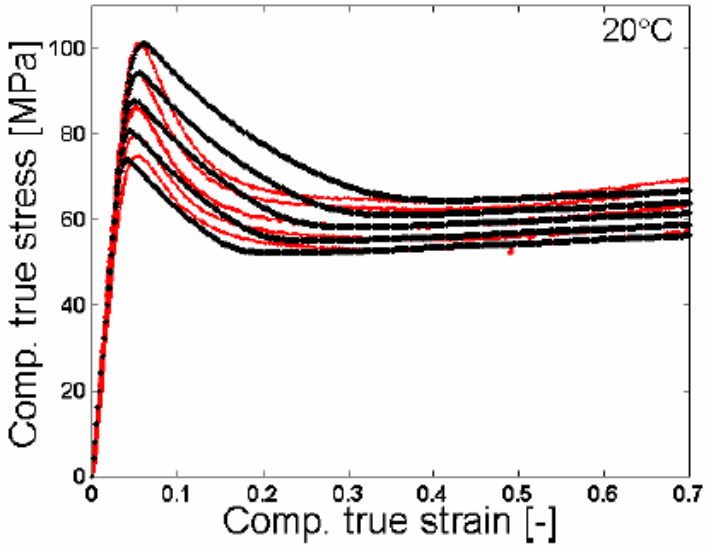

Figure 2.10 Comparing the fitted stress strain curves (black) of PS with the measured data (red) at various strain rates [12]

Baselmans obtained a reasonable curve-fit for the yield point and the strain hardening region of the stress-strain curve. However, the numerical calculation did not curve-fit the strain softening of the stress-strain curve accurately. He suggested in his study that a better and accurate curve-fit can be obtained if the compression Leonov model is to be modeled in further detail.

In a recent development of material models for unreinforced thermoplastics by Michael Junginger[16], the Eyring equation was used to model the yield surface for the material model. The material model is based on the assumption of linear elastic behavior and a non-associated flow rule. A similar approach was then used by Haufe, Kolling, Feucht and Du Bois [8] in the development of *Material 187* in LS-DYNA using the Drucker-Prager model.

2.7. Impact Properties of Plastic Materials

Impact properties of plastic material are interrelated to the toughness of the material itself [17]. As defined by Shah [17], the impact resistance of a material is the ability of the material to resist breaking under a shock loading. Ward and Hadley [13] defined impact resistance of a material as the ability of the material to maintain its integrity and to absorb a sudden impact.

For plastic materials, there are 4 common types of failures due to impact load. They are [17]:

i. Brittle Failure
ii. Slight Cracking
iii. Yielding
iv. Ductile Failure

The impact properties of plastic materials are closely related to [9]:

i. Rate of loading
ii. Notch sensitivity
iii. Temperature
iv. Orientation
v. Degree of crystallinity

For this study, the focus will be on the effect of rate of loading and temperature towards the impact properties of plastic materials. The rate of loading can be related to the strain rate. The rate of loading will affect the impact behavior of plastic materials. For instance, at high rates of loading, plastic materials tend to fail in a brittle manner. But at low loading rates, plastic materials might exhibit a ductile behavior.

According to Shah [17], each and every plastic material has a critical impact velocity where the materials will behave as brittle materials. The effect of loading rate is reflected by the study conducted by Lopez-Puente, Zaera and Navarro [18]. The effects of loading rate are illustrated in Figure 2.11.

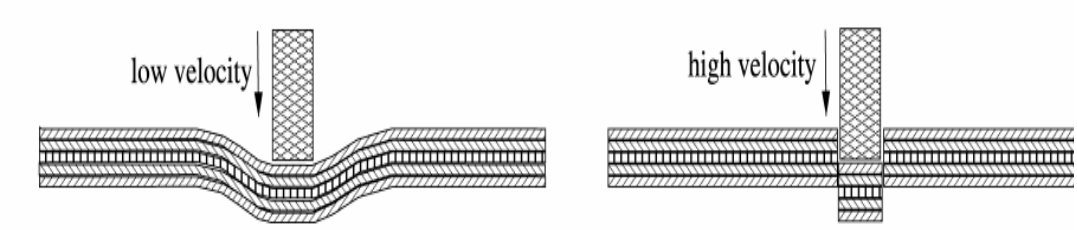

Figure 2.11 Effect of loading rate on the impact properties of plastics [18]

For the temperature effect, impact strength of the plastic materials will increase as the temperature increases [9]. The increment of impact strength is very significant when the temperature is near the glass transition temperature of the plastic material itself. The temperature effect on polypropylene (PP) is illustrated in Figure 2.12.

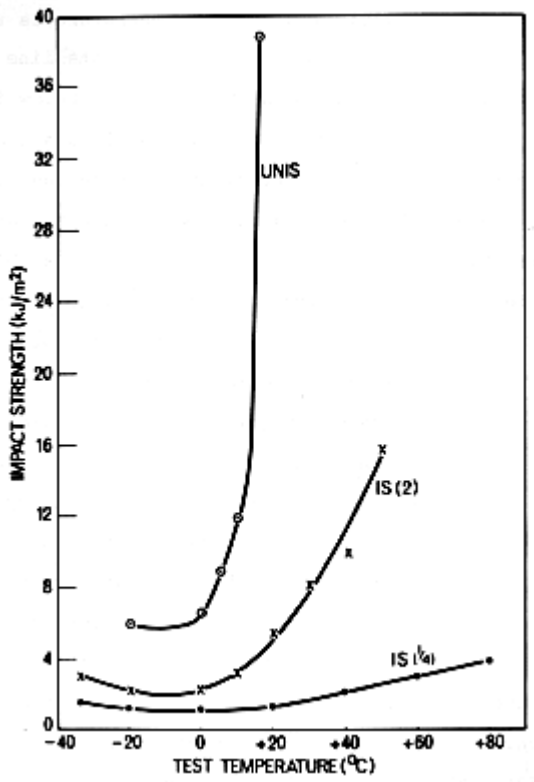

Figure 2.12 Effect of Temperature on the impact strength of PP [9]

There are 3 curves in the plot shown in Figure 2.12. The plot reflects the effect of temperature towards the impact strength of a polymer. Besides this, the notch effect on the impact properties of PP is also being highlighted in Figure 2.12. UNIS is referring to unnotched impact strength while IS (2) and IS (1/4) referred to notch impact strengths for notch diameters of 2 mm and 0.25 mm respectively.

2.8. Summary

As a summary, this chapter covered the stress-strain behavior of plastic materials. Reviews were also done on the factors affecting the stress-strain behavior of these materials. The factors discussed were strain rate and temperature effect. The Eyring equation used to relate the strain rate and temperature effect was also discussed. For the next chapter, a review will be covered on the existing material models used to represent plastic materials in LS-DYNA.

3.0. Review of Material Models in LS-DYNA

There are a total of 220 types of material models readily available in the LS-DYNA package [19]. Most of the material models are developed based on material laws derived from stress-strain curves obtained from physical testing. The main categories of the material laws used in the LS-DYNA package include [20]:

i. Hyperelasticity
ii. Viscosity
iii. Plasticity
iv. Elastomers
v. Foams
vi. Thermoplastics

For this study, the focus will be on *Material 24* (Piecewise Linear Plasticity) which is based on the plasticity material law. Another material model of interest will be *Material 187* (Semi Analytical Model for Polymers) which is developed based on the thermoplastic material laws.

3.1. Material 24 – Piecewise Linear Plasticity

Elastic-plastic material laws are originally developed for metallic materials. *Material 24* is one of the material models developed based on the plasticity laws in LS-DYNA. This material model is commonly used for crash and impact related simulations [16].

This material model is an elasto-plastic material with an arbitrary stress versus strain curve. The arbitrary strain rate dependency can also be defined for this material model [19].

The material model assumes that the elastic deformation as linear. Strain rate effect is also included in the model based on the yield stress shift. Stress-strain curves for various strain rates are used to model the plastic material behavior [19].

The stress-strain behavior can be expressed as a bilinear stress-strain curve by defining the tangent modulus, ETAN. As an alternative, an effective stress against effective plastic strain can be defined. The effective stress and effective plastic strain can be defined using 2 methods, which is by

i. Defining 8 points of effective stress and effective plastic strain values
ii. Defining an effective stress-effective plastic strain curve

For UNIAXIAL stress considerations, the effective stress against effective plastic strain is equivalent to the true stress against the true plastic strain curve obtained through physical tests [21].

The strain rate effects included in the material model can be defined using 3 different methods. The methods are:

i. Cowper-Symonds Equation

Cowper-Symonds equation represents a perfectly rigid plastic material by taking into consideration the Dynamic yield that depends on strain rate, $\dot{\varepsilon}$ [22]. The expression used to represent the Cowper-Symonds equation is as follows [21]:

$$\frac{\sigma_d}{\sigma_y} = 1 + \left[\frac{\dot{\varepsilon}}{C}\right]^{\frac{1}{p}}$$

Where

p	=	Material constants
C	=	Material constants
σ_y	=	Yield stress
σ_d	=	Dynamic yield stress

The ratio of the dynamic yield stress and the yield stress represents the scaling factor for the yield stress.

However, the Cowper-Symonds equation is originally developed for metallic materials. Using the expression in scaling the yield stress for polymer or plastic materials must be done with care to avoid inaccuracy to the simulation results. This is one of the problems faced by [23] when using this method in defining yield stress scaling factor for plastic materials.

ii. Load Curve defining the yield stress scaling factor
iii. Stress-strain curve for various strain rates

As it can be seen, most of the parameters required by *Material 24* can be defined using the stress-strain curve obtained through a physical test on the desired material. The common physical test used to obtain the parameters required is the UNIAXIAL Tensile test which will be discussed later in the study.

3.2. Material 187 – Semi Analytical Model for Polymers (SAMP1)

Material 187 or also known as SAMP1 applies an isotropic smooth yield surface for the description of non-reinforced plastics [19]. According to Kolling, Haufe, Feucht and Du Bois [8], all effects related to plastics can be considered using simple material models consisting of:

i. Necking effect through the elastic-plastic law
ii. Unloading behavior through a damage model
iii. Pressure dependent behavior through Drucker-Prager model

To be able to define the yield surface formulation in LS-DYNA, it is recommended that physical tests of tension, compression and shear should be conducted [8]. This is because the yield surface formulation takes into consideration that plastics have a varied modulus of elasticity and yield point in tension, compression and shear based on the Drucker-Prager model. Figure 3.1 illustrates the recommended physical tests for the definition of yield surface formulations in SAMP1 with subscript *t*, *c* and *s* representing tensile, compression and shear.

.

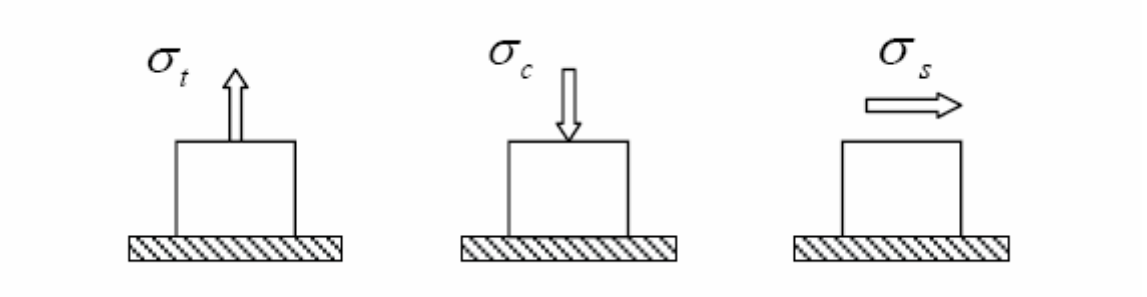

Figure 3.1 Recommended Physical Tests for SAMP 1 [8]

The hardening formulation of SAMP1 can be defined using the stress against plastic strain curves obtained from the physical tests mentioned above. Another curve of interest is the plastic Poisson's ratio curve which can be obtained from a tensile test. The formulation does not require any coefficient inputs. The curves required to determine the hardening formulations are shown in Figure 3.2 and Figure 3.3.

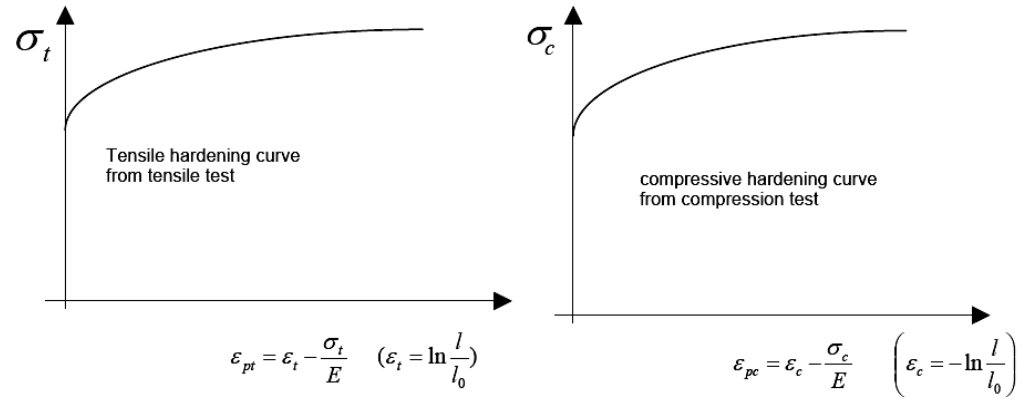

Figure 3.2 Hardening curve in tension and compression for SAMP1 [8]

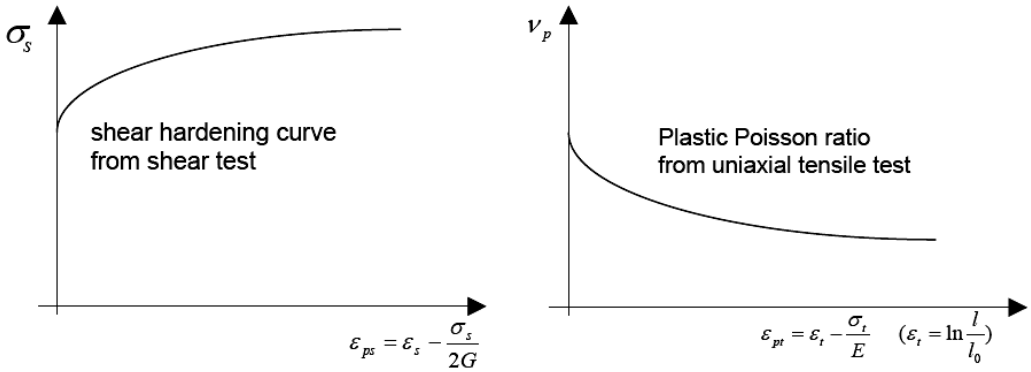

Figure 3.3 Hardening curve in shear and plastic Poisson's ratio for SAMP1 [8]

Another critical parameter when dealing with plastic material modelling is the strain rate effects on the material. In SAMP1, the strain rate effects can be determined using data from dynamic tests [8]. For strain rate consideration, SAMP1 assumes that the rate effect in compression and shear to be similar to the tensile condition. Figure 3.4 illustrates the tensile hardening curve from Dynamic tensile tests required for SAMP1.

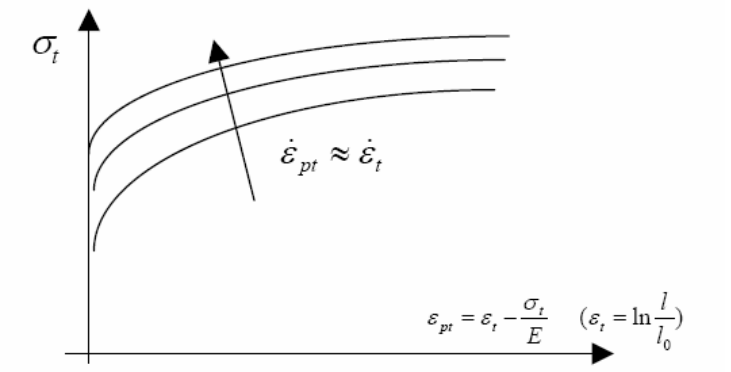

Figure 3.4 Tensile hardening curve from Dynamic tensile tests for SAMP1 [8]

To consider the damage model used to model the unloading behavior, SAMP1 uses an elastic damage concept. The concept is defined using the damage parameter as a function of plastic strain. This parameter reduces the modulus of elasticity to reflect the unloading behavior of the material. The damage parameter is defined as [8]:

$$d = 1 - \frac{E_d}{E}$$

Where

d	=	Damage parameter
E_d	=	Damaged modulus of elasticity
E	=	Modulus of elasticity

The damage curve derivation for SAMP1 input is shown in Figure 3.5. The damage parameter is expressed in the function of plastic strain.

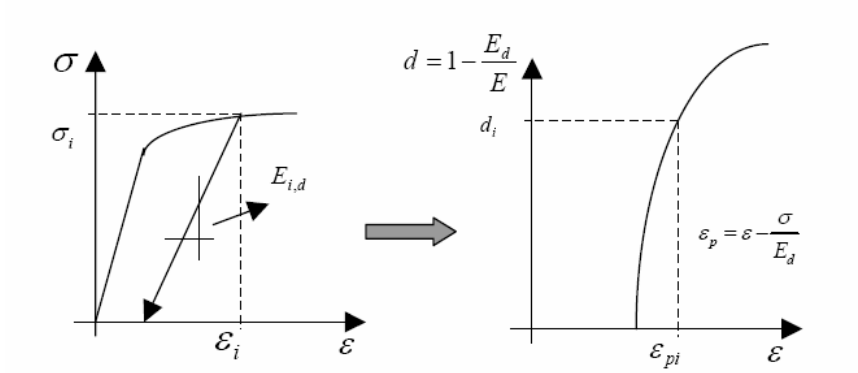

Figure 3.5 Determination of damage as a function of plastic strain [8]

By using the damage parameter obtained, the stress-strain curve for a particular strain rate is then converted into the effective hardening curve as illustrated in Figure 3.7.

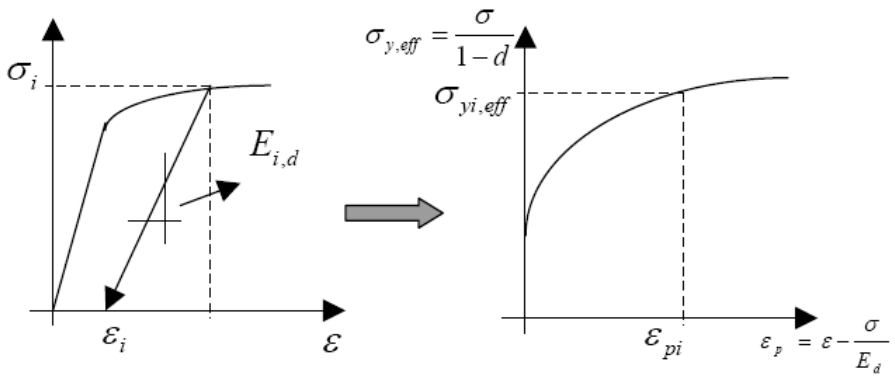

Figure 3.6 True stress to effective hardening curve conversion [8]

However, this material model was not used for the simulations covered for the study. This was mainly due to the difficulty in obtaining reliable and accurate data required for most of the parameters of SAMP1.

3.3. Summary

As a summary, the chapter reviewed on the existing material models in LS-DYNA. The focus of the review was on *Material 24* and *Material 187* or SAMP1. The review covered the basis of the material modelling used for both the material models. The next chapter will be covering the experimental method for the UNIAXIAL Tensile test.

4.0. Experimental Method - UNIAXIAL Tensile Test

The objectives of running the UNIAXIAL Tensile test are:

i. To observe the behavior of the plastic material under various strain rates and test temperatures
ii. To obtain the stress-strain curve for the material tested
iii. To validate the Eyring's equation and compute the equation's coefficients
iv. To obtain the parameters required for *Material 24* in LS-DYNA

However, due to the difficulty in obtaining the DYLARK 480P16 material, the study had to resort to the use of another plastic material, LEXAN EXL1414H. The replacement material is of a PC blend. The test pieces required were prepared and provided by JCL. Figure 4.1 shows the dumb-bell shaped test piece and its dimensions with a thickness of 4mm.

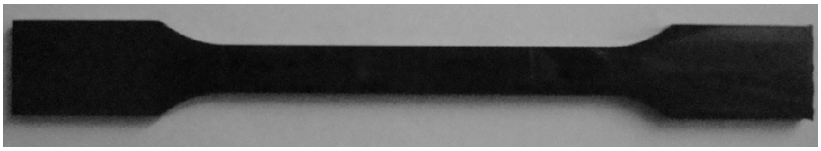

a. Dumb-bell shaped Test Piece

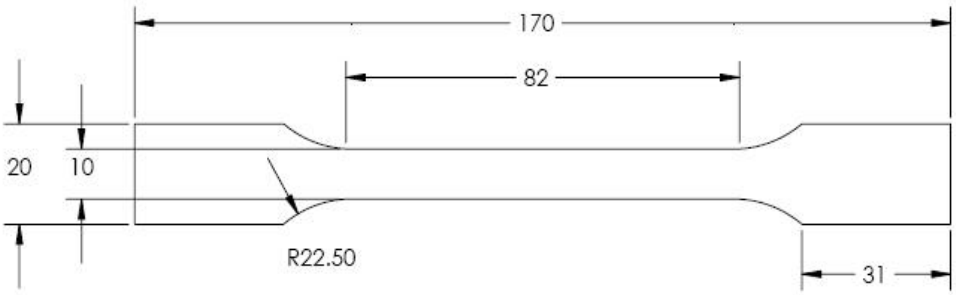

b. Test Piece with critical dimensions

Figure 4.1 Dumb-bell shaped test piece of LEXAN EXL1414H

The mechanical properties of the LEXAN EXL1414H tested at 50mm/min are as shown in Table 4.1. The detailed data sheet for the material is attached as **Appendix A**. The parameters shown in Table 4.1 were used as test validation parameters.

Table 4.1 Mechanical Properties for LEXAN EXL1414H

	Parameters	Symbol	Input	Unit
1	Modulus of Elasticity	E	2020	MPa
2	Yield Stress (Tensile)	σ_y	56.0	MPa
3	Yield Strain (Tensile)	ε_y	6	%

UNIAXIAL Tensile test was conducted to observe the behavior of the material under various strain rates. Therefore, stress-strain curves for the material at different strain rates are required. The variation of strain rates can be obtained by changing the crosshead test velocities. The test velocities used for the test are tabulated in Table 4.2.

Table 4.2 Test Velocity and number of test done

	Test Velocity (mm/min)	No of Test
1	1	3
2	10	3
3	20	3
4	50	3

However, the test could not take into consideration the test temperature effect. This was mainly because the environmental chamber available can only be fitted to a universal testing machine with a minimum load cell of 100kN for static tests and 200kN for dynamic tests. To be able to obtain a reasonably accurate test result, the test piece should at least withstand a minimum of 5% of the load cell's load. Based on the data sheet, the estimated maximum force for LEXAN EXL1414H should be in the range of 1.0 to 2.0kN. The estimated load is less than 5% of the minimum load required by the load cell of the universal testing machine. Forcefully using the load cell of 100kN might produce results with high inaccuracy.

As the tested material was a replacement for the material of interest, the objectives for running the test were modified as follow.

i. To understand the procedure of conducting a UNIAXIAL Tensile Test
ii. To observe the behavior of LEXAN EXL1414H under various strain rates
iii. To obtain the stress-strain curve for the material tested
iv. To validate the Eyring's equation and compute the equation's coefficients

However, the studied material on the dynamic behavior of plastic materials remained the same. The material model with stress-strain related parameters was provided by JCL for material DYLARK 480P16. The material model was produced by NOVA Chemicals for *Material 24*.

4.1. UNIAXIAL Tensile Test – Apparatus

The test was conducted using a universal testing machine which is the INSTRON 1195 using a load cell of 1000lb based on ASTM D638M [4] testing requirements. The test machine used is as shown in Figure 4.2. The controls and settings of the machine were done using the control panel and data logger as shown in Figure 4.3.

Figure 4.2 INSTRON 1195 Universal Testing Machine

a. Data Logger

b. Control Panel

Figure 4.3 Controls for INSTRON 1195

For the strain measurement, an extensometer with a gauge length of 50mm and a maximum strain measurement of 6% strain was used. The extensometer was fixed to the test piece as shown in Figure 4.4. As stated in the data sheet for LEXAN EXL1414H, the strain at break is estimated to be 120% strain. Therefore, after the strain reading exceeds 6%, the extensometer was removed as the extensometer no longer provides any strain measurement data. However, the test piece was still loaded till it breaks.

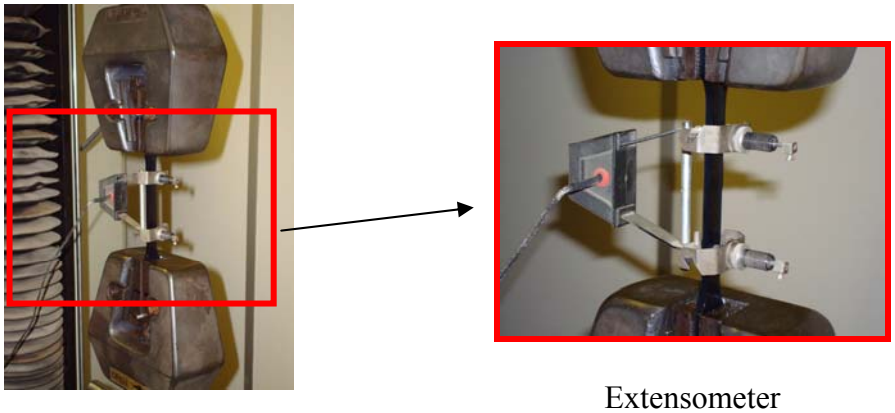

Extensometer

Figure 4.4 Extensometer

4.2. UNIAXIAL Tensile Test – Test Results

Through observation, the test piece started to show obvious necking soon after the extensometer was removed at 6% strain. The necking of the test piece is illustrated in Figure 4.5 (i). The necking effect stretched in 2 directions towards the upper and lower grip of the INSTRON machine. The necking stopped at the fillet radius of the test piece. This can be observed as shown in Figure 4.5 (ii) and (iii). Finally, the test piece stopped showing any continuous necking effect and break as reflected in Figure 4.5 (iv).

i ii

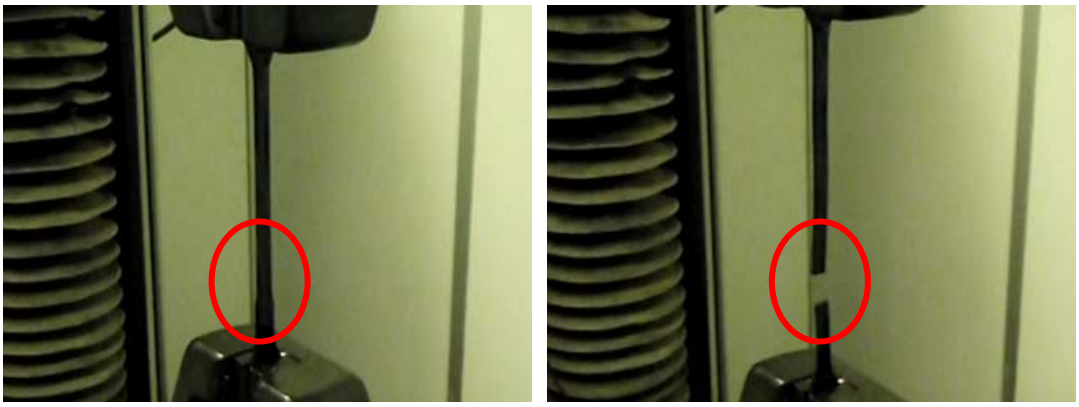

iii iv

Figure 4.5 UNIAXIAL Tensile Test Observation

The failed test pieces tested at 50mm/min are shown in Figure 4.6. As it can be seen, the material is of a ductile type. The test data was converted to true values of stress and strain based on the equations provided by ASTM D638M [4]. The true stress against true strain curve for the LEXAN EXL1414H tested at 50mm/min is shown in Figure 4.7. The strain values after 6% strain were extrapolated based on the strain rate of the test piece up to 6% strain with the assumption that the strain rate remained the same throughout the test.

Figure 4.6 Failed Test Pieces tested at 50mm/min

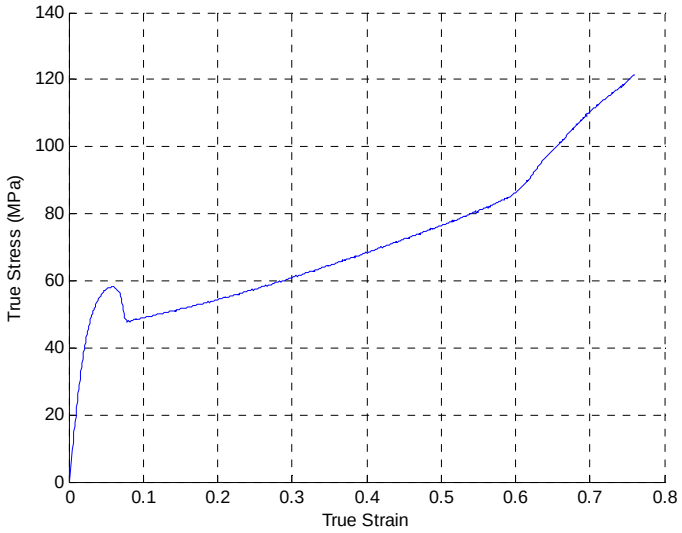

Figure 4.7 True Stress vs True Strain curve for LEXAN EXL1414H at 50mm/min

The UNIAXIAL tensile test was conducted for various test velocities. The true stress-true strain curves for various test velocities are shown in Figure 4.8. It can be observed that as the test velocity is increased, the stress-strain curve is being shifted upwards gradually. The curves shown were plotted up till a strain value of 6% only.

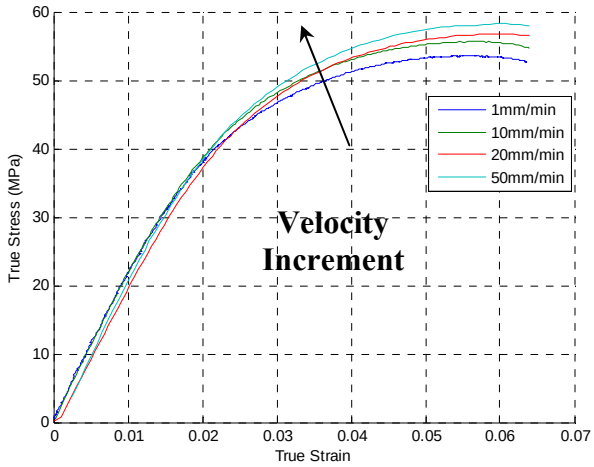

Figure 4.8 True Stress vs True Strain curves for various test velocities

Based on ASTM D638M [4], to be able to estimate the yield stress of a plastic material, an offset yield strength curve should be plotted at an offset value of 0.1% strain as shown in Figure 4.9. The intersection of the offset yield strength curve and the stress-strain curve is the estimated yield point of the tested material. As the parameter of interest is the yield stress, the stress-strain curves are shown up to a strain value of 6% strain.

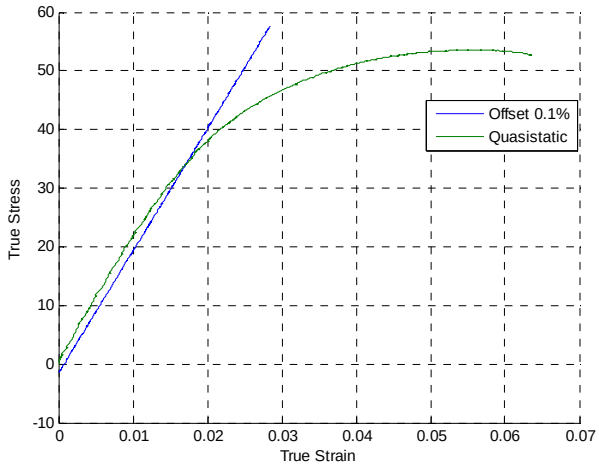

Figure 4.9 Offset 0.1% and True Stress vs True Strain curve at 1mm/min

To determine the strain rate, $\dot{\varepsilon}$ for the UNIAXIAL Tensile test at various test velocities, the strain-time response should be obtained. The strain-time responses for the various test velocities are plotted in Figure 4.10.

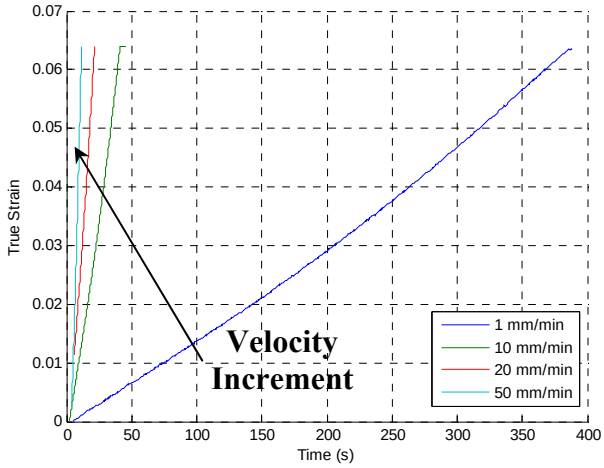

Figure 4.10 Strain-Time Response for UNIXIAL Tensile Test for LEXAN EXL1414H with various test velocities

As strain rate can be defined as:

$$\because \dot{\varepsilon} = \frac{d\varepsilon}{dt}$$

For the study, the strain rate was linearly approximated as:

$$\therefore \dot{\varepsilon} = Slope \quad of \quad Curve$$

By using the equation above, the strain rates for the UNIAXIAL Tensile tests conducted were approximated as in Table 4.3. The processed data for the tests conducted are tabulated in Table 4.4 for the yield stress and Table 4.5 for the modulus of elasticity for LEXAN EXL1414H.

Table 4.3 Strain Rates of UNIAXIAL Tensile Tests for LEXAN EXL1414H at various test velocities

	Test Velocity (mm/min)	Strain Rate (1/s)			
		Test 1	Test 2	Test 3	Average
1	1	0.0002	0.0002	0.0002	**0.0002**
2	10	0.0016	0.0016	0.0016	**0.0016**
3	20	0.0034	0.0032	0.0031	**0.0032**
4	50	0.0082	0.0083	0.0083	**0.0083**

Table 4.4 Yield Stress for LEXAN EXL1414H at various test velocities

Test Velocity (mm/min)	Strain Rate (1/s)	Yield Stress (MPa)			
		1	2	3	Average
1	0.0002	32.06	32.09	30.36	**31.50**
10	0.0016	33.13	33.28	33.08	**33.16**
20	0.0032	33.55	33.81	33.54	**33.64**
50	0.0083	34.30	34.32	34.15	**34.26**

Table 4.5 Modulus of Elasticity for LEXAN EXL1414H at various test velocities

Test Velocity (mm/min)	Strain Rate (1/min)	Modulus of Elasticity (MPa)			
		1	2	3	Average
1	0.0002	2103.8	2143.2	2195.8	**2147.6**
10	0.0016	2158.0	2134.7	2146.2	**2146.3**
20	0.0032	2091.3	2115.0	2134.2	**2113.5**
50	0.0083	2178.2	2159.2	2142.9	**2160.1**

To validate the test results, the yield stress at 6% strain and modulus of elasticity of LEXAN EXL1414H as provided in the data sheet were compared to the values obtained through the experimental test conducted. The values provided in the data sheet were obtained for a test velocity of 50mm/min based on ASTM D638M [4]. The comparison is tabulated in Table 4.6.

Table 4.6 UNIAXIAL Tensile Test Validation for LEXAN EXL1414H at 50mm/min

	Parameter	Data Sheet (MPa)	Experiment (MPa)	Error (%)
1	Yield Stress @ 6% strain	56.0	58.17	3.88
2	Modulus of Elasticity	2020	2160.1	6.94

The experimental yield stress of LEXAN EXL1414H at 6% strain was 3.88% off the value provided by the data sheet. The experimental modulus of elasticity was 2160.1 MPa. The value showed a deviation error of 6.94%. The experimental values showed a good correlation to the data sheet of LEXAN EXL1414H. This means that the strain measurement method using the extensometer produced reasonably accurate results up to 6% strain.

4.3. UNIAXIAL Tensile Test – Eyring Equation

As the UNIAXIAL Tensile test was conducted at various test velocities, a plot of the ratio for yield stress and temperature against the natural logarithm of the strain rate can be obtained. A linear curve was obtained as shown in Figure 4.11. As the test was carried out at low strain rates, a single process of activation was obtained based on the Eyring equation.

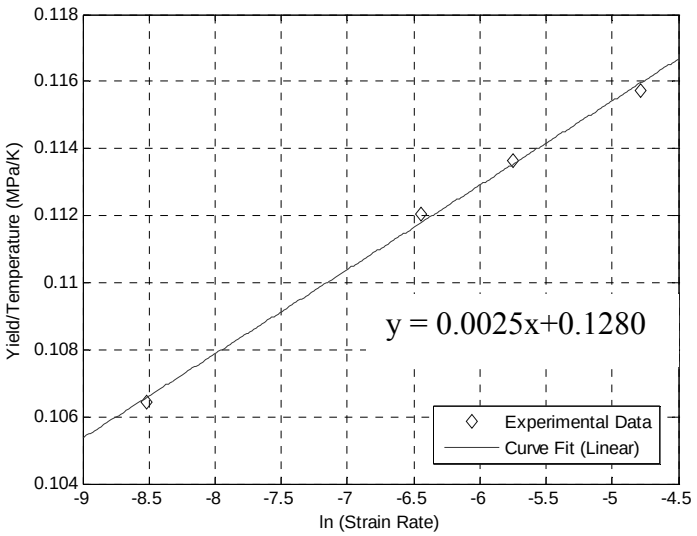

Figure 4.11 Plot of σ_y/T against ln $\dot{\varepsilon}$ for LEXAN EXL1414H

By comparing the single process of activation for the Eyring equation and a linearized approximation,

Eyring Equation :- $$\frac{\sigma_y}{T} = [\frac{\Delta H}{vT} + \frac{R}{v} \ln \frac{2\dot{\varepsilon}}{\dot{\varepsilon}_o}]$$

Linearized Approximation :- $$y = displacement + slope \cdot x$$

It can be approximated that the coefficients for the single process of activation for the Eyring equation are as shown below:

$$\frac{R}{v} = slope \quad of \quad curve \quad ; \quad \frac{\Delta H}{v} = displacement \times T$$

To be able to calculate the final coefficient for the Eyring equation, the steps below were followed.

Step 1:-

$$\frac{\sigma_y}{T} = (\frac{\sigma_y}{T})_a$$

Step 2:-

$$\ln \frac{2}{\dot{\varepsilon}_o} = -\frac{1}{slope}[displacement - (\frac{\sigma_y}{T})_a] - \ln \dot{\varepsilon} @ (\frac{\sigma_y}{T})_a$$

Based on the calculations discussed above, the coefficients of the Eyring equation for LEXAN EXL1414H are tabulated in Table 4.7.

Table 4.7 Coefficients of Eyring Equation for LEXAN EXL1414H

	Eyring Coefficients	Value
1	$\frac{R}{v}$	0.0025
2	$\frac{\Delta H}{v}$	37.8880
3	$\ln \frac{2}{\dot{\varepsilon}_o}$	-0.1060

By replacing the coefficients of the Eyring equation with the values computed in Table 4.6, the single process of activation of the Eyring equation for LEXAN EXL1414H is as shown below:

$$\frac{\sigma_y}{T} = [\ \frac{37.8880}{T} - 2.6500\times10^{-4} + 0.0025 \ln \dot{\varepsilon}\ ]$$

The Eyring equation shown above can be used to relate the strain rate and temperature effect onto the LEXAN EXL1414H at low strain rates.

4.4. Summary

The chapter included brief explanations on the UNIAXIAL Tensile test setups and procedures. The test observations and results were presented in the chapter. Based on the test results, the coefficients of the Eyring equation were computed for LEXAN EXL1414H to relate the strain rate effect on the material. The following chapter will discuss on the experimental method for the Drop Weight Impact test for DYLARK 480P16.

5.0. Experimental Method - Drop Weight Impact Test

The objective for conducting the Drop Weight Impact test on DYLARK 480P16 by JCL using DYNA-Tup 8250 is to obtain the dynamic behavior of the material at various temperatures. The experimental setups for the test are shown in Figure 5.1 and Figure 5.2. The test area on the test piece is also shown in Figure 5.2. The illustrations shown are courtesy of JCL.

a. DYNA-Tup 8250

b. Impact tup

Figure 5.1 DYNA-Tup 8250 and the Impact tup

a. Test Fixture

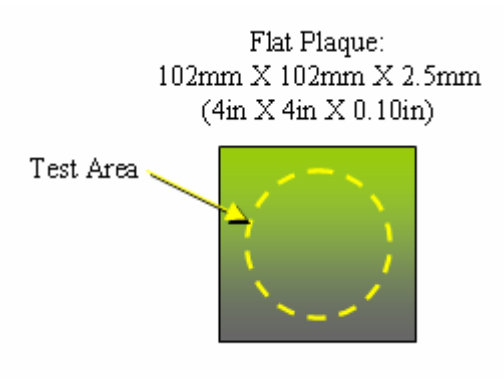

b. Test Piece

Figure 5.2 Test Fixture and Test Piece for drop weight impact test using DYNA-Tup 8250

For the data provided by JCL, the test was conducted using an impact tup with a mass of 5 kg. The test velocity of the tup was set to 6.7 m/s. The diameter of the tup is 12.7 mm. The values are summarized in Table 5.1.

Table 5.1 Parameters for Drop Weight Impact test using DYNA-Tup 8250

	Dimension	Input	Unit
1	Impact Tup Diameter	12.7	mm
2	Impact Tup Mass	5.0	kg
3	Test Velocity	6.7	m/s

5.1. Drop Weight Impact Test Results

The test was conducted on DYLARK 480P16 test piece at ambient temperature, 85°C and -40°C. Figure 5.3 shows the plot of force against displacement for the test done on ambient temperature provided by JCL. The test results for 85°C and -40°C are illustrated in Figure 5.4 and 5.5.

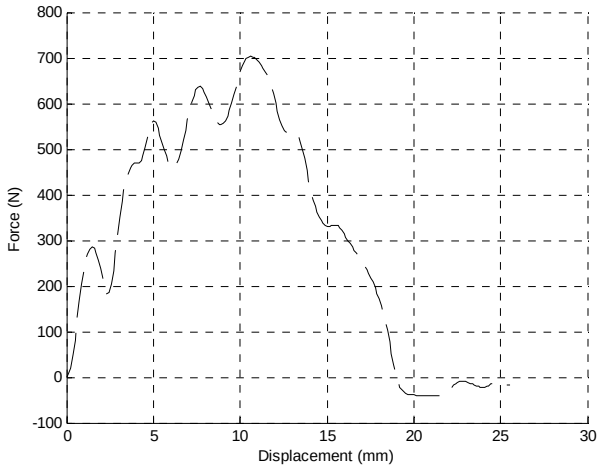

Figure 5.3 Force against Displacement plot for Drop Weight Impact test for DYLARK 480P16 at ambient temperature (Provided by JCL)

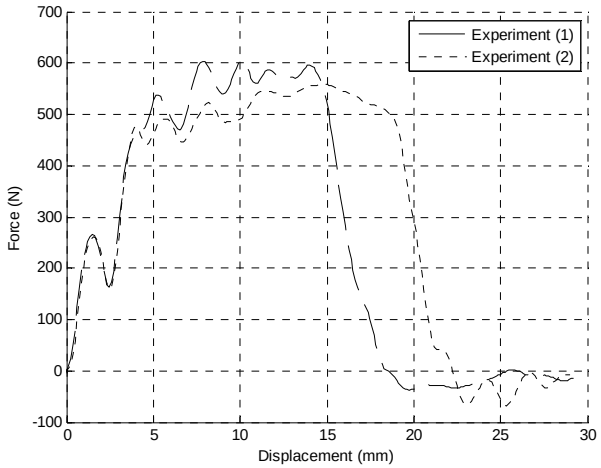

Figure 5.4 Force against Displacement plot for Drop Weight Impact test for DYLARK 480P16 at 85°C (Provided by JCL)

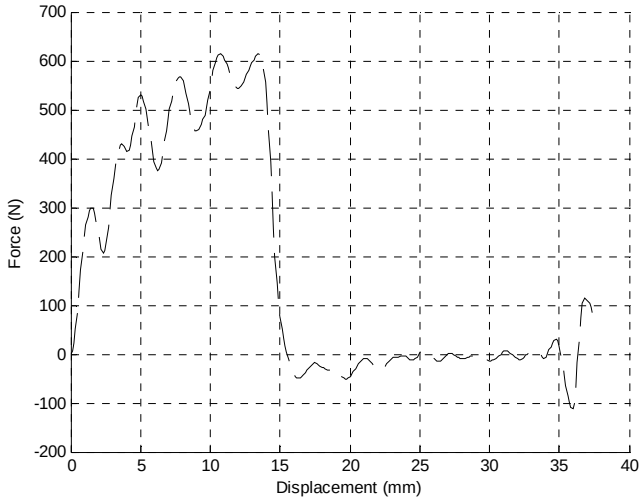

Figure 5.5 Force against Displacement plot for Drop Weight Impact test for DYLARK 480P16 at -40°C (Provided by JCL)

5.2. Summary

As a summary, this chapter covered the Drop Weight Impact test using the DYNA-Tup 8250. The results for the test at ambient temperature, 85°C and -40°C were included. For the next chapter, a brief background study will be covered on the FE method using LS-DYNA. The FE modelling considerations required will also be discussed.

6.0. LS-DYNA

The aim of the study is to simulate the dynamic properties for DYLARK 480P16 based on an empirical method. A Drop Weight Impact test was used to obtain the dynamic behavior of the material. Then, an FE analysis was carried out to simulate the dynamic response for DYLARK 480P16. The numerical analysis is categorized as a wave propagation problem. The wave propagation problem can be solved using the explicit FE method.

LS-DYNA is a type of explicit, transient and non-linear FE analysis package. The package applies explicit direct integration method to calculate the response history using step-by-step integration of the equation of motion [24]. For the study, *LS-PrePost* was used as the pre-processor and post-processor. The LS-DYNA models were modelled and meshed using *LS-PrePost*. Then, the model was solved using *ANSYS LS-DYNA* solver. The simulated model was post-processed using *LS-PrePost*. All the simulation models for the study used the standard units as shown in Table 6.1 to avoid any dynamic inconsistencies when post processing the simulation results.

Table 6.1 LS-DYNA model Standard Units for the study

	Parameter	Unit
1	Mass	tonne
2	Length	Millimeter (mm)
3	Time	Seconds (s)
4	Force	Newton (N)
5	Stress	MPa

6.1. Effect of Time Step on an LS-DYNA Simulation

The explicit FE method is conditionally stable. The condition for the method to be stable is to not exceed the critical time step, Δt_{cr} which is also the maximum time step. If the time step used for the integration exceeds Δt_{cr}, the numerical calculation will become unstable. Hence, produces irrelevant analysis results. The effect of Δt_{cr} is reflected in Figure 6.1.

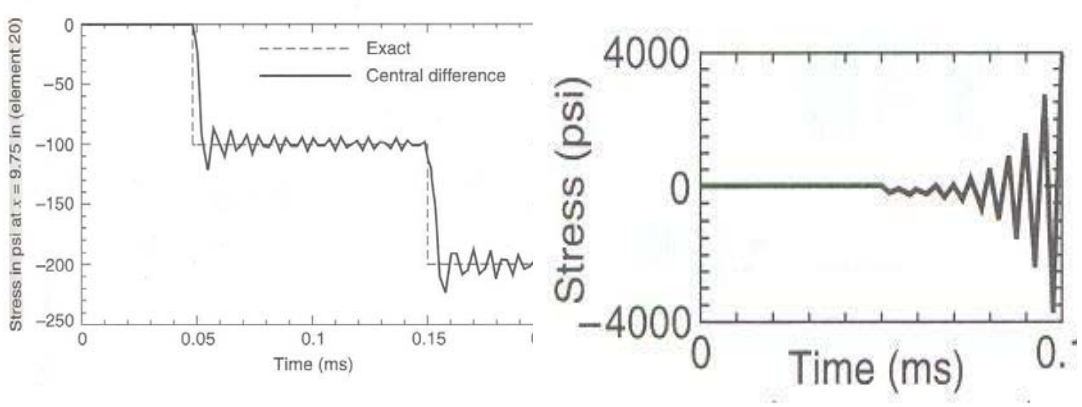

a. $\Delta t = 2.4$ μs b. $\Delta t = 2.5$ μs

Figure 6.1 Effect of time step on the response history of an explicit FE analysis with Δt_{cr} = 2.484 μs [24]

The FE model used for this study is of shell-elements. In LS-DYNA, the critical time step for shell elements is given as [21]:

$$\Delta t_{cr} = \frac{L_s}{c}$$

With $c = \sqrt{\frac{E}{\rho\,(1-\nu^2)}}$

Where

c = Speed of sound

L_s = Characteristic length of the shell element

The characteristic length mentioned above is illustrated in Figure 6.2 for (a) 4-node shell element and (b) warped 4-node element.

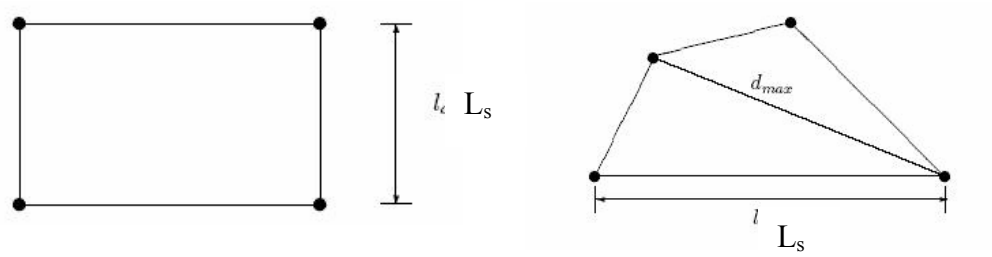

(a) 4-node shell element (b) 4-node warped shell element

Figure 6.2 Characteristic length of shell elements in LS-DYNA [21]

6.2. LS-DYNA Modelling Considerations

To simulate the UNIAXIAL Tensile and Drop Weight Impact tests in LS-DYNA, the modelling considerations as below were followed accordingly.

i. Element Length/Mesh Density
ii. Element Type
iii. Material Properties
iv. Stress-Strain data for Material 24
v. Boundary Conditions
vi. Impact Contact
vii. Failure Plastic Strain (FPS)
viii. Sliding Interface Penalty Coefficient (SLSFAC)
ix. Element Formulation
x. Simulation data Filtering

The details of how the modelling considerations mentioned were applied will be discussed in the Chapter 7 to 10.

6.3. Summary

The chapter covered a brief background study on explicit FE method and also the LS-DYNA modelling considerations for the study. The next chapter will discuss on the modelling of the physical problems for the study in LS-DYNA.

7.0. LS-DYNA Models

This chapter covers the LS-DYNA models for the study. The models include FE simulations for:

i. UNIAXIAL Tensile test
ii. Drop Weight Impact test

All the FE simulations covered in the study was done using *Material 24* as the material model to represent DYLARK 480P16. *Material 187* or SAMP1 was not included in the study due to the lack of reliable and accurate data required by the material model for DYLARK 480P16. The general material properties for the material are provided by NOVA Chemicals. The data sheet for the material is attached in **Appendix B**. However, JCL modified the modulus of elasticity based on tests they conducted. The modified material properties for DYLARK 480P16 are tabulated in Table 7.1.

Table 7.1 Material Properties for DYLARK 480P16

	Parameters	Symbol	Input	Unit
1	Modulus of Elasticity	E	5117	MPa
2	Density	ρ	1.18E-09	tonne/mm^3
3	Poisson's Ratio	ν	0.279	

7.1. Effective Stress against Effective Plastic Strain

To represent DYLARK 480P16 using *Material 24*, the true values of the stress-strain curves for various strain rates must be converted into effective stresses and effective plastic strains. Figure 7.1 shows the true stress-true strain plot for the studied material tested at ambient temperature for various strain rates.

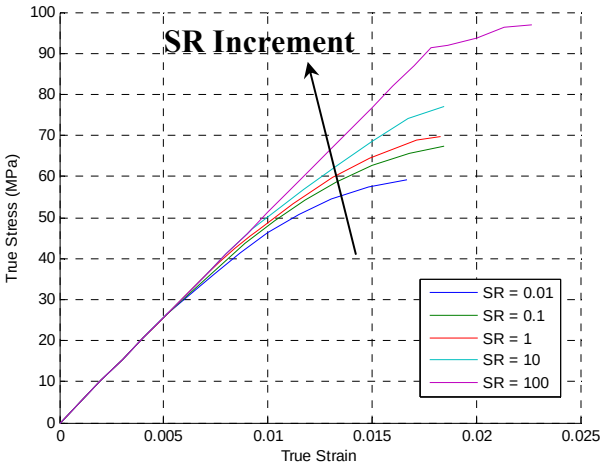

Figure 7.1 True Stress vs True Strain for DYLARK 480P16 at ambient temperature for various strain rates

To be able to convert the true stress-true strain curves into the desired parameters for *Material 24*, the steps as discussed below were followed.

Step 1: Determine Elastic-Plastic Region of Stress-Strain Curve

Firstly, the elastic and plastic region for the stress-strain curves must be clearly identified. There are a few methods to determine the regions. The first method is by defining the yield point of the stress-strain curve based on ASTM D638M [4] as discussed earlier using an offset yield strength curve. However, NOVA Chemicals' approach to separate both the elastic and plastic regions is by defining the proportional limit point as the yield point instead. The proportional limit is the elastic limit of the material where Hooke's law applies. The proportional limit and the elastic-plastic region for the stress-strain curve at strain rate, SR = 0.01 are shown in Figure 7.2.

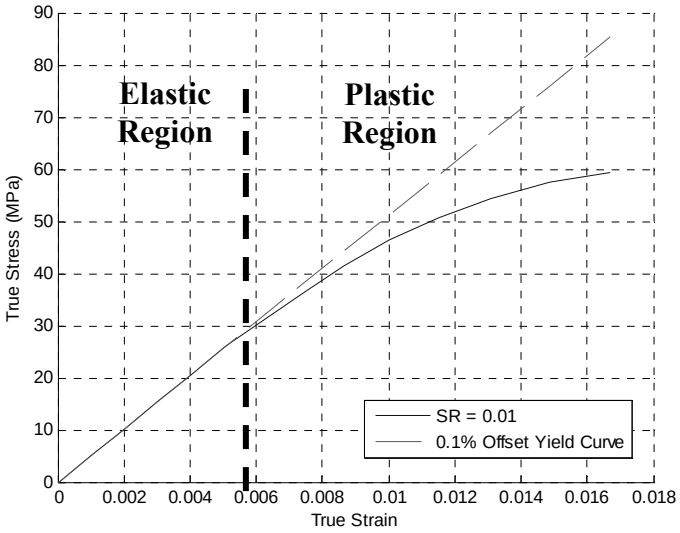

Figure 7.2 Elastic-Plastic region of True Stress vs True Strain curve for DYLARK 480P16

Step 2: Removing the Elastic Region of Stress-Strain Curve

Then, the elastic region is removed leaving only the plastic region of the true stress-true strain curve as shown in Figure 7.3.

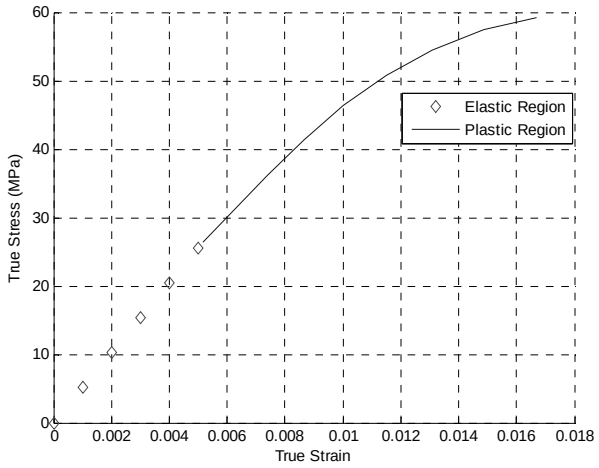

Figure 7.3 True Stress vs True Strain curve for DYLARK 480P16 (With the elastic region removed)

Step 3: Converting the Plastic Strain to Effective Plastic Strain

As the true stress of the stress-strain curve was obtained through UNIAXIAL Tensile test, the true stress is actually equivalent to the effective stress. To convert the plastic strain values to effective plastic strain, the equation below is used:

$$\varepsilon_p = \varepsilon_{total} - \varepsilon_{elastic}$$

With

$$\varepsilon_{elastic} = \frac{\sigma_y}{E}$$

The resultant curve is illustrated in Figure 7.4 for strain rate, SR = 0.01.

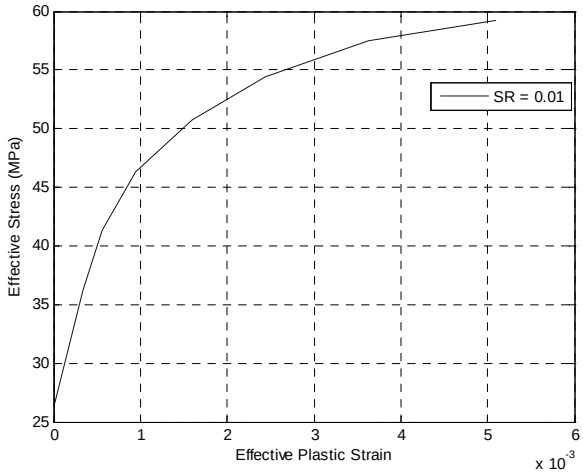

Figure 7.4 Effective Stress vs Effective Plastic Strain for DYLARK 480P16 at SR = 0.01

The steps discussed above were converted into a MATLAB script as attached in **Appendix C**. By repeating the steps discussed above using the MATLAB script, the stress-strain curves for other strain rates were converted into the desired parameter for *Material 24* as discussed in Chapter 3.

The converted curves are shown in Figure 7.5. The LS-DYNA keyword for the material model is included in **Appendix D**. Besides the mechanical properties shown in Table 7.1, the curves were used to take into consideration the strain effects on DYLARK 480P16 using *Material 24* in LS-DYNA.

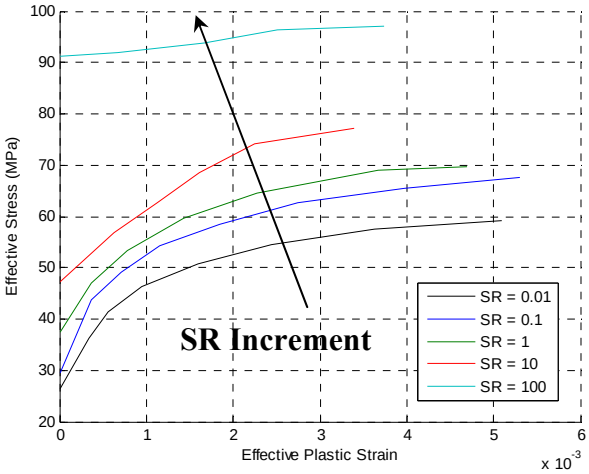

Figure 7.5 Effective Stress vs Effective Plastic Strain for DYLARK 480P16 for various strain rates

7.2. LS-DYNA Model – UNIAXIAL Tensile Test

Before proceeding to model the Drop Weight Impact test, a simple UNIAXIAL Tensile test model is generated to ensure that the *Material 24* is working in a desired manner. A 2-dimensional 'dumb bell' specimen is modeled in LS-DYNA.

The mesh of the model consists of shell elements only. The boundary conditions are set based on the actual UNIAXIAL Tensile test condition as described in ASTM D638M [4]. *Prescribed-motion-node* is used to apply the tensile load while *Boundary-SPC-Node* is used as the restraints.

A load curve is used to define the *Prescribed-Motion-Node* which also represents the test velocity required. For the simulation, the time step option is set to default where the solver will compute the time step. As the simulation was of a simple physical problem, the number of integration points used was a value of 2. The parameters used for the UNIAXIAL Tensile test simulation model are summarized in Table 7.2.

Table 7.2 Parameters for UNIAXIAL Tensile Test Simulation Model

	Parameter	Dumb-bell Shaped Test Piece
1	Element Type	Shell Elements
2	Element Formulation	Default (Belytschko-Tsay)
3	Load	Prescribed-Motion-Node
4	Restraints	Boundary-SPC-Node
5	No. of Integration Points	2

For the simulation, a convergence study was executed to evaluate a suitable mesh density for the simulation model. Besides this, an iteration process involving the Failure Plastic Strain (FPS) was conducted. The FPS value is used to delete an element when the strain of the element reaches the value set. By deleting elements when the strain of the elements reached the FPS value set, the failure mode of the model can be simulated accordingly. The iteration process for the UNIAXIAL Tensile test simulation model is simplified in Figure 7.6.

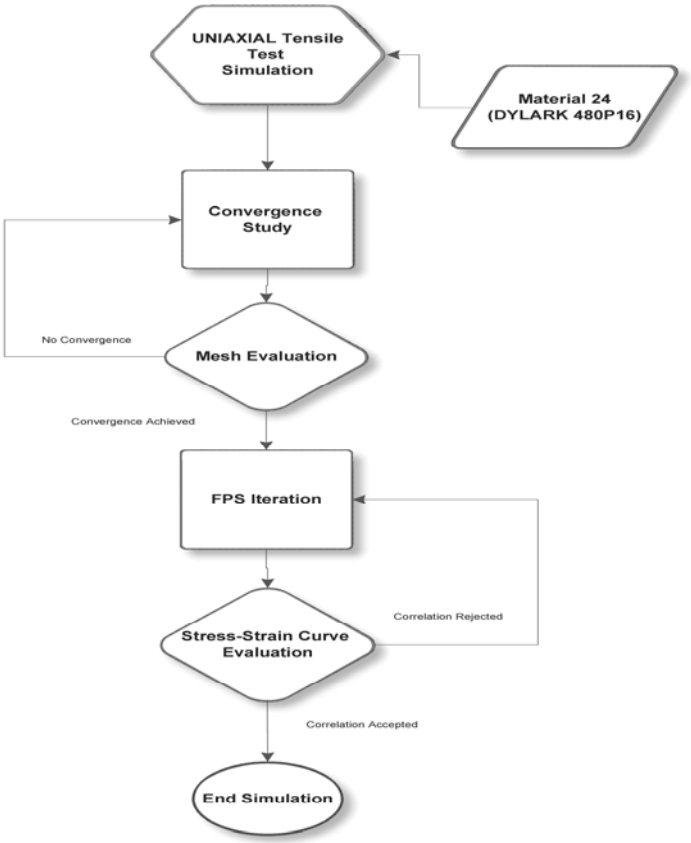

Figure 7.6 Iteration Process Flow for UNIAXIAL Tensile Test Simulation Model

Step 1: Geometry Preparation

Firstly, the dumb-bell shaped test piece geometry was prepared. The dimensions for the geometry used were based on the test piece provided by JCL for the UNIAXIAL Tensile test for LEXAN EXL1414H. The simulation geometry is shown in Figure 7.7. The region where the boundary condition and loading as stated in Table 7.2 was applied is also illustrated in Figure 7.7. The region 'X' where the stress-strain data was extracted is highlighted in Figure 7.7. The LS-DYNA keyword for the model is included in **Appendix E**.

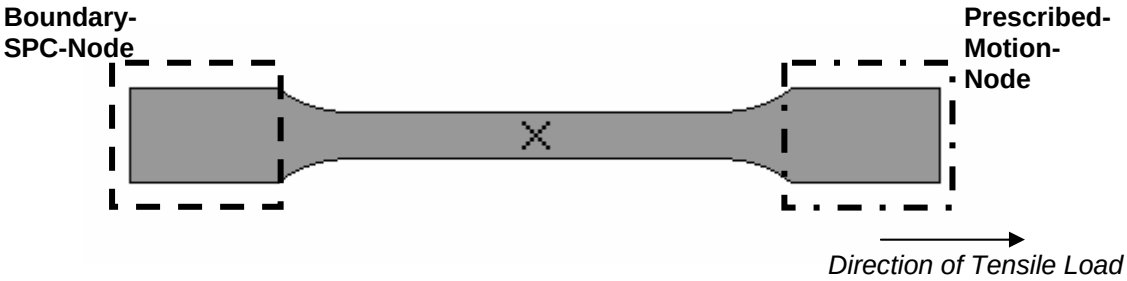

Figure 7.7 Dumb-bell Shaped Geometry for the UNIAXIAL Tensile Test Simulation for DYLARK 480P16

Step 2: Convergence Study

Next, a simple convergence study was carried out using the geometry as shown in Figure 7.7. To correlate the simulation results to physical test results for this study, the simulation results should be within the ±5% error range. A deviation error was allowed as the material model used is developed using metallic material laws instead of polymer material laws. The mesh of the model was refined by varying the Element Length (EL). The simulation results for different EL ranging between 0.5mm to 2mm using a trial test velocity of 500mm/s for SR = 10 are shown in Figure 7.8. The stress-strain data was obtained for elements at the central region of the test piece.

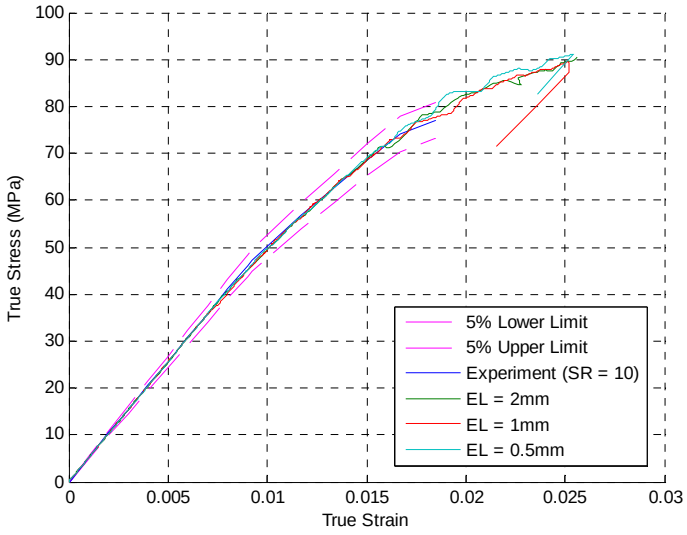

Figure 7.8 True Stress-True Strain of UNIAXIAL Tensile Test for DYLARK 480P16 with various EL (Test Velocity = 500mm/s, SR = 10)

Based on the observation of the plots in Figure 7.8, the results showed reasonable convergence for the different EL simulated. Therefore, to decide on the suitable EL for the simulation model, the failure mode of the simulation model for various EL were compared. The failure modes for different EL are reflected in Figure 7.9.

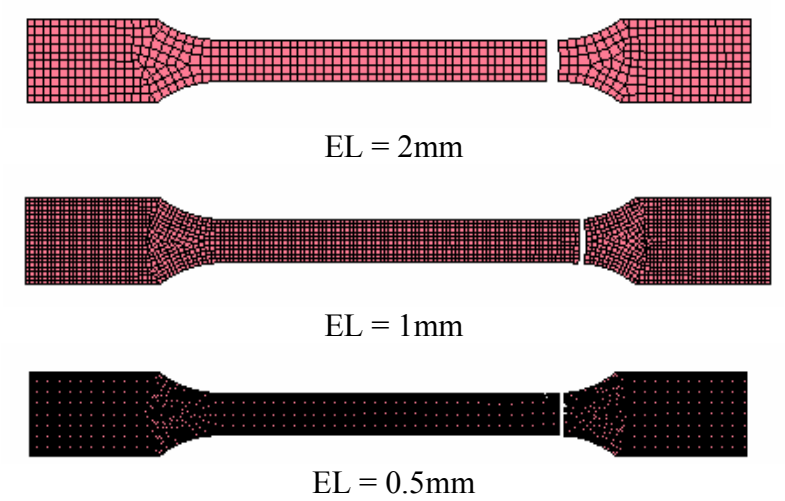

Figure 7.9 Simulated failure modes of UNIAXIAL Tensile Test for DYLARK 480P16 with various EL (Test Velocity = 500mm/s)

However, the failure mode for all the simulated models showed similarity and was difficult to determine which EL was the best. Therefore, another parameter was looked into. The strain rate of the simulation model for various EL was plotted as shown in Figure 7.10.

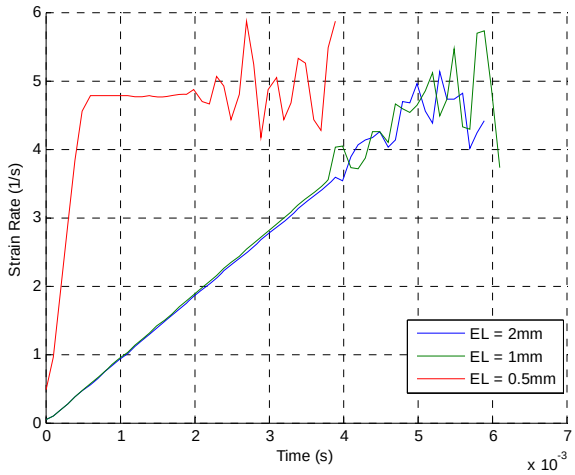

Figure 7.10 Strain rate response of UNIAXIAL Tensile Test for various EL

Based on the simulated strain rate response which was obtained by differentiating the strain response of the simulation models, the strain rate response for the model with EL = 0.5mm showed convergence. With that, it was decided that EL = 0.5mm enabled the simulation study to be done by undergoing a constant strain rate before the test piece break. Then, another iterative study was carried by varying the value of the test velocity till a strain rate of 10 was achieved. The iteration process can be seen in Figure 7.11.

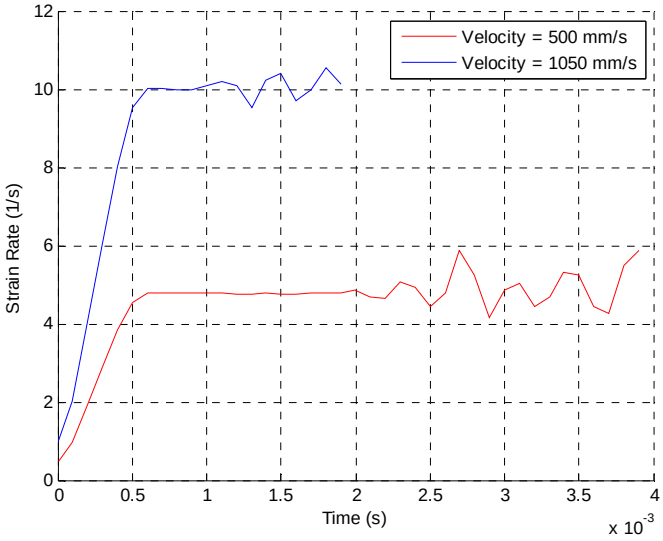

Figure 7.11 Strain rate response of UNIAXIAL Tensile Test for various test velocity

Step 3: FPS Iteration

Based on the convergence study discussed above, an EL of 0.5 mm was chosen for the FPS iteration. EL of 0.5 mm was selected due to the constant strain rate achieved as shown in Figure 7.11. By simulating the model for various FPS values, the plot as shown in Figure 7.12 was obtained.

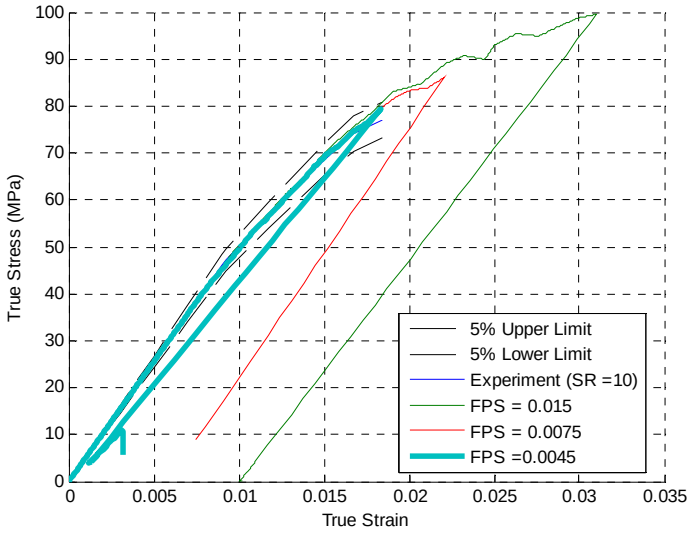

Figure 7.12 True Stress-True Strain of UNIAXIAL Tensile Test for DYLARK 480P16 with various FPS (EL = 0.5mm, SR = 10)

Based on the observation of the plot showed in Figure 7.12, it can be seen that the curve with FPS = 0.0045 showed the most reasonable correlation to the experimental test result. The final simulation model parameters are summarized in Table 7.3.

Table 7.3 Final FPS value for UNIAXIAL Tensile Test Simulation Model

	Strain Rate (1/s)	Test Velocity (mm/s)	EL (mm)	FPS
1	10	1050	0.5	0.0045

7.3. LS-DYNA Model – Drop Weight Impact Test

After achieving a reasonable level of confidence for the material model's simulated behavior, the Drop Weight Impact test on material DYLARK 480P16 was modeled in LS-DYNA. The proposal for the test based on the discussion done in an earlier chapter is illustrated in Figure 7.13.

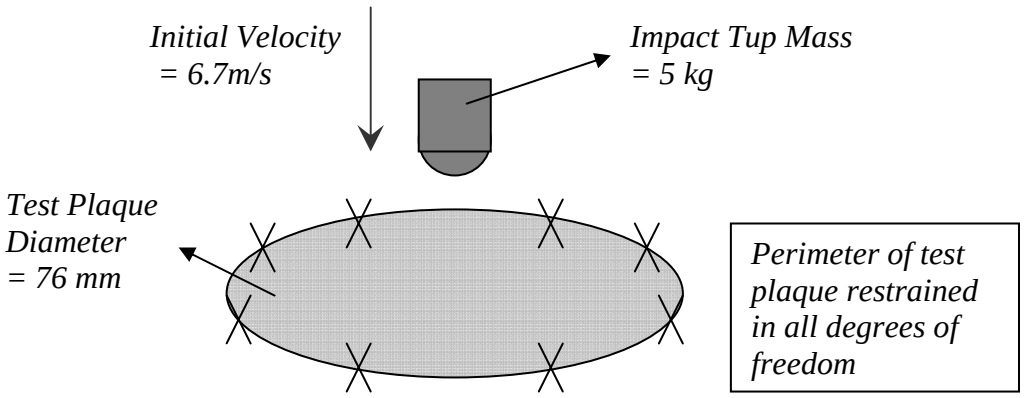

Figure 7.13 Proposed model for drop weight impact test

As shown in Figure 7.13, the impact tup was modeled using a bullet-shaped geometry. The purpose of using the geometry was to enable the application of the *Seat-Belt Accelerometer Element* for the analysis. The element was used to provide acceleration, velocity and displacement data of the impactor. The elements used for the model consist only of shell elements.

The mass of the impact tup was taken into consideration by obtaining the ratio of the mass over the volume of the tup. The material properties for the impact tup are tabulated in Table 7.4.

Table 7.4 Material Properties for Impact Tup

	Parameters	Symbol	Input	Unit
1	Modulus of Elasticity	E	210000	MPa
2	Density	ρ	5.61E-06	tonne/mm^3
3	Poisson's Ratio	ν	0.3	

For the model, the boundary condition of the circular test plaque was set using *SPC* function restraining 6 degrees of freedom of the test plaque's perimeter. The contact used to describe the impact problem is of the *Automatic-Surface-To-Surface* function. For this impact contact, the impact tup was set to *Master* while the test plaque was set to *Slave*. The FE model for the test was illustrated in Figure 7.14. The location of the accelerometer was shown in Figure 7.15. The parameters used for the Drop Weight Impact simulation model are summarized in Table 7.5.

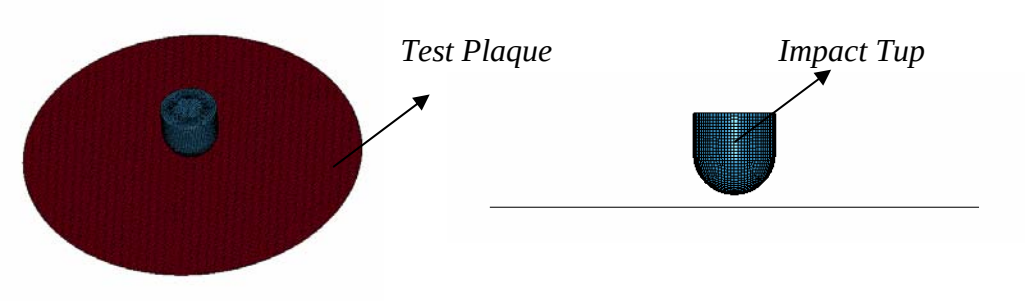

Figure 7.14 FE model for Drop Weight Impact test

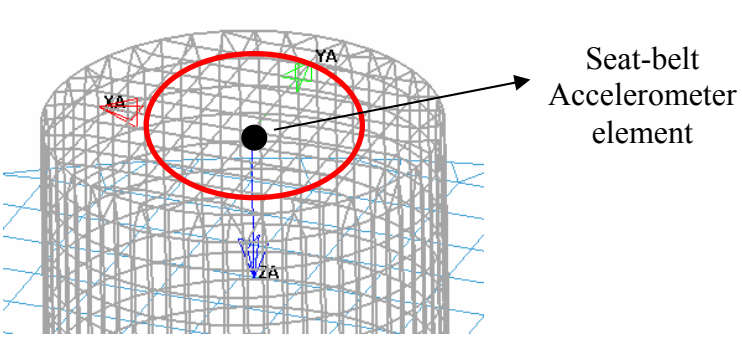

Figure 7.15 Location of seat-belt accelerometer element on the impact tup

Table 7.5 Parameters for Drop Weight Impact Test Simulation Model

	Parameter	**Test Plaque**	**Impact Tup**
1	Material Model	*Material 24*	*Material 20 (Rigid)*
2	Element Type	Shell Elements	Shell Elements
3	Element Formulation	Default (Belytschko-Tsay)	Default (Belytschko-Tsay)
4	Impact Velocity	-	Initial Velocity
5	Boundary Condition	Boundary-SPC-Node	-
6	Impact Contact	Surface-Surface (Slave)	Surface-Surface (Master)
7	No of Integration Point	5	2

As for the initial time step, the model was tested on different values of time step, which were 0.2 μs and also a default time step. The default time step refers to the time step value computed by LS-DYNA which was 0.0616 μs for this particular simulation model. The outcome of using both the step sizes is shown in Figure 7.16.

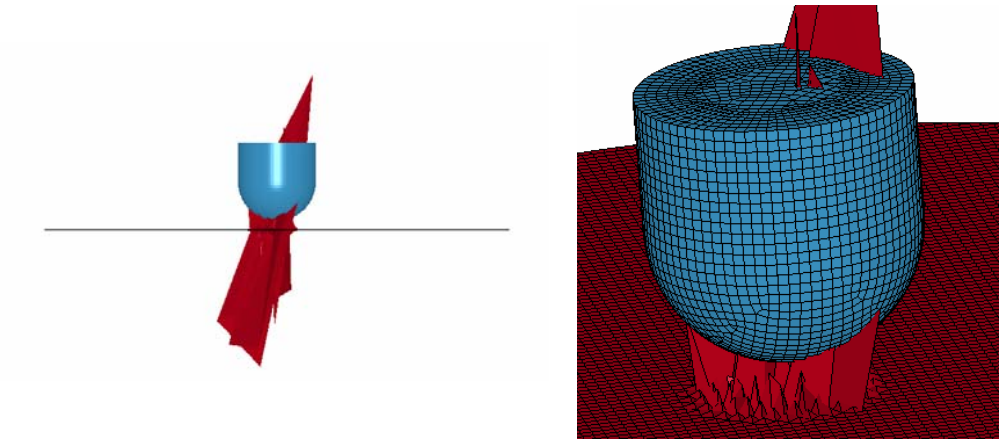

a. Step size = 0.2 μs

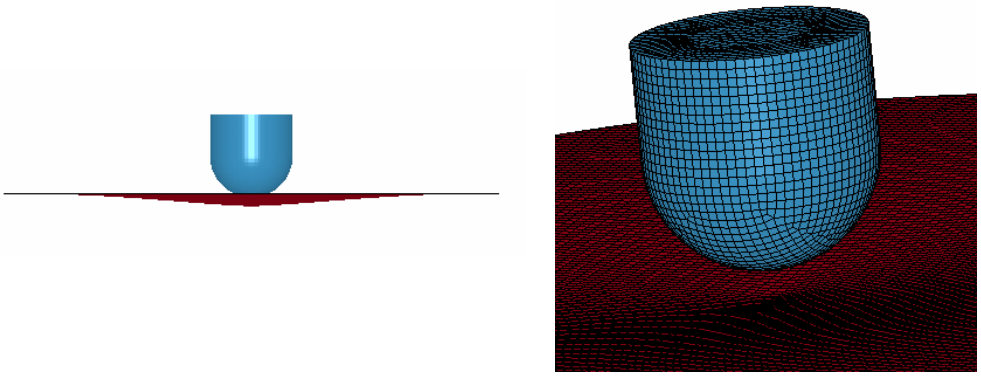

b. Step size = Default (0.0616 μs)

Figure 7.16 Model test on various step size

Through observation, at a larger time step, the FE model became unstable as discussed earlier. When a smaller time step is used, the stability of the model increased. However for the simulations, the minimum time step definition for shell elements is set to default as the step size iterated by the LS-DYNA solver is able provide a reasonable value for the simulation. The LS-DYNA keyword for the model is included in **Appendix F**.

For the Drop Weight Impact test simulation, a convergence study was not carried out as the EL chosen was based on the common element length used by JCL, which is 0.5mm. Therefore, the simulation was focused on the FPS iteration process to obtain a reasonable correlation between the simulation and experimental results for the Drop Weight Impact test. The iterative study is summarized in Figure 7.17.

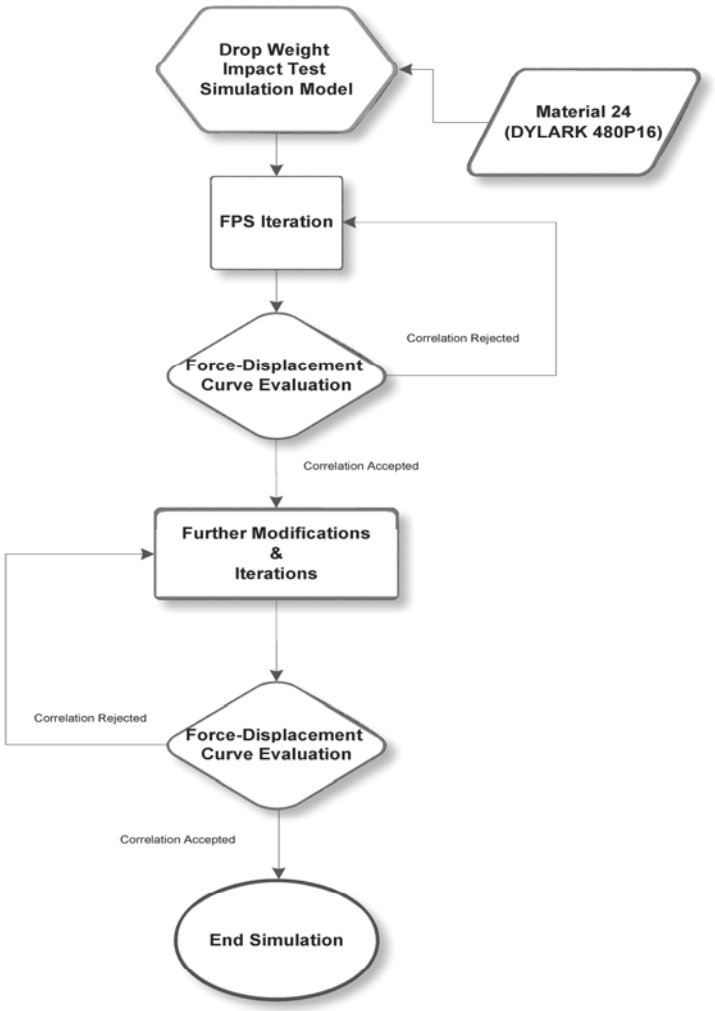

Figure 7.17 Iteration Process Flow for Drop Weight Impact Test Simulation Model

The simulation process and results for the Drop Weight Impact test model will be discussed in the following chapters based on the flow chart as shown in Figure 7.17.

7.4. Summary

To summarize up the chapter, a discussion was covered on the conversion of stress-strain curves to effective stress-effective plastic strain curves. The chapter also included discussions on LS-DYNA models for the UNIAXIAL Tensile and Drop Weight Impact test simulations. For the following chapter, a discussion on the simulation results of the Drop Weight Impact test simulation model will be covered for ambient temperature.

8.0. Numerical and Experimental Results Comparison (Ambient Temperature 23^{o}C)

For the Drop Weight Impact Test simulation, 2 basic criteria had been selected to correlate the simulation force-displacement curve to the experimental results. The basic correlation criteria are:

i. Peak load and corresponding displacement
ii. Final displacement at zero force

As a comparison for the study, the basic correlation criteria values should be within a deviation error range of ±10% of the experimental values to be considered acceptable. After fulfilling the basic criteria, the simulated force-displacement curve was correlated by comparing it with the experimental curve shape. The basic criteria for the correlation are illustrated in Figure 8.1.

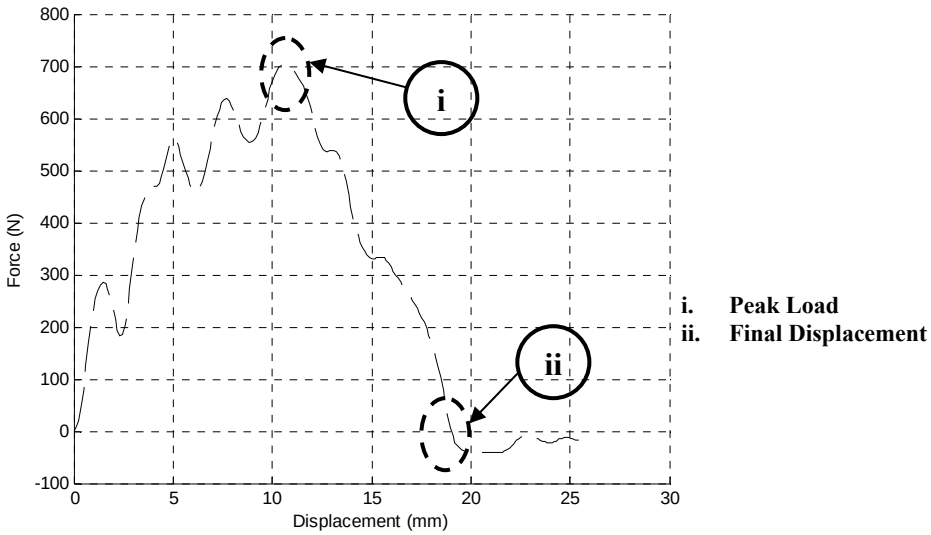

Figure 8.1 Force Vs Displacement plot for DYLARK 480P16 at ambient temperature with basic correlation criteria

As the simulation was of an impact simulation, SAE filter using Channel Frequency Class (CFC) with a limiting frequency of 1000 Hz was used to filter the high frequency noise produced during contact [19] filter type suggested by JCL uses Fourier series to digitally filter off unwanted high frequency vibrations and noise from the simulation raw data.

8.1. Drop Weight Impact Test Simulation Results at Ambient Temperature

Step 1: FPS Iteration

Firstly, the FE model of the Drop Weight Impact test was simulated by varying the FPS value. The simulated results were then being compared to the experimental test results. The simulated force-displacement curves are illustrated in Figure 8.2. The results for various FPS values were being compared to the experimental results.

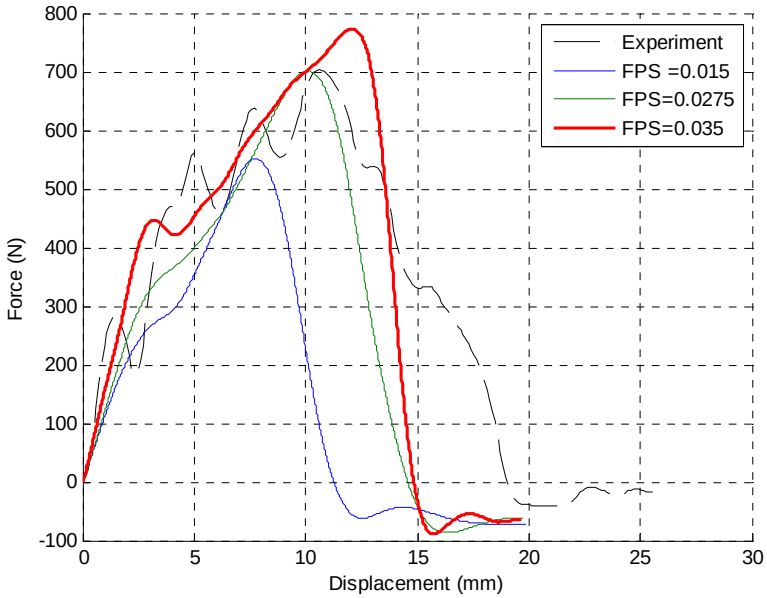

Figure 8.2 Force Vs Displacement plots for DYLARK 480P16 at ambient temperature with FPS variation

Through observation, the simulated peak load nearest to the experimental result was obtained by using FPS = 0.0275. However, the basic correlation criterion also includes the final displacement at zero force. At FPS = 0.0275, the final displacement value seemed to be too far off the experimental value. Therefore, the simulated curve which best fulfill both the basic correlation criteria was by using FPS = 0.035.

Step 2: Sliding Interface Penalty Factor Iteration

The simulated force-displacement curve for FPS = 0.035 showed a reasonable correlation based on the basic criteria mentioned. However, the final displacement for the simulation result seemed to exceed the ±10% deviation error range set for the study. Therefore, an iterative study was done by varying the Sliding Interface Penalty Factor (SLSFAC) using FPS = 0.035. The SLSFAC is a penalty factor used to scale contact stiffness for all penalty-based contact. The plots for a variation of SLSFAC are included in Figure 8.3.

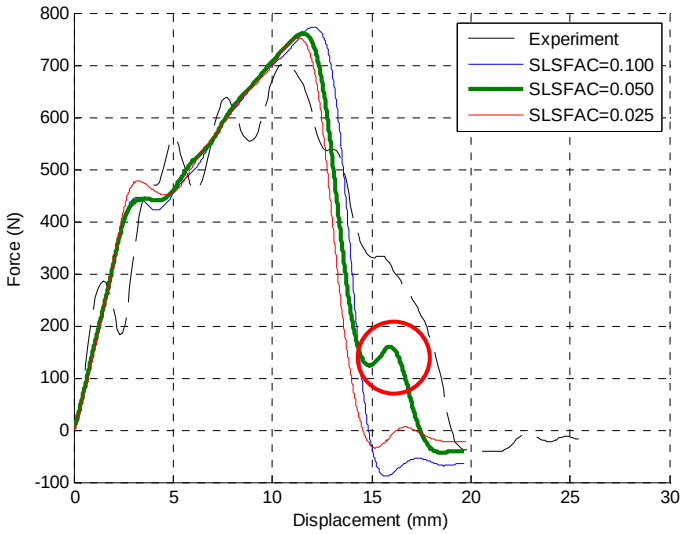

Figure 8.3 Force Vs Displacement plots for DYLARK 480P16 at ambient temperature with SLSFAC variation (FPS = 0.035)

As it can be seen in Figure 8.3, the simulated force-displacement curve which correlates the best was obtained by using SLSFAC = 0.05 for an FPS value of 0.035. The final displacement for the curve showed a better correlation as compared to using a default value for SLSFAC which is 0.1. For SLSFAC = 0.05, the additional 'hump' as highlighted in Figure 8.3 also further improved the curve shape correlation.

Step 3: Curve Shape Correlation

For the curve shape correlation, the simulated force-displacement curve for FPS = 0.035 with SLSFAC of 0.05 was chosen as graphical comparison. It can be seen that the filtered simulation curve showed shape correlations in 3 regions as highlighted in Figure 8.4.

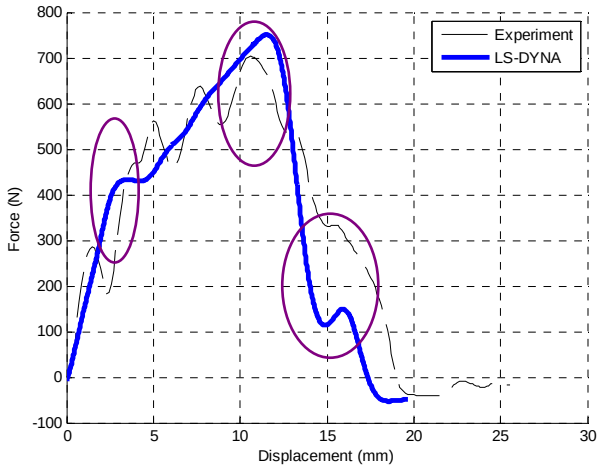

Figure 8.4 Force Vs Displacement plot comparison for DYLARK 480P16 at ambient temperature indicating shape correlation regions (FPS = 0.035, SLSFAC = 0.05)

However, it was observed that if the comparison was made using the raw simulation data, there was another shape correlation region at the beginning of the force-displacement curve between the simulation and experimental data. The correlation region is shown in Figure 8.5.

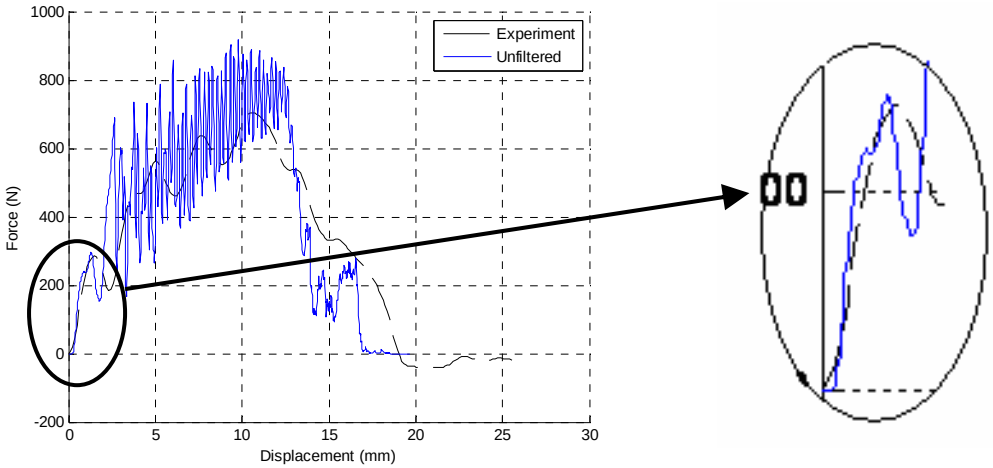

Figure 8.5 Force Vs Displacement plot comparison for DYLARK 480P16 at ambient temperature indicating shape correlation region (Unfiltered Simulation Data)

Step 4: Element Formulation Variation

The default Element Formulation (ELFORM) used for the simulation model above is of Belytschko-Tsay formulation. To further investigate the reliability of the ELFORM used for the simulation models discussed thus far, a simple study was conducted by changing the formulation to a Fully Integrated Shell Element (FISE) type.

The simulation results are shown in Figure 8.6. The comparison of the basic correlation criteria between the various element formulations is tabulated in Table 8.1.

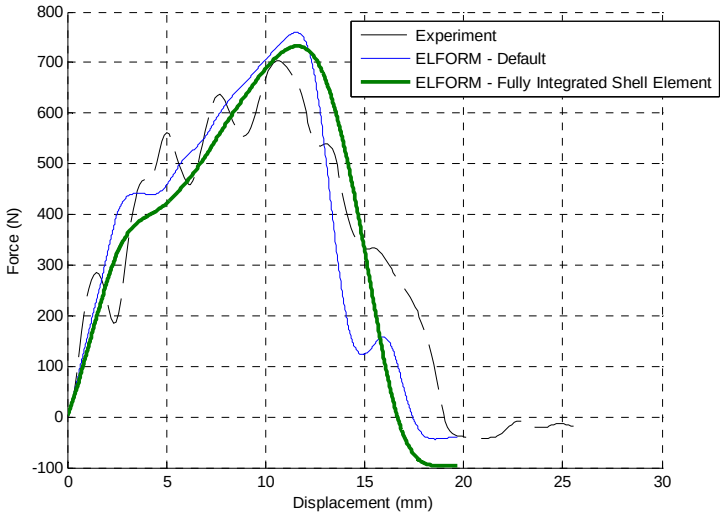

Figure 8.6 Force Vs Displacement plot comparison for DYLARK 480P16 at ambient temperature with ELFORM variation (FPS = 0.035, SLSFAC = 0.05)

Table 8.1 Experimental and Simulation results comparison for basic correlation parameters (Various ELFORM) – Ambient Temperature

	Parameter	Experimental	Default	FISE
1	Peak Load (N)	703.10	758.90	731.90
2	Displacement @Peak Load (mm)	10.60	11.56	11.69
3	Final Displacement @Zero Load (mm)	18.95	17.42	16.66

By comparing the results between the various ELFORM, it can be observed that the results produced by the FISE formulation showed a better correlation in terms of the peak load only. In all, the result produced by using the default ELFORM produced a better correlation in terms of basic criteria and curve shape correlation.

8.2. Final Simulation Model Parameter – Ambient Temperature

Based on the iterations done in *Step 1* to *3*, the final simulation parameters which best correlate the experimental force-displacement curve tested at ambient temperature are tabulated in Table 8.2.

Table 8.2 Final Simulation Parameter for Drop Weight Impact test Simulation Model for DYLARK 480P16

	Temperature	FPS	SLSFAC	ELFORM
1	Ambient	0.035	0.05	Default

The comparison values for the basic correlation criteria are summarized in Table 8.3. The error values for the criteria are within the 10% error range set for the study. The simulated peak load is 7.94% off the experimental peak load. The furthest offset error was the displacement corresponding to the peak load which is 9.06%. The failure mode for the simulation with these parameters is illustrated in Figure 8.7.

Table 8.3 Experimental and Simulation results comparison for basic correlation parameters – Ambient Temperature

	Parameter	Experimental	LS-DYNA	Offset Error (%)
1	Peak Load (N)	703.10	758.90	7.94
2	Displacement @Peak Load (mm)	10.60	11.56	9.06
3	Final Displacement @Zero Load (mm)	18.95	17.42	8.07

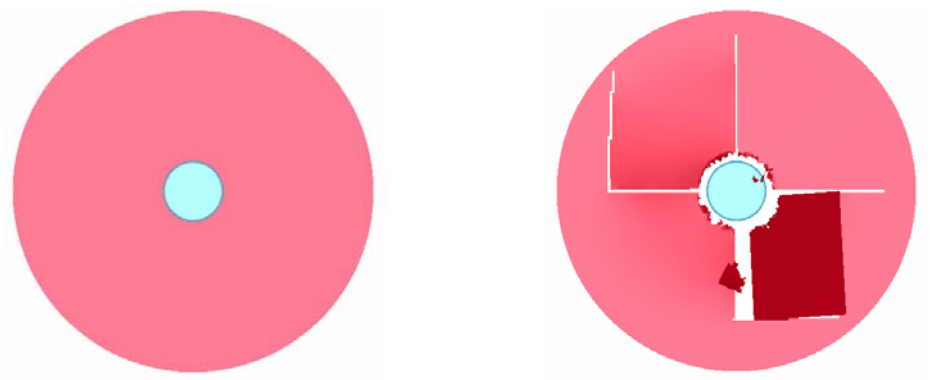

a. Initial b. End

Figure 8.7 Failure Mode for Drop Weight Impact Test Simulation at ambient temperature (FPS = 0.035, SLSFAC = 0.05) – Top View

8.3. Summary

As a summary to the chapter, the simulation results for the Drop Weight Impact test simulation model for ambient test temperature were presented. Iteration studies conducted were also included. The next chapter will be about the simulation of the Drop Weight Impact test conducted at 85°C.

9.0. Simulation and Experimental Results Comparison (Hot Temperature 85°C)

For the elevated test temperature at 85°C, the correlation was done by comparing the simulation results with 2 experimental results. The basic correlation criteria are highlighted in Figure 9.1. The peak load of the simulation model is aimed at a range in between both the experimental results. Therefore, the ±10% deviation error range was not applied for this set of simulation results.

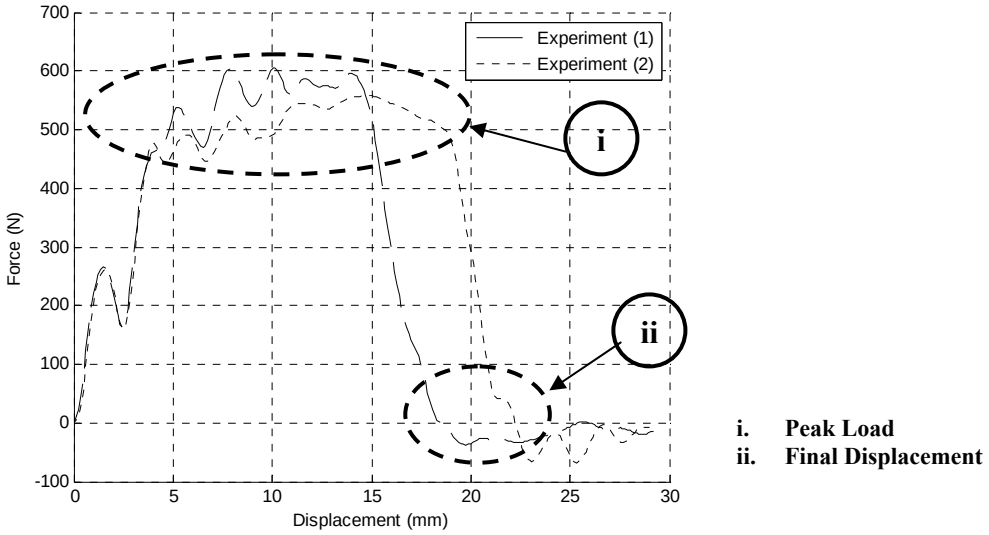

Figure 9.1 Force against Displacement plot for Drop Weight Impact test for DYLARK 480P16 at 85°C with basic correlation criteria

9.1. Preliminary Drop Weight Impact Test Simulation Results at 85°C

For the hot temperature test, a set of stress-strain curves for DYLARK 480P16 obtained through UNIAXIAL Tensile test at 85°C was provided by JCL. The stress-strain curves are plotted in Figure 9.2. By using the MATLAB script as attached in **Appendix C**, the stress-strain curves were converted into effective stress-effective plastic strain values. The effective stress-effective plastic strain curves for test temperature at 85°C are illustrated in Figure 9.3. The keyword file produced by the MATLAB script was imported into the simulation model as *Material 24*.

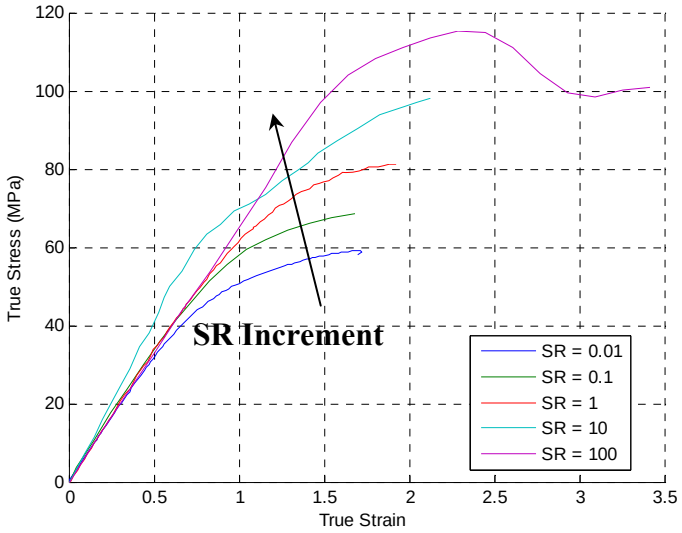

Figure 9.2 True Stress vs True Strain for DYLARK 480P16 at 85°C for various strain rates

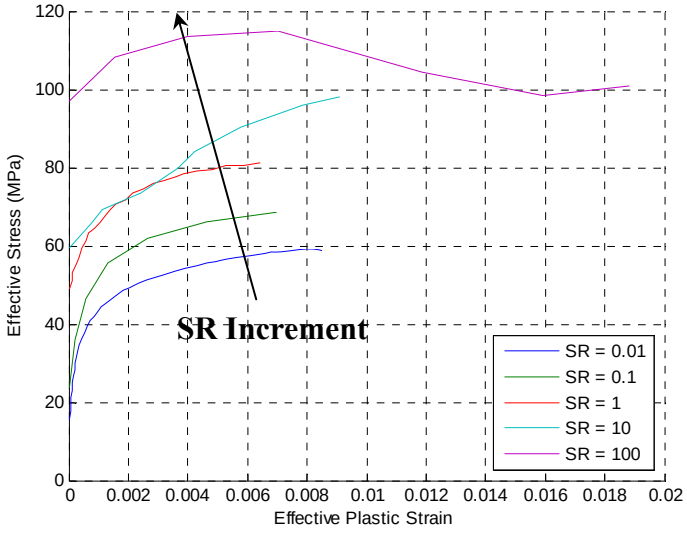

Figure 9.3 Effective Stress vs Effective Plastic Strain for DYLARK 480P16 at 85°C for various strain rates

Step 1: FPS Iteration

By using the effective stress-effective plastic strain values shown in Figure 9.3, the Drop Weight Impact test simulation model was simulated under various FPS values. The simulated results are shown in Figure 9.4.

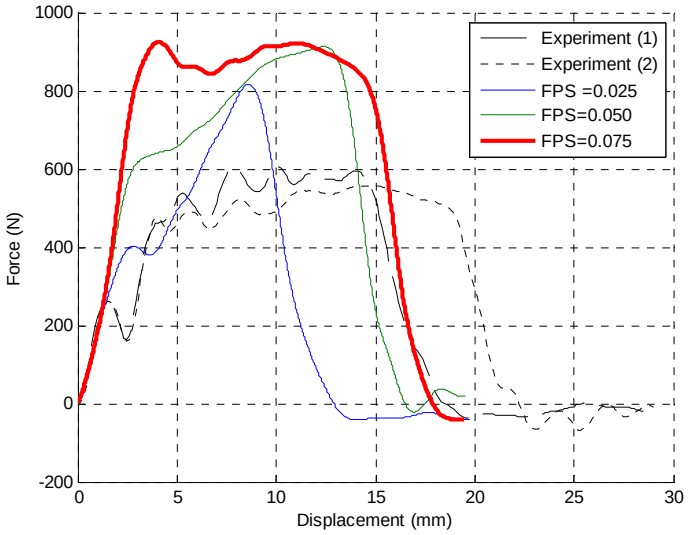

Figure 9.4 Force Vs Displacement plots for DYLARK 480P16 at 85°C with FPS variation

However, the simulated force-displacement curves using the stress-strain curves provided by JCL for the hot temperature test did not show a reasonable correlation in terms of peak load. The peak load for the curve which showed a reasonable curve shape correlation was at least 1.5 to 2 times higher than the ones produced through experimental testing.

Another noticeable problem with the stress-strain curves provided by JCL at 85°C was that the average modulus of elasticity is in the range of 6000MPa which is higher than the value at ambient temperature, 5117 MPa. The expected modulus of elasticity at hotter temperature should be lower than the one at ambient temperature as stated in the review covered earlier.

Based on the problems raised above, the stress-strain curves shown in Figure 9.2 were considered irrelevant. Therefore, to be able to simulate the Drop Weight Impact test at 85°C, the study reverted to scaling down the effective stress value of the ambient temperature material model based on the Eyring equation mentioned in the earlier review. The effective plastic strain values were assumed to remain the same.

9.2. Eyring Equation – DYLARK 480P16

To be able to scale down the effective stress of the ambient temperature stress-strain curve, the coefficients of the Eyring equation was computed for DYLARK 480P16. Firstly, the yield points for the ambient temperature stress-strain curves at various strain rates were computed based on the criterion set by ASTM D638M [4]. Then, the plot for σ_y/T against ln $\dot{\varepsilon}$ was obtained as shown in Figure 9.5.

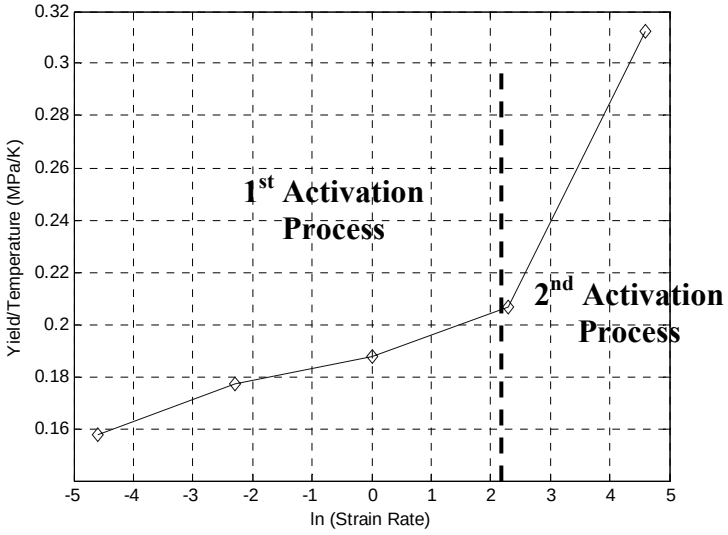

Figure 9.5 Plot of σ_y/T against ln $\dot{\varepsilon}$ for DYLARK 480P16 at ambient temperature

As it can be seen in Figure 9.5, the plot showed a second process of activation as mentioned in the reviews covered. Therefore, to be able to compute the coefficients for the Eyring equation with a second process of activation, the σ_y/T against ln $\dot{\varepsilon}$ plot was divided into 2 sections. The first and second process of activation plots are illustrated in Figure 9.6 and 9.7 respectively. The curves were curve fitted using a linear approximation. The linear curve fit equations for each of the activation process were included in each of the plots.

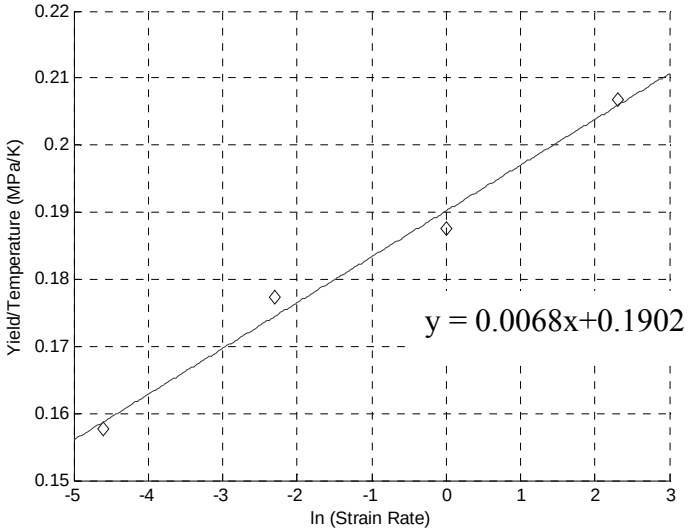

Figure 9.6 1st process of activation of the Eyring equation plot for DYLARK 480P16 at ambient temperature

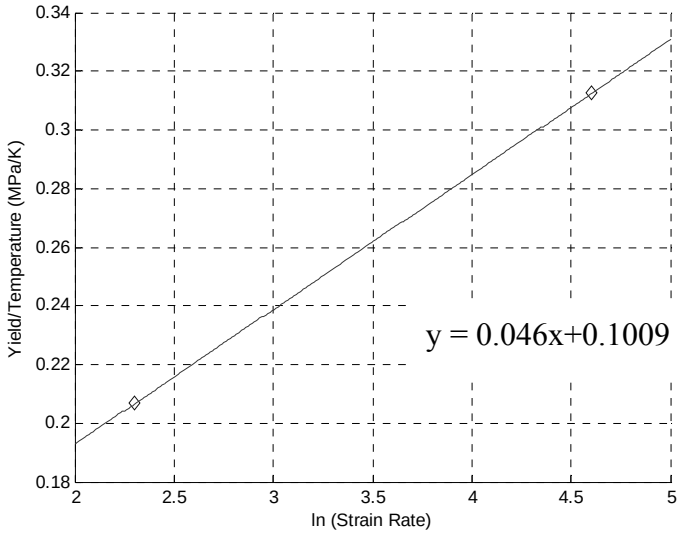

Figure 9.7 2nd process of activation of the Eyring equation plot for DYLARK 480P16 at ambient temperature

1st Activation Process of the Eyring Equation

Based on the calculation method discussed in Chapter 4.3, the coefficients of the Eyring equation for DYLARK 480P16 are tabulated in Table 9.1.

Table 9.1 Coefficients of Eyring Equation for the 1st activation process for DYLARK 480P16

	Eyring Coefficients	Value
1	$\frac{R}{v}$	0.0068
2	$\frac{\Delta H}{v}$	56.2992
3	$\ln \frac{2}{\dot{\varepsilon}_o}$	0.1779

By replacing the coefficients of the Eyring equation with the values computed in Table 9.1, the 1st activation process of the Eyring equation for DYLARK 480P16 is as shown below:

$$(\frac{\sigma_y}{T})_\alpha = [\ \frac{56.2992}{T} + 1.2097\times10^{-3} + 0.0068 \ln \dot{\varepsilon}\ ]$$

2nd Activation Process of the Eyring Equation

Based on the reviews done in Chapter 2.6, the additional component to the Eyring equation to represent the 2nd activation process is as shown below:

Eyring equation :- $$(\frac{\sigma_y}{T})_\beta = \frac{R}{\nu_2}\sinh^{-1}[\frac{\dot{\varepsilon}}{\dot{\varepsilon}_{02}}\exp\frac{\Delta H_2}{RT}]$$

By using the approximation approach for the 1st activation process, the coefficients for the remainder of the Eyring equation can be approximated as follow:

$$\frac{R}{\nu} = slope \quad ; \quad \frac{\Delta H}{R} = \frac{displacement}{slope} \times T$$

To be able to compute the remaining coefficient, the calculation steps below were followed.

Step 1:- $$\Delta_{\alpha\beta} = (\frac{\sigma_y}{T})_\beta - (\frac{\sigma_y}{T})_\alpha$$

Step 2:- $$\dot{\varepsilon}_{02} = \frac{\dot{\varepsilon}}{\sinh^{-1}[\frac{\Delta_{\alpha\beta}}{slope}]}\exp[\frac{displacement}{slope}]$$

By replacing the unknowns for the equations above, the coefficients for the additional component of the Eyring equation are as shown in Table 9.2.

Table 9.2 Coefficients of Eyring Equation for the 2nd activation process for DYLARK 480P16

	Eyring Coefficients	Value
1	$\frac{R}{\nu}$	0.0046
2	$\frac{\Delta H}{R}$	649.2760
3	$\dot{\varepsilon}_{02}$	245.3319

The Eyring equation for the 2nd process of activation is as shown below:

$$(\frac{\sigma_y}{T})_\beta = 0.0046 \sinh^{-1}[\frac{\dot{\varepsilon}}{245.3319}\exp^{\frac{649.2760}{T}}]$$

By substituting all the coefficients shown in Table 9.1 and Table 9.2 into the full Eyring equation which comprises of a 1st and 2nd activation process, the equation as follows can be obtained:

$$(\frac{\sigma_y}{T}) = [\frac{56.2992}{T} + 1.2097\times10^{-3} + 0.0068 \ln \dot{\varepsilon}\ ] + 0.0046 \sinh^{-1}[\frac{\dot{\varepsilon}}{245.3319}\exp^{\frac{649.2760}{T}}]$$

The equation shown above can be used to compute the value of σ_y/T for any temperature and strain rates. As a validation for the accuracy of the equation above, the equation above was used to curve fit the experimental data for DYLARK 480P16 at ambient temperature. The curve fit plot is illustrated in Figure 9.8.

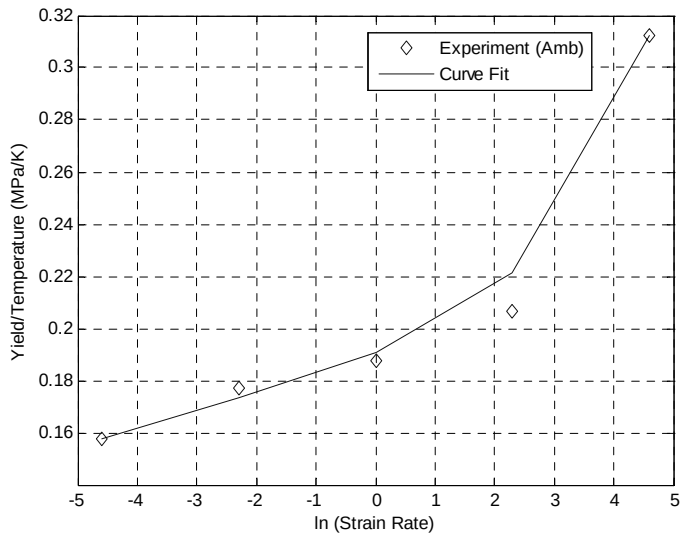

Figure 9.8 Plot of σ_y/T against ln $\dot{\varepsilon}$ for DYLARK 480P16 at ambient temperature with curve fitting using Eyring Equation

The Eyring equation was then used to extrapolate the curve of σ_y/T - ln $\dot{\varepsilon}$ for temperatures 85°C and -40°C. The plot for the extrapolated curves is shown in Figure 9.9.

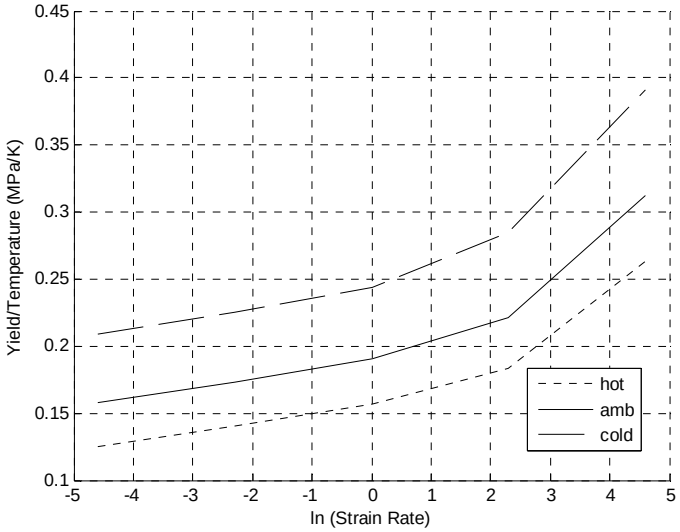

Figure 9.9 Plot of σ_y/T against ln $\dot{\varepsilon}$ for DYLARK 480P16 with curve fitting using Eyring Equation for various test temperatures

In order to scale the effective stress of DYLARK 480P16 for other temperatures using the ambient temperature as the reference point, the equation as follow was used:

$$SC = \frac{\left(\sigma_y / T\right)_2}{\left(\sigma_y / T\right)_{amb}}$$

With

SC = Scaling Coefficient
Notation 2 = Required Temperature

As the effective stress for a UNIAXIAL Tensile test is equivalent to the true stress, the SC can be applied directly to the effective stress values. The values for σ_y/T are calculated using the Eyring equation. The SC for 85°C at various strain rates is tabulated in Table 9.3. However, the SC for each of the strain rates varies. To avoid confusion of having various SC for different strain rates, an average value of SC was used for the simulation model instead. The SC was applied only to the effective yield stress of the curves shown in Figure 7.5.

Table 9.3 SC of Effective Stress for temperature 85°C

	$\dot{\varepsilon}$ (1/s)	ln $\dot{\varepsilon}$	σ_y/T (MPa/K)	SC	SC_{Ave}
1	0.01	-4.6056	0.1247	0.7915	
2	0.1	-2.3028	0.1405	0.8103	
3	1	0.0000	0.1572	0.8248	
4	10	2.3028	0.1831	0.8281	
5	100	4.6056	0.2631	0.8417	
					0.82

9.3. Drop Weight Impact Test Simulation Results at 85°C based on Ambient Temperature material model

Step 1: FPS Iteration (SC = 0.82)

By using the average SC of 0.82 computed in Table 9.3, the effective stresses for various strain rates in *Material 24* used for the ambient temperature simulation were scaled down. The modified material model was used to simulate the Drop Weight Impact test at 85°C for various FPS values. The simulated force-displacement curves are presented in Figure 9.10.

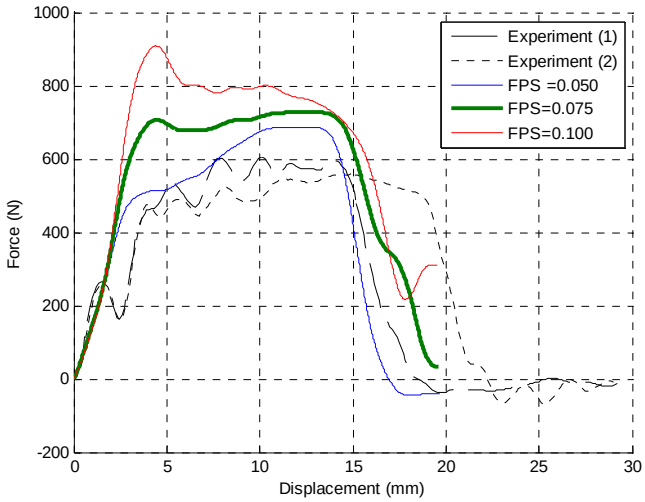

Figure 9.10 Force Vs Displacement plot comparison for DYLARK 480P16 at 85°C with various FPS (SC = 0.82)

Step 2: SC Iteration

As it can be seen in Figure 9.10, the best correlation obtained for SC = 0.82 was by using an FPS value of 0.075. However, the peak load was still too

large as compared to the experimental values. Therefore, an iterative study was carried out on the SC values. The results of using a variation of SC values are shown in Figure 9.11.

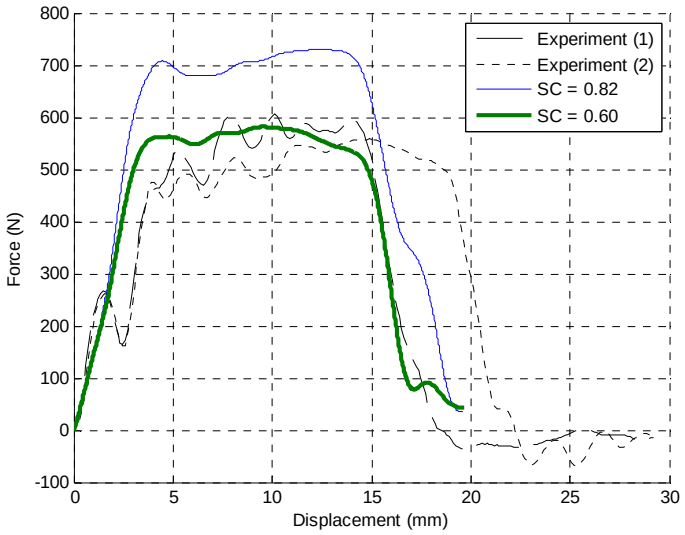

Figure 9.11 Force Vs Displacement plot comparison for DYLARK 480P16 at 85°C with various SC (FPS = 0.075)

By reducing the SC down to 0.60, the simulated force-displacement curve showed an improved correlation as compared to previous simulation results. The peak load was reduced to a range in between both the experimental results. Based on the simulation observation, the SC of 0.6 can be obtained by adding a correction factor as shown in the equation below:

$$SC_{\text{mod}} = \frac{\left(\sigma_y / T\right)_2}{\left(\sigma_y / T\right)_{amb}} - \underbrace{\left|\frac{T_2 - T_{amb}}{T_{amb}}\right|}_{\text{Correction Factor}}$$

Correction Factor

Step 3: FPS Iteration (SC = 0.60)

By using the SC of 0.60, the Drop Weight Impact test was simulated for various FPS values. The effect of varying FPS values is represented in Figure 9.12.

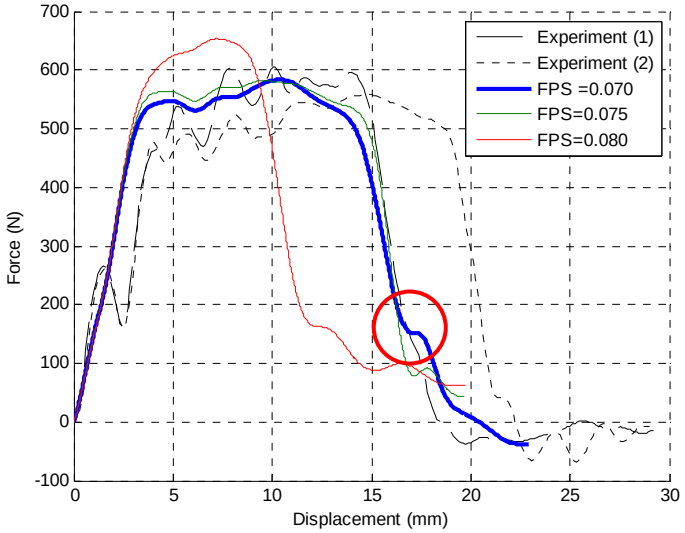

Figure 9.12 Force Vs Displacement plot comparison for DYLARK 480P16 at 85°C with various FPS (SF = 0.60)

Through observation, the force-displacement curve for FPS = 0.070 showed a better curve shape correlation than the rest of the simulated curves as highlighted in Figure 9.12.

Step 4: Modulus of Elasticity for DYLARK 480P16 at 85°C

Up till this stage, the only modification done on *Material 24* meant for ambient temperature was to scale the effective stress. The simulations covered above were done using the modulus of elasticity obtained at ambient temperature. This is not the actual situation as the modulus of elasticity is also temperature dependent.

To be able to estimate the modulus of elasticity for 85°C, the stress-strain curves for DYLARK 480P16 at ambient temperature were modified based on the modified SC. The modified stress-strain curves were also adjusted to obtain the yield stress computed using the modified SC based on ASTM D638M [4].

The stress-strain curve for SR = 0.01 for 85°C were plotted in Figure 9.13 as comparison to the curve at ambient temperature. The modified stress-strain curves for various strain rates at 85°C are shown in Figure 9.14.

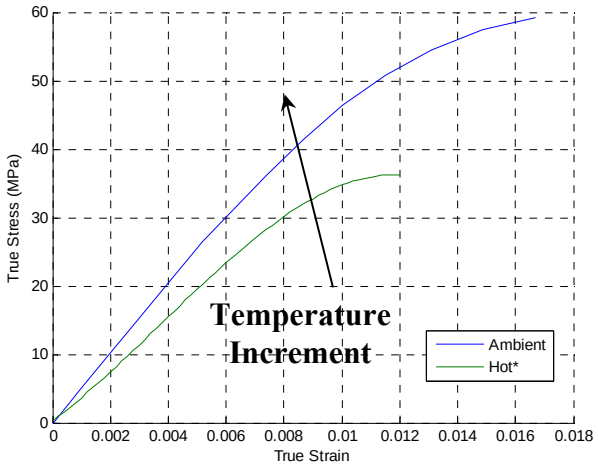

Figure 9.13 True Stress-True Strain curve for DYLARK 480P16 at different temperatures (SR = 0.01)

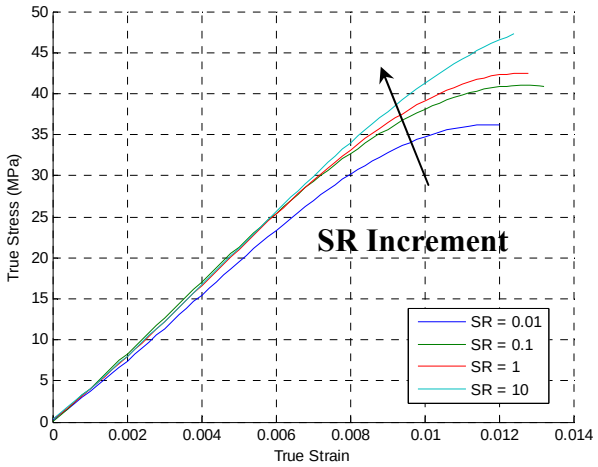

Figure 9.14 True Stress-True Strain curve for DYLARK 480P16 with various strain rates at 85°C

Based on the stress-strain curves in Figure 9.14, the modulus of elasticity computed is 4094 MPa. The new modulus of elasticity was then used to simulate the Drop Weight Impact test model. The simulated results are shown in Figure 9.15 showing the effect of changing the modulus of elasticity.

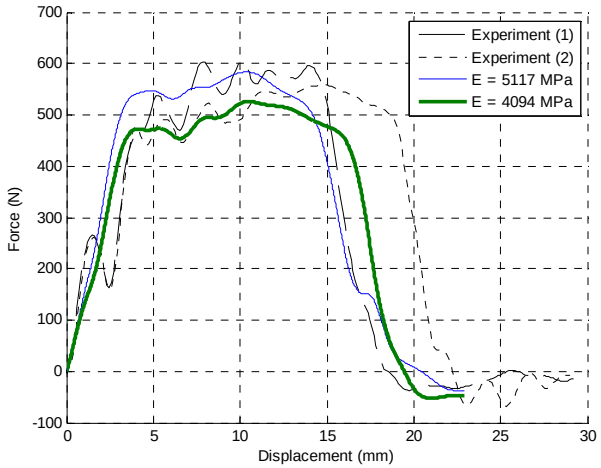

Figure 9.15 Force Vs Displacement plot comparison for DYLARK 480P16 at 85°C with different Modulus of Elasticity (FPS = 0.070, SC = 0.60)

Step 5: Curve Shape Correlation

The main focus for the curve shape correlation for this set of simulation results was focused on the peak load region. The curve for the simulation result using FPS = 0.070 and SC = 0.60 showed reasonable curve shape correlation as compared to the experimental results. The correlation is highlighted in Figure 9.16.

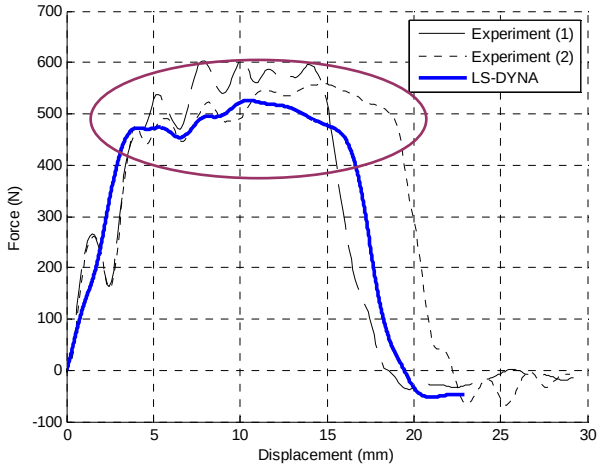

Figure 9.16 Force Vs Displacement plot comparison for DYLARK 480P16 at 85°C indicating shape correlation regions (FPS = 0.070, SC = 0.60)

By looking at the unfiltered force-displacement curve of the same simulation model, a curve shape correlation was observed at the beginning of the curve. The curve shape correlation is shown in Figure 9.17.

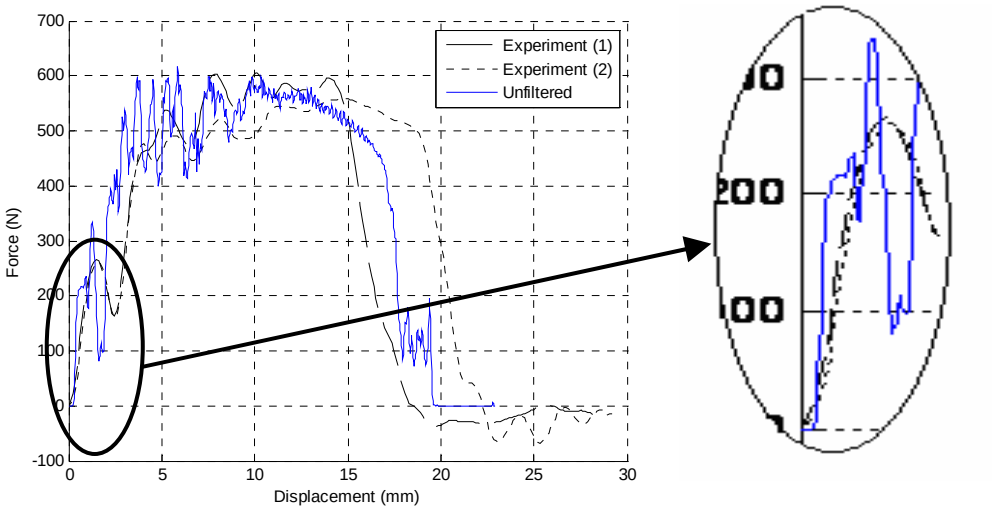

Figure 9.17 Force Vs Displacement plot comparison for DYLARK 480P16 at 85°C indicating shape correlation region (Unfiltered Simulation Data- FPS = 0.070, SC = 0.60)

Step 6: Element Formulation Variation

The ELFORM for the simulation model of the Drop Weight Impact test at 85°C were put to the reliability test. The simulated results shown up till now for the test at hot temperature were conducted using the default ELFORM. For a complete ELFORM, the FISE formulation was used for this simple study. The simulated force-displacement curves are presented in Figure 9.18.

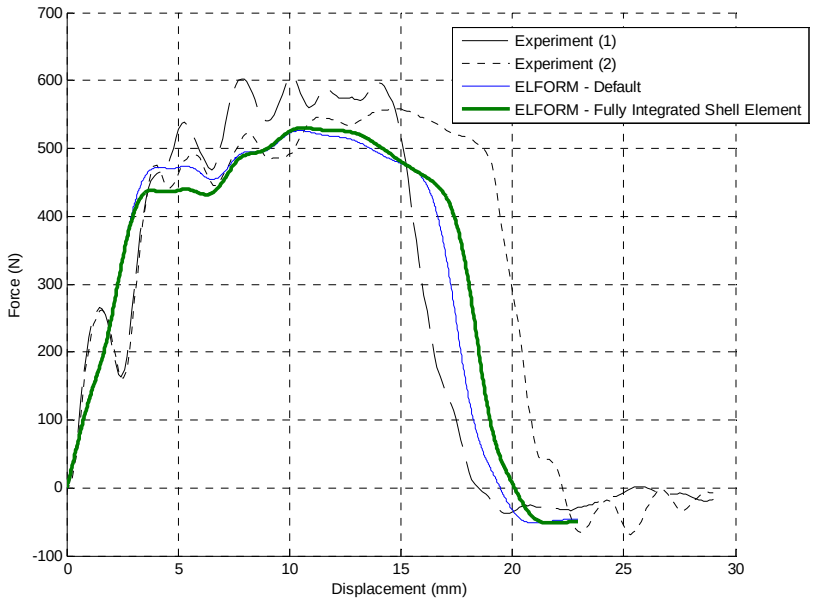

Figure 9.18 Force Vs Displacement plot comparison for DYLARK 480P16 at 85°C with ELFORM variation (FPS = 0.070, SC = 0.60)

Through observation, it can be seen that the filtered result obtained using the FISE formulation did not differ too much from the results produced using the default ELFORM. The numerical comparison of the experimental and simulation method using various ELFORM is tabulated in Table 9.4.

Table 9.4 Experimental and Simulation results comparison for basic correlation parameters at 85°C (Various ELFORM)

	Parameter	Experimental (Test 1/Test2)	Default	FISE
1	Peak Load (N)	605.40/558.00	526.40	531.40
2	Displacement @Peak Load (mm)	10.14/14.89	10.52	10.45
3	Final Displacement @Zero Load (mm)	18.55/22.24	19.45	20.29

9.4. Final Simulation Model Parameter – Hot Temperature

From the iterative study discussed above, the final simulation parameters for the test conducted at 85°C are summarized in Table 9.5. As the correlation was carried out by comparing 2 sets of experimental data, it was not possible to determine the error range for the basic correlation criteria set. Therefore, no values of error for the correlation criteria were computed as shown in Table 9.6. The failure mode for the simulation model based on the parameters tabled in Table 9.5 is illustrated in Figure 9.19.

Table 9.5 Final Simulation Parameter for Drop Weight Impact test Simulation Model for DYLARK 480P16 at 85°C

	Temperature (°C)	FPS	SC	Modulus of Elasticity (MPa)	ELFORM
1	85	0.070	0.60	4094	Default/FISE

Table 9.6 Experimental and Simulation results comparison for basic correlation parameters for 85°C

	Parameter	Experimental (Test 1/Test 2)	LS-DYNA	Offset Error (%)
1	Peak Load (N)	605.40/558.00	526.40	-
2	Displacement @Peak Load (mm)	10.14/14.89	10.52	-
3	Final Displacement @Zero Load (mm)	18.55/22.24	19.45	-

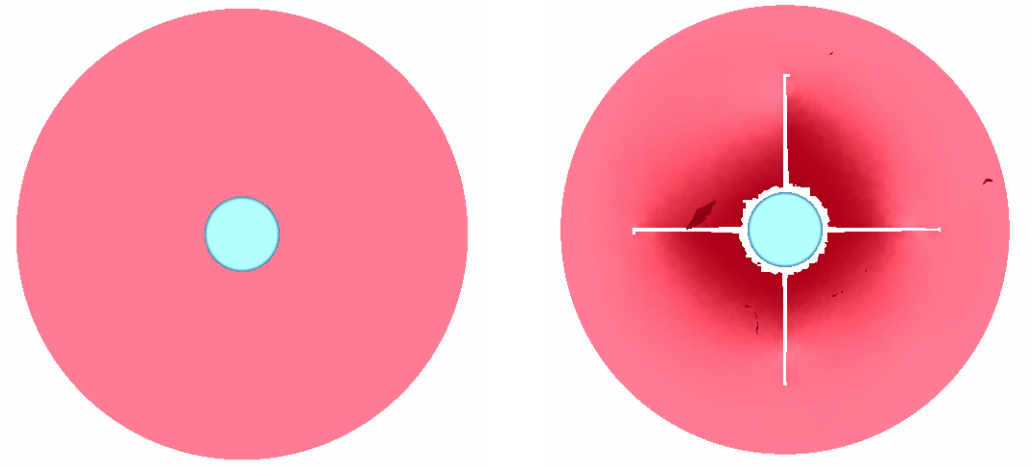

a. Initial b. End

Figure 9.19 Failure Mode for Drop Weight Impact Test Simulation at 85°C (FPS = 0.070, SC = 0.60, E = 4094MPa) – Top View

9.5. Drop Weight Impact Test Simulation at 85°C using Approximated Stress-Strain Curve based on Eyring Equation

As shown in Figure 9.14, the stress-strain curve of up to SR = 10/s for 85°C was approximated based on the Eyring equation. The curves were converted into effective values for stress and plastic strain using the Matlab script as attached in **Appendix C**. Due to the lack of data in approximating the actual stress-strain curve at 85°C for SR =100/s, the data used were scaled down using SC = 0.60 based on the ambient temperature curve. The purpose of running this set of simulation was to validate the approximated stress-strain curves at 85°C.

The simulated force-displacement curve for the approximated data is shown in Figure 9.20. The simulation result using the approximated data showed graphical similarity in terms of curve shape correlation. The iterative study and numerical comparison for the simulation are attached in **Appendix G.**

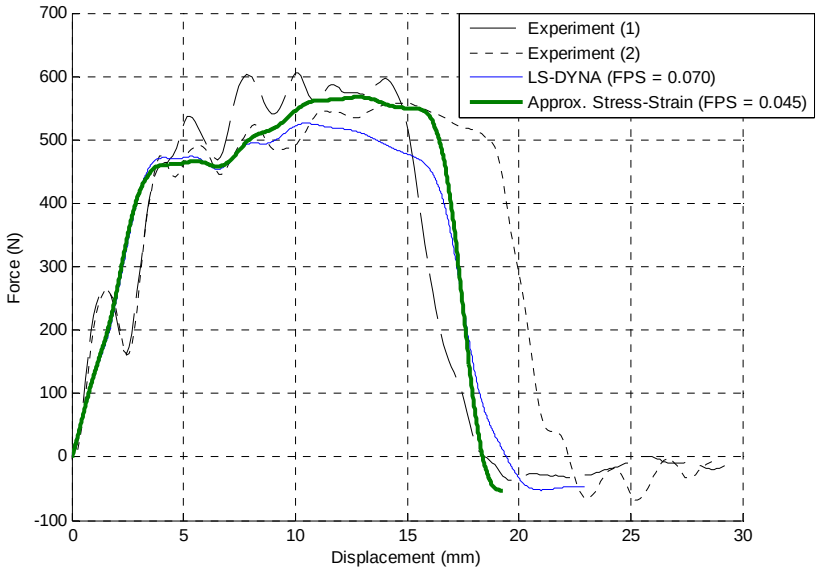

Figure 9.20 Force Vs Displacement plot comparison for DYLARK 480P16 at 85°C using Approximated Stress-Strain Curves

9.6. Summary

The chapter covered an iterative study on the correlation of the Drop Weight Impact test simulation conducted at 85°C. The chapter also discussed on the application of the Eyring equation in modifying the ambient temperature stress-strain parameters to approximate the ones at 85°C. The following chapter will present on the simulation model of the Drop Weight Impact test at -40°C.

10.0. Simulation and Experimental Results Comparison (Cold Temperature -40°C)

For the test conducted at -40°C, the same initial step was taken as the ones for ambient temperature and 85°C, which is by defining the basic correlation criteria as shown in Figure 10.1.

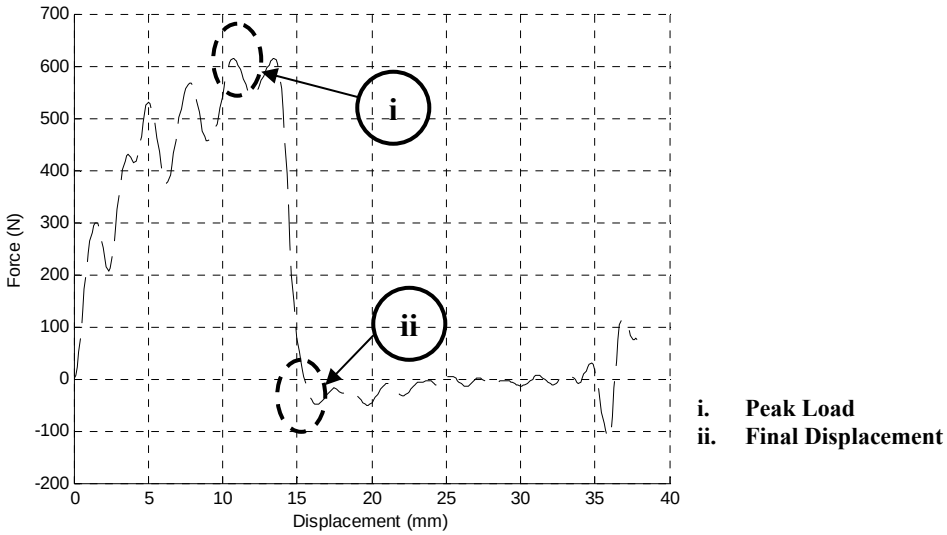

Figure 10.1 Force against Displacement plot for Drop Weight Impact test for DYLARK 480P16 at -40°C with basic correlation criteria

10.1. Preliminary Drop Weight Impact Test Simulation Results at -40°C

Before proceeding to the simulation of the test, the modified SC of the Eyring equation for -40°C was calculated as shown in Table 10.1. The average value of the modified SC was then used to scale up the effective stress at ambient temperature to approximate the stress value at -40°C. The SC was applied only to the effective yield stress of the curves shown in Figure 7.5.The LS-DYNA model for the test at this temperature was then tried out for various FPS values. The resultant plots are illustrated in Figure 10.2.

Table 10.1 SC of Effective Stress for temperature 85°C

	$\dot{\varepsilon}$	ln $\dot{\varepsilon}$	σ_y/T (MPa/K)	Modified SC	Modified SC_{Ave}
1	0.01	-4.6056	0.2091	0.1576	
2	0.1	-2.3028	0.2251	0.1734	
3	1	0.0000	0.2435	0.1906	
4	10	2.3028	0.2846	0.2211	
5	100	4.6056	0.3908	0.3126	
					1.07

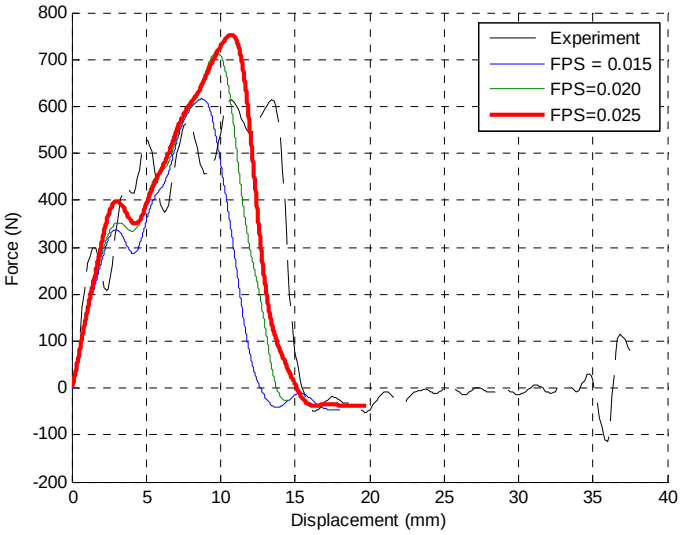

Figure 10.2 Force Vs Displacement plots for DYLARK 480P16 at -40°C with FPS variation (SC = 1.07)

It can be seen in Figure 10.2 that the best correlation for the force-displacement curve was for the FPS value of 0.025. However, the peak load produced using this FPS value was too large as compared to the experimental value which was 614.2 N.

By looking back at the review covered in Chapter 2 on the effect of temperature and strain rate on a plastic material, it was said that the behavior of the material will change from ductile to brittle as the material temperature is decreased till sub zero conditions. For brittle behavior, there will be no plastic deformation. Hence, there will be no effective plastic strain value.

As there was no test data to determine the point of behavior change for the DYLARK 480P16 at -40°C, an iterative study was carried out by removing the higher strain rates of the scaled effective stress-effective plastic strain for -40°C one by one to attempt to achieve a reasonable correlation for the Drop Weight Impact test. The force-displacement plots of the iteration study are shown in Figure 10.3.

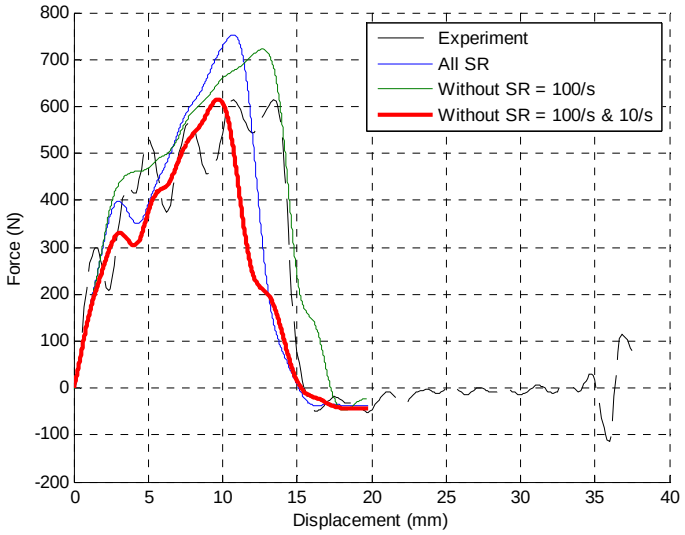

Figure 10.3 Force Vs Displacement plots for DYLARK 480P16 at -40°C with SR set variation (FPS = 0.025)

By observing the plots shown in Figure 10.3, the effect of removing the parameters for higher SR was very obvious. The best correlation for force-displacement curve was achieved by removing SR = 100/s and 10/s. It can be seen that the peak load and the final displacement showed reasonable correlation to the experimental values.

10.2. Final Simulation Model Parameter – Cold Temperature (Without SR = 100/s & 10/s)

By running a detailed iterative study as attached in **Appendix H**, the final simulation parameters for the model tested -40°C are summarized in Table 10.2. The simulated force-displacement plot based on these parameters is shown in Figure 10.4.

Table 10.2 Final Simulation Parameter for Drop Weight Impact test Simulation Model for DYLARK 480P16 at -40°C

	Temperature (°C)	FPS	SC	Modulus of Elasticity (MPa)	ELFORM
1	-40	0.030	1.07	5594	Default

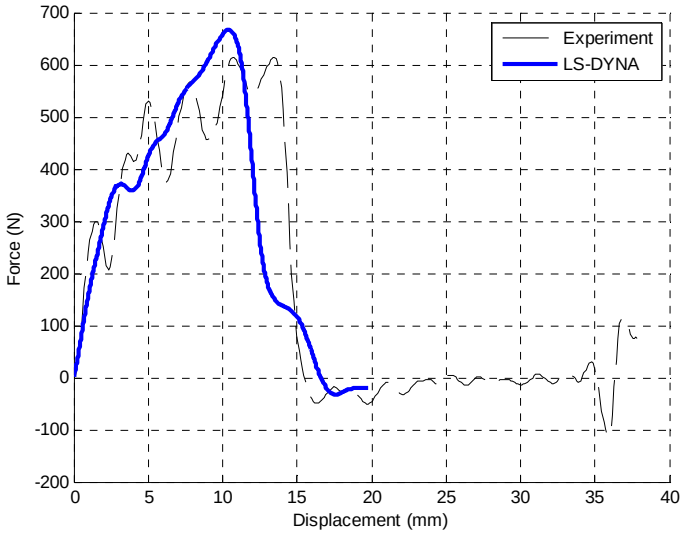

Figure 10.4 Force Vs Displacement plot comparison for DYLARK 480P16 at -40°C (FPS = 0.030, SC = 1.07, E=5549 MPa)

For the numerical comparison of the basic correlation criteria, the computed error values are presented in Table 10.3. The highest error value was for the peak load with a value of 8.55%. The lowest or best correlated criterion was the displacement at peak load, which was 2.43% error of deviation. The failure mode of this simulated model for the Drop Weight Impact test is shown in Figure 10.5.

Table 10.3 Experimental and Simulation results comparison for basic correlation parameters for -40°C

	Parameter	Experimental	LS-DYNA	Offset Error (%)
1	Peak Load (N)	614.2	666.70	8.55
2	Displacement @Peak Load (mm)	10.69	10.43	2.43
3	Final Displacement @Zero Load (mm)	15.48	16.61	7.30

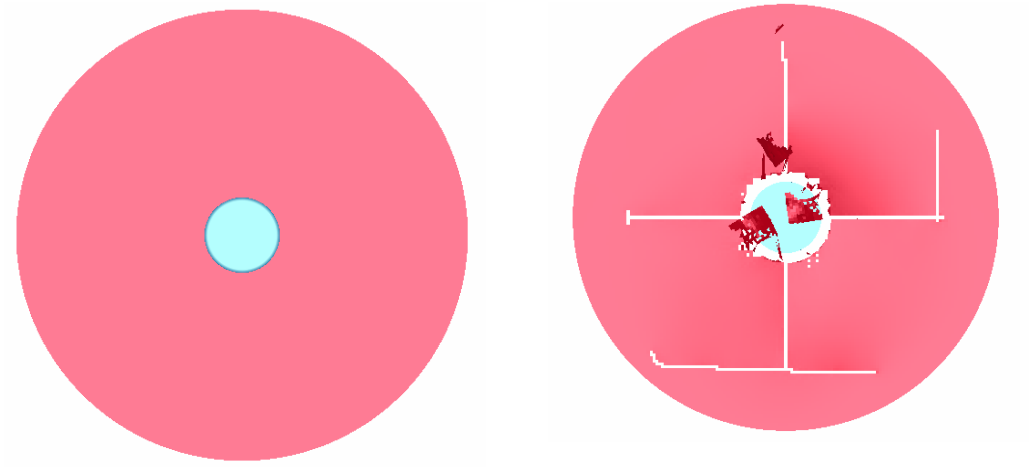

a. Initial b. End

Figure 10.5 Failure Mode for Drop Weight Impact Test Simulation at -40°C (FPS = 0.030, SC = 1.07, E = 5549MPa) – Top View

However, according to JCL, the standard SR values for a material model used by them should have at least a SR value of up to 10/s. Therefore, to be able to comply with the needs of JCL, a detailed iterative study was carried out for the material model by removing only SR = 100/s.

10.3. Final Simulation Model Parameter – Cold Temperature (Without SR = 100/s)

By running iterative studies as attached in **Appendix I**, the final simulation parameters for this set of simulation are tabulated in Table 10.4. The resultant force-displacement curve using the tabulated parameters is illustrated in Figure 10.6.

Table 10.4 Final Simulation Parameter for Drop Weight Impact test Simulation Model for DYLARK 480P16 at -40°C

	Temperature (°C)	FPS	SC	Modulus of Elasticity (MPa)	ELFORM
1	-40	0.0175	1.07	5594	Default

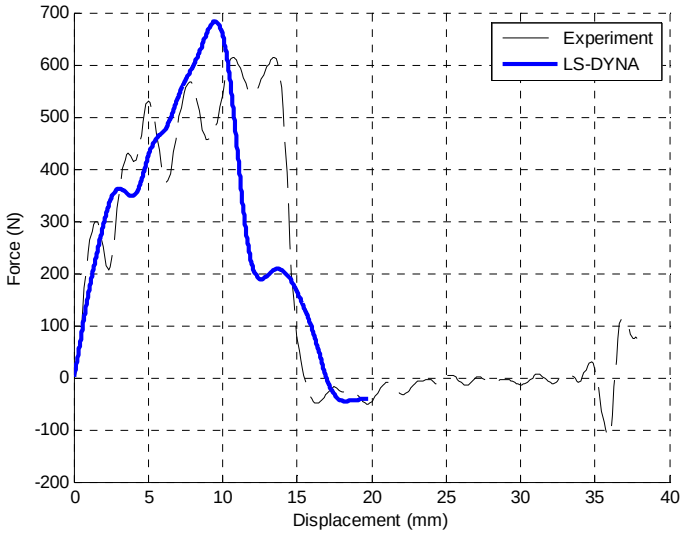

Figure 10.6 Force Vs Displacement plot comparison for DYLARK 480P16 at -40°C (FPS = 0.0175, SC = 1.07, E=5549 MPa)

The numerical comparison of the basic correlation criteria is presented in Table 10.5. The best possible error deviation values for simulation model by removing SR = 100 exceeded the ±10% deviation range set for the study by an estimated 1%. The failure mode for this set of simulation is presented in Figure 10.7.

Table 10.5 Experimental and Simulation results comparison for basic correlation parameters for -40°C

	Parameter	Experimental	LS-DYNA	Offset Error (%)
1	Peak Load (N)	614.2	682.1	11.06
2	Displacement @Peak Load (mm)	10.69	9.53	10.85
3	Final Displacement @Zero Load (mm)	15.48	16.95	9.50

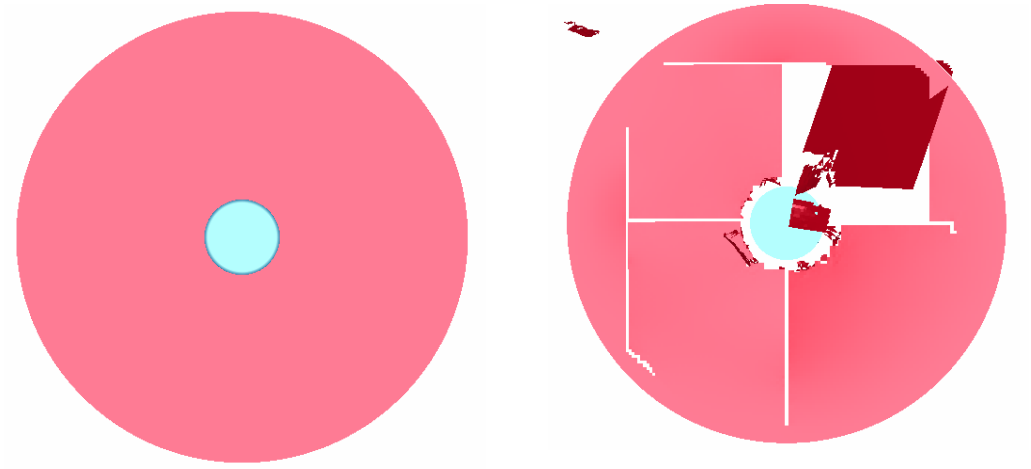

a. Initial b. End

Figure 10.7 Failure Mode for Drop Weight Impact Test Simulation at -40°C (FPS = 0.0175, SC = 1.07, E = 5549MPa) – Top View

10.4. Drop Weight Impact Test Simulation at -40°C using Approximated Stress-Strain Curve based on Eyring Equation

As the stress-strain curves for -40°C were also approximated as shown in **Appendix H**, a study was conducted to verify the validity of the approximation. The simulation results produced using the approximated curves for both the SR sets showed a correlation to the simulation results obtained using the scaled stress-strain curves. The iterative studies and numerical comparisons for the simulations are attached in **Appendix J**.

10.5. Summary

The chapter covered the correlation for the simulation results for the Drop Weight Impact Test at -40°C. The chapter covered the application of the Eyring equation in scaling the stress-strain parameters at ambient temperature to -40°C. The chapter also considered the effect of removing higher strain rate data of *Material 24* onto the dynamic response of the Drop Weight Impact simulation model.

11.0. Discussion

11.1. Discussion based on Deliverable 1

Correlation of strain rate and temperature effect on the stress-strain behavior of DYLARK 480P16 through the Eyring equation

The Eyring equation in the function of temperature as shown below was used to relate the strain rate and temperature effect on the stress-strain behavior of DYLARK 480P16. The equation showed good correlation to the stress-strain data provided by JCL at ambient temperature as shown in Figure 9.8.

$$\left(\frac{\sigma_y}{T}\right) = \left[\frac{56.2992}{T} + 1.2097\times10^{-3} + 0.0068 \ln \dot{\varepsilon}\right] + 0.0046 \sinh^{-1}\left[\frac{\dot{\varepsilon}}{245.3319}\exp^{\frac{649.2760}{T}}\right]$$

However, the derivation of the equation was based solely on the stress-strain data at ambient temperature. To further increase the level of confidence of the Eyring equation for DYLARK 480P16, stress-strain data for the material should be obtained at various temperatures. The data will provide concrete validation to the equation.

The 2nd process of activation of the Eyring equation was derived based only on yield points obtained for two values of strain rates. This might not produce an accurate approximation for the equation. In order to increase the accuracy of the approximation, more data should be obtained for higher strain rates.

11.2. Discussion based on Deliverable 2

Stress-strain behavior of LEXAN EXL1414H through UNIAXIAL Tensile Test

The UNIAXIAL Tensile test was supposed to be done to obtain the stress-strain parameters for DYLARK 480P16. However, due to the difficulty in obtaining the material, a replacement material, LEXAN EXL1414H was used. The material model for DYLARK 480P16 was provided by JCL.

For the UNIAXIAL Tensile test, the stress-strain behavior of the replacement model, LEXAN EXL1414H was observed when the crosshead test velocity was varied. As the crosshead test velocity was increased, the strain rate of the test was increased. When the strain rate was increased, the stress values of the material were increased as shown in Figure 4.8. The stress-strain behavior obtained through the study showed consistent agreement with the reviews shown in Figure 2.3 and 2.4.

As the test was conducted using an extensometer, the strain of the material could only be measured up to 6% strain. The strain data was not enough to be used to accurately estimate the strain rate. For the study, the strain of the material was assumed to behave linearly in respect to the time of strain measurement till the test piece breaks. To be able to improve the accuracy of the strain rate estimation, a high speed camera capturing the elongation of the test piece could be used. By using the high speed camera, the strain of the material can be measured till it breaks.

Dynamic behavior of DYLARK 480P16 through Drop Weight Impact Test

The Drop Weight Impact test was conducted at different temperatures. Theoretically, the peak load for test temperature -40^{o}C is expected to be higher than the one of the ambient temperature. However, the test results showed otherwise as can be seen in Figure 5.5. The reason for the lower peak load might be due to the change of material behavior from ductile to brittle. This means that the material might have already exceeded the ductile-brittle transition point for the material at -40^{o}C. This was the basis of the removal of stress-strain parameters at higher strain rates.

11.3. Discussion based on Deliverable 3

Validation of FE model through experimental test results for a Drop Weight Impact test on DYLARK 480P16 using LS-DYNA

For the Drop Weight Impact test simulation on DYLARK 480P16, an accurate and reliable stress-strain behavior of the material should be prepared. Besides this, the Failure Plastic Strain (FPS) parameter showed significant effect on the dynamic response of the model. The correlation of the simulation model for the ambient temperature was achieved by fine tuning the FPS value.

For test temperature 85^{o}C and -40^{o}C, the stress parameter for *Material 24* was scaled using the modified SC derived from the Eyring equation as shown below. The SC used the ambient temperature data as the basis for scaling the stress value at the desired temperature. The additional correction factor meant that the behavior of the DYLARK 480P16 did not comply fully with the Eyring equation which is derived based on glassy polymers. This is most probably due to the fact that the DYLARK 480P16 is a type of reinforced plastic.

$$SC_{\text{mod}} = \frac{(\sigma_y / T)_2}{(\sigma_y / T)_{amb}} - \underbrace{\left| \frac{T_2 - T_{amb}}{T_{amb}} \right|}_{\text{Correction Factor}}$$

For -40°C, higher strain rate data were removed by assuming that the material had surpassed the ductile-brittle transition point. However, the correlation based on the minimum requirements set by JCL for having strain rates of up to 10/s is just at a barely acceptable range. Improvements on the simulation model can be achieved by further detailing the iterative study.

A correlation of the force-displacement curve was obtained using this scaling coefficient shown above besides the fine tuning of the FPS value. However, the scaling was done with the assumption than there were no changes to the strain when the test temperature changes. In fact, the strain value at failure at different test temperature varies. This might affect the simulated final displacement of the model.

The simulated failure modes for the Drop Weight Impact Test simulation were illustrated in Figure 8.7 (ambient temperature), Figure 9.19 (85°C), Figure 10.5 and 107 (-40°C). The simulated failure for ambient temperature and -40oC can be considered to be of brittle failure. At 85oC, the impactor can be seen to punch through the test plaque without shattering the plaque. The type of failure is categorized as ductile failure.

The failure modes showed agreement to the behavior of plastic materials where the material will become more brittle as the material temperature is reduced and vice versa. However, for further validation, actual failure modes at various test temperatures should be used as comparison.

11.4. Summary

As a summary, the chapter included the discussions based on the research deliverables. The next chapter will conclude the findings of the study.

12.0. Conclusion

Based on the reviews covered, the effects of strain rate and temperature on plastic material can cause a shift in stress-strain curve of that material as shown in Figure 2.3 and 2.4. The test data produced for the LEXAN EXL1414H and DYLARK 480P16 showed agreement to the stress-strain shift due to the change of strain rates.

The Eyring equation was used to correlate the strain rate effects on LEXAN EXL1414H and DYLARK 480P16 at ambient temperature. The equation provided a reasonable curve fit to the experimental data as shown in Figure 4.11 for LEXAN EXL1414H and Figure 9.8 for DYLARK 480P16. The equation was generalized in the function of temperature and can be used to predict the behavior of the material at various temperatures.

A review on existing material models suitable for plastic materials in LS-DYNA was covered. Based on the review, *Material 24* and *Material 187* are the two most common and suitable material models used to model a plastic material in LS-DYNA. *Material 187* is developed purely for polymer materials while *Material 24* is originally developed for metallic materials.

However, the simulation results obtained in the study by using *Material 24* showed reasonable correlation to the characteristics of plastic materials. The critical parameter of *Material 24* required for simulating the dynamic behavior of DYLARK 480P16 based on the Drop Weight Impact test is the Failure Plastic Strain (FPS) value. To simulate the dynamic behavior of the material at various temperatures, a Scaling Coefficient (SC) derived based on the Eyring equation for DYLARK 480P16 was used to scale the yield stress. The SC used for the simulation models for different test temperatures produced reasonable correlation to experimental data.

As a conclusion in all, the dynamic properties of DYLARK 480P16 for an FE analysis were simulated based on an empirical method. The dynamic properties of DYLARK 480P16 for an FE analysis can be obtained by fine tuning the Failure Plastic Strain (FPS) values of *Material 24* . As for various test temperatures, the dynamic properties of DYLARK 480P16 can be simulated by applying the Scaling Coefficient (SC) derived from the Eyring equation on the ambient temperature.

12.1. Recommendations for future work

As recommendations for future work, further studies can be done on:

i. The detailed application of the Eyring equation in developing an improved material model for plastic materials for dynamic situations

ii. Further validation and application of the scaling coefficient derived based on the Eyring equation using the stress-strain data at ambient temperature in predicting the dynamic behavior of plastic material for various test temperatures

iii. The application and validation of the material model parameters obtained for the study on an actual automotive plastic component simulation

13.0. References

[1] WT Li, Plastic Designs, China Daily. Business Weekly (2007) pg 6.

[2] Society of Automotive Engineers., Plastics in the automotive industry, SAE International ; Woodhead, Warrendale, Pa. : Cambridge, 1994.

[3] ER Johnston, FP Beer, Mechanics of materials, 2nd ed. in SI units. ed., McGraw-Hill, London, 1992.

[4] American Society of Testing and Materials (ASTM). ASTM D638M Standard Test Method for Tensile Properties of Plastics (Metric), (1993).

[5] LSTC, Effective Plastic Strains, (2004).

[6] C Bauwens-Crowet, J Bauwens, G HomÃ¨s. The temperature dependence of yield of polycarbonate in uniaxial compression and tensile tests, J.Mater.Sci. 7 (1972) 176-183.

[7] LE Nielsen, Mechanical properties of polymers and composites., Dekker, New York, 1974.

[8] S Kolling, A Haufe, M Feucht, PA Du Bois. SAMP-1 : A Semi-Analytical Model for the Simulation of Polymers, (2005) A-II-27-A-II-52.

[9] LE Nielsen, Mechanical properties of polymers and composites., Dekker, New York, 1974.

[10] GM Swallowe, Mechanical properties and testing of polymers : an A-Z reference, Kluwer Academic, Dordrecht ; London, c1999.

[11] EM Arruda, MC Boyce, R Jayachandran. Effects of strain rate, temperature and thermomechanical coupling on the finite strain deformation of glassy polymers, Mechanics of Materials,. 19 (1995) 193-212.

[12] Baselmans H., A new modelling approach of rate dependent softening in glassy polymers. (2002).

[13] D Hadley, IM Ward, Introduction to the mechanical properties of solid polymers, Wiley, Chichester, 1993.

[14] JA Roetling. Yield stress behaviour of polymethylmethacrylate, Polymer,. 6 (1965) 311-317.

[15] C Bauwens-Crowet, JC Bauwens, G Homès. Tensile yield-stress behavior of glassy polymers, Journal of Polymer Science Part A-2: Polymer Physics. 7 (1969) 735-742.

[16] F Huberth, S Hiermaier, M Neumann. Material Models for Polymers under Crash Loads - Existing LS-Dyna Models and Perspective, (2005) H-I-1-H-I-12.

[17] V Shah, Handbook of plastics testing and failure analysis, 3rd ed., John Wiley & Sons, Hoboken, N.J, 2007.

[18] J López-Puente, R Zaera, C Navarro. The effect of low temperatures on the intermediate and high velocity impact response of CFRPs, Composites Part B: Engineering,. 33 (2002) 559-566.

[19] LSTC, LS-Dyna Keyword User's Manual, Version 971 ed. 2007.

[20] PA Du Bois, M Koesters, T Frank, S Kolling. Crashworthiness Analysis of Structures Made from Polymers, (2004) C-I-1-C-I-12.

[21] LSTC. LS-Dyna Theory Manual, (2006).

[22] TX Yu, WJ Stronge, Dynamic models for structural plasticity, [Corrected 2nd printing] ed., Springer-Verlag, Berlin, 1995.

[23] I Lage-Canellas, Material Model Validation in LS-Dyna For Car-Interior Head Impact Situation, (2005).

[24] RD Cook, SM David, ME Plesha, RJ Witt, Concepts and applications of finite element analysis, 4th ed., Wiley, New York, 2001.

Appendix A: LEXAN EXL1414H

IDES Prospector
www.ides.com/prospector

Combined Data Sheet

Wednesday, July 02, 2008

LEXAN* EXL1414H Resin

SABIC Innovative Plastics - *Polycarbonate*

Unit System: SI

Actions **Legend (Open)**

General Information

Product Description

Opaque PC-Siloxan copolymer with excellent processability. Medium flow, extreme low temperature ductile. Enhanced hydrolytic stability.

General			
Material Status	• Commercial: Active		
Availability	• North America		
Features	• Copolymer • Ductile	• Good Processability • Hydrolytically Stable	• Medium Flow
Appearance	• Opaque		
Forms	• Pellets		
Processing Method	• Injection Molding		

ASTM and ISO Properties [1]

Physical	**Nominal Value**	**Unit**	**Test Method**
Specific Gravity	1.18	g/cm³	ASTM D792
Density	1.19	g/cm³	ISO 1183
Melt Mass-Flow Rate (MFR) (300°C/1.2 kg)	10	g/10 min	ASTM D1238
Melt Volume-Flow Rate (MVR) (300°C/1.2 kg)	9.00	cm³/10min	ISO 1133
Molding Shrinkage (Flow, 3.20 mm)	0.40 to 0.80	%	ASTM D955
Water Absorption Sat/23C	0.35	%	ISO 62
Water Absorption 23C/50RH	0.15	%	ISO 62
Mechanical	**Nominal Value**	**Unit**	**Test Method**
Tensile Modulus [2]	2020	MPa	ASTM D638
Tensile Modulus	2150	MPa	ISO 527-1, -2/1
Tensile Strength [3] (Yield)	56.0	MPa	ASTM D638
Tensile Stress (Yield)	57.0	MPa	ISO 527-1, -2/50
Tensile Strength [3] (Break)	50.0	MPa	ASTM D638
Tensile Stress (Break)	60.0	MPa	ISO 527-1, -2/50
Tensile Elongation [3] (Yield)	6.0	%	ASTM D638
Tensile Strain (Yield)	6.0	%	ISO 527-1, -2/50
Tensile Elongation [3] (Break)	98	%	ASTM D638
Tensile Strain (Break)	120	%	ISO 527-1, -2/50
Flexural Modulus [4] (50.0 mm Span)	2230	MPa	ASTM D790
Flexural Modulus [5]	2250	MPa	ISO 178
Flexural Strength [5,6]	85.0	MPa	ISO 178
Flexural Strength [4] (Yield, 50.0 mm Span)	92.0	MPa	ASTM D790
Impact	**Nominal Value**	**Unit**	**Test Method**
Charpy Notched Impact Strength [7]			ISO 179/1eA
(-30 °C)	65.0	kJ/m²	
(23 °C)	70.0	kJ/m²	
Charpy Unnotched Impact Strength [7]			ISO 179/1eU
(-30 °C)	No Break		
(23 °C)	No Break		

http://prospector.ides.com/datasheet.aspx?I=34&E=82417 7/2/2008

Notched Izod Impact			ASTM D256
(-30 °C)	774	J/m	
(23 °C)	865	J/m	
Notched Izod Impact Strength [8]			ISO 180/1A
(-30 °C)	60.0	kJ/m²	
(23 °C)	70.0	kJ/m²	
Unnotched Izod Impact Strength [8]			ISO 180/1U
(-30 °C)	No Break		
(23 °C)	No Break		
Instrumented Dart Impact - Total Energy			ASTM D3763
(-30 °C)	77.0	J	
(23 °C)	70.0	J	
Thermal	**Nominal Value**	**Unit**	**Test Method**
Deflection Temperature Under Load (0.45 MPa, Unannealed, 3.20 mm)	139	°C	ASTM D648
Heat Deflection Temperature [9] (0.45 MPa, Unannealed)	140	°C	ISO 75B-1, -2
Deflection Temperature Under Load (1.8 MPa, Unannealed, 3.20 mm)	124	°C	ASTM D648
Heat Deflection Temperature [9] (1.8 MPa, Unannealed)	128	°C	ISO 75A-1, -2
Vicat Softening Point (Rate B, Loading 2 (50 N))	145	°C	ASTM D1525
Vicat Softening Temperature			
(--)	145	°C	ISO 306/B50
(--)	146	°C	ISO 306/B120
CLTE, Flow (TMA) (-40 to 40 °C)	0.000070	cm/cm/°C	ASTM E831
Coefficient of Linear Thermal Expansion, Flow (23 to 80 °C)	0.000072	cm/cm/°C	ISO 11359-1, -2
CLTE, Transverse (TMA) (-40 to 40 °C)	0.000070	cm/cm/°C	ASTM E831
Coefficient of Linear Thermal Expansion, Transverse (23 to 80 °C)	0.000072	cm/cm/°C	ISO 11359-1, -2
Ball Pressure Test, 125 °C	Pass		IEC 60695-10-2

Processing Information

Injection	**Nominal Value**	**Unit**
Drying Temperature	121	°C
Drying Time	3.0 to 4.0	hr
Drying Time, Maximum	48	hr
Suggested Max Moisture	0.020	%
Suggested Shot Size	40 to 60	%
Rear Temperature	271 to 293	°C
Middle Temperature	282 to 304	°C
Front Temperature	293 to 316	°C
Nozzle Temperature	288 to 310	°C
Processing (Melt) Temp	293 to 316	°C
Mold Temperature	71.1 to 93.3	°C
Back Pressure	0.345 to 0.689	MPa
Screw Speed	40 to 70	rpm
Vent Depth	0.025 to 0.076	mm

Notes

[1] Typical properties: these are not to be construed as specifications.

[2] 50 mm/min

[3] Type I, 50 mm/min

[4] 1.3 mm/min

[5] 2.0 mm/min

[6] Yield

[7] 80*10*3 sp=62mm

[8] 80*10*3

[9] Edgewise, 120*10*4 mm, 100 mm

Appendix B: DYLARK 480P16

NOVA Chemicals®

High Performance Styrenics

PRODUCT DATA SHEET FOR:

DYLARK® 480P16

GLASS REINFORCED ENGINEERING RESIN

FEATURES:	APPLICATIONS:
• Very high modulus • High heat resistance • Excellent flow characteristics • Excellent adhesion to urethane	• Instrument panel substrates • Consoles • Cluster housings • Interior trim

Properties (1)	Method	Typical Values (2,3)
Specific gravity	ISO 1183	1.18
Melt Flow, gm/10 minutes (230/2.16)	ISO 1133	0.5
Glass Fiber Content, %	ISO 3451/1	16
Tensile Strength, MPa	ISO 527-2	74
Tensile Elongation, %	ISO 527-2	2.2
Tensile Modulus, MPa	ISO 527-2	5900
Flexural Strength, MPa	ISO 178	118
Flexural Modulus MPa	ISO 178	5550
Izod Impact (notched), $^{kJ}/_{m2}$ at 23°C at –40°C	ISO 180/1A	 8.1 7.7
Charpy Impact (notched), $^{kJ}/_{m2}$ at 23°C	ISO 179/1eA	8.4
Charpy Impact (unnotched), $^{kJ}/_{m2}$ at 23°C	ISO 179/1eU	27.5
Mold shrinkage, inch/inch (cm/cm)	ISO 2577	0.0025-0.0045
DTUL at 1.82 MPa, °C (unannealed, 4.0 mm bar)	ISO 75-2	120
Coefficient of Linear Thermal Expansion	NOVA Chemicals Laboratory Procedure	
cm/cm/°C		5.1×10^{-5}
inch/inch/°F		2.8×10^{-5}

(1) Properties designated in this standard have been determined in accordance with the current issues of the specified testing methods.
(2) Typical Values represent average laboratory values and are intended as guides only, not as specific specification limits.
(3) For Engineering Analysis Data, please contact NOVA Chemicals.

June 3, 2004 Document is uncontrolled 24 hours after printing

DYLARK

NOVA Chemicals

PRODUCT DATA SHEET
(Continued)

DYLARK Engineering Resin

PROCESSING

Molding Machines

- Clamp tonnage of 2-3 tons per square inch are generally adequate
- Shot weight should be 50-75% of rated capacity
- General-purpose screws typically used for ABS, PS, PC can be used to process *DYLARK* Engineering Resins. Compression ratios should be in the 2.0:1 to 2.5:1 range. Zero metering screws are also satisfactory. Ring check valves are preferred over ball check type.

Pre-Dry Requirements

DYLARK Engineering Resins can be molded as received without predrying.

Mold Design

- *DYLARK* Engineering Resins are molded in all standard mold designs, including hot runner manifolds with multiple drops (nozzles).
- *DYLARK* Engineering Resins have a very high modulus and fast set up times dictating generous draft angles (3°-5°) and no undercuts for trouble free automatic molding.
- The recommended grade of tool steel is AISI Grade P-20, prehardened to a RC of mid-30's

Regrind

Up to 20% regrind may be used without loss of physical properties.

START-UP CONDITIONS

	Range	Typical
*Melt temperature	500-550°F / 260-288°C	525°F/274°C
Profile temperatures	480-550°F/249 - 288°C	Front 525°F/274°C Center 510°F/266°C Rear 490°F/254°C
**Mold temperatures	Core 110-140°F / 43-60°C Cavity 130-160°F / 54-71°C	120°F / 49°C 150°F / 66°C
Screw RPM	80-125	100
Injection speed	medium-fast	Fast
Back pressure, psi	50-100	50

* Air purge at equilibrium conditions

** Mold surface temperature at equilibrium conditions

This information is of a general nature to serve as a guide in starting-up operation of an injection-molding machine. It may be necessary to modify these conditions as experience indicates, depending upon the characteristics of the processing equipment and of the mold or die in order to obtain the desired results.

NOVA Chemicals Inc.
DYLARK Engineering Resins
29201 Telegraph Road
Suite 500
Southfield, Michigan 48034

Customer and Technical Services

Phone: 248/353-6730
Fax: 248/353-6195

NOVA Chemicals

CAUTION: This product is a combustible thermoplastic. The products of combustion, as from other commonly used materials such as wood, may be hazardous to life or health, particularly in confined spaces. Do not exceed recommended processing temperatures. This material is attacked by many organic solvents. Chemical resistance information is available on request.

June 3, 2004

Appendix C: MATLAB M-File for Eff. Stress Vs Eff. Plastic Strain

```
%*****************************************************************
% TITLE
%*****************************************************************

% Effective Stress Vs Effective Plastic Strain

%*****************************************************************
% OBJECTIVE
%*****************************************************************

% To define the elastic and plastic region of a stress-strain
  curve
% To define the Effective Stress Vs Effective Plastic Strain curve
  required for MAT24 in LS-Dyna

%*****************************************************************
% KEYWORD FILE FOR MAT24
%*****************************************************************

% Open keyword file
fid = fopen ('keyword.k','w') ;
fprintf(fid,'*KEYWORD\n');
fprintf(fid,'*TITLE\n');
fprintf(fid,'$# title\n');
fprintf(fid,'LS-DYNA keyword deck by LS-Prepost\n');

% L = no. of test data
L = input('No. of test data = ');
% rho = Density
rho = input('Density (tonne/mm3) =');
% e = Modulus of Elasticity
e = input('Modulus of Elasticity (MPa) =');
% pr = poisson_s ratio
pr = input('Poisson_s ratio =');
%fps = Failure Plastic Strain
fps = input('Failure Plastic Strain =');

% Print general material properties
fprintf(fid,'*MAT_PIECEWISE_LINEAR_PLASTICITY\n');
fprintf(fid,'$#     mid        ro         e        pr      sigy
etan      fail      tdel\n');
fprintf(fid,'         1 %3.2e %2.4f    %2.4f     0.000     0.000
%2.4f\n',[rho;e;pr;fps]);
fprintf(fid,'$#       c         p      lcss      lcsr
vp\n');
fprintf(fid,'     0.000     0.000     %1.0f\n',[L+1]);
fprintf(fid,'$#    eps1      eps2      eps3      eps4      eps5
eps6      eps7      eps8\n');
fprintf(fid,'     0.000     0.000     0.000     0.000     0.000
0.000     0.000     0.000\n');
fprintf(fid,'$#     es1       es2       es3       es4       es5
es6       es7       es8\n');
```

```
fprintf(fid,'     0.000     0.000     0.000     0.000     0.000
0.000     0.000     0.000\n');

% sr = strain rate
sr = input('Strain rate =');

% Define Table for curves generated
fprintf(fid,'*DEFINE_TABLE\n');
fprintf(fid,'$#    tbid\n');
fprintf(fid,'         %1.0f\n',[L+1]);
fprintf(fid,'$#             value      lcid\n');
fprintf(fid,'           %2.7f         %1.0f\n',[sr;1:L']);

%*****************************************************************
% DEFINE DATA FOR STRESS-STRAIN CURVE
%*****************************************************************

for p= 1:L

    data = input('Test Data Input = ');

    ytan = 0;

    i = length(data);

    % teps = true strain
    teps = data(1:i,1);

    % tsigma = true stress
    tsigma = data(1:i,2);

%*****************************************************************
% CALCULATE MODULUS OF ELASTICITY (E)
%*****************************************************************

    % E = Modulus of Elasticity based on test data
    E = polyfit(data(1:5,1),data(1:5,2),1);
    e(p) = E(1);

%*****************************************************************
% DEFINE TANGENTIAL CURVE
%*****************************************************************

    for k = 1:0.5*i

        ytan(k) = E(1).*teps(k)+E(2);

    end

 % Plot True Stress-True Strain and Offset Yield Strength Curves
    figure(1)
    hold all
    grid on
    %plot (teps(1:k),ytan)
    plot (teps,tsigma)
```

```
    xlabel ('True Strain ')
    ylabel ('True Stress (MPa)')
    hold off

%*****************************************************************
% DEFINE DATA FOR TRUE STRESS-PLASTIC STRAIN CURVE
%*****************************************************************

    for n = 1:k

    z(n)=ytan(n)-tsigma(n);

        if abs(z(n)) <= 0.005*E(1)

            N(p) = n;

        else

        end

    end

    % sigma = true stress for True Stress-Plastic Strain curve
    % peps = plastic strain
    sigma = tsigma(N(p):1:i);
    q = length(sigma);
    peps = abs([teps(N(p):1:i)-(sigma(1:q)-E(2))/E(1)]);

 % Plot of True Stress-Plstic Strain Curve
    figure (L+1)
    hold all
    plot (peps,sigma)
    grid on
    xlabel('Effective Plastic Strain ')
    ylabel('Effective Stress (MPa)')

%*****************************************************************
% SETUP KEYWORD FILE FOR TRUE STRESS-PLASTIC STRAIN CURVE
%*****************************************************************

   fprintf(fid,'*DEFINE_CURVE_TITLE\n')
   fprintf(fid,'%2.2f\n',[sr(p)]);
   fprintf(fid,'$#    lcid      sidr       sfa       sfo      offa
offo    dattyp\n')
   fprintf(fid,'         %1.0f         0  1.000000
1.000000\n',[p])

fprintf(fid,'$#                a1                  o1\n')
fprintf(fid,'           %2.7f          %2.7f\n',[peps';sigma'])
end
fclose(fid)
hold off
 e(1)
%*****************************************************************
% END
%*****************************************************************
```

Appendix D: LS-DYNA Keyword for *Material 24* (DYLARK 480P16)

```
$# LS-DYNA Keyword file created by LS-PREPOST 2.2 -
20Mar2008(16:12)
$# Created on Jul-22-2008 (18:27:18)
*KEYWORD
*TITLE
$# title
LS-DYNA keyword deck by LS-Prepost
*MAT_PIECEWISE_LINEAR_PLASTICITY
$480P16 23C LS-Dyna MAT24 LCSS Material Card
$HMNAME MATS       1DYLARK480P16
$#     mid        ro         e        pr      sigy      etan
fail      tdel
         4 1.1800E-9 5117.0000  0.279000     0.000     0.000
0.027500
$#       c         p      lcss      lcsr        vp
     0.000     0.000         1
$$ HM Entries in Stress-Strain Curve =
$#    eps1      eps2      eps3      eps4      eps5      eps6
eps7      eps8
     0.000     0.000     0.000     0.000     0.000     0.000
0.000     0.000
$#     es1       es2       es3       es4       es5       es6
es7       es8
     0.000     0.000     0.000     0.000     0.000     0.000
0.000     0.000
*DEFINE_TABLE_TITLE
LCSS Table
$#    tbid
         1
$$ HM Entries in number of values =         5
$#             value      lcid
           0.0100000         2
(.. ..)
         100.0000000         6
*DEFINE_CURVE
$HMNAME CURVES       2480P16_SR0.01
$HMCOLOR CURVES       2       1
$HMCURVE     2    2 LoadCurve1
$#    lcid      sidr       sfa       sfo      offa      offo
dattyp
         2         0  1.000000  1.000000
$#               a1                  o1
              0.000          26.3675995
(.. ..)
           0.0051000          59.2760010
*DEFINE_CURVE
$HMNAME CURVES       3480P16_SR0.1
$HMCOLOR CURVES       3       1
$HMCURVE     3    3 LoadCurve2
$#    lcid      sidr       sfa       sfo      offa      offo
dattyp
         3         0  1.000000  1.000000
$#               a1                  o1
              0.000          29.4930992
```

```
(.. ..)
           0.0053000          67.4855957
*DEFINE_CURVE
$HMNAME CURVES       4480P16_SR1.0
$HMCOLOR CURVES       4       1
$HMCURVE     1    1 LoadCurve3
$#    lcid      sidr       sfa       sfo      offa      offo
dattyp
         4         0  1.000000  1.000000
$#                a1                  o1
               0.000          37.5430031
(.. ..)
           0.0047000          69.6080017
*DEFINE_CURVE
$HMNAME CURVES       5480P16_SR10
$HMCOLOR CURVES       5       1
$HMCURVE     2    2 LoadCurve4
$#    lcid      sidr       sfa       sfo      offa      offo
dattyp
         5         0  1.000000  1.000000
$#                a1                  o1
               0.000          47.2814980
(.. ..)
           0.0033930          77.0909958
*DEFINE_CURVE
$HMNAME CURVES       6480P16_SR100
$HMCOLOR CURVES       6       1
$HMCURVE     3    3 LoadCurve5
$#    lcid      sidr       sfa       sfo      offa      offo
dattyp
         6         0  1.000000  1.000000
$#                a1                  o1
               0.000          91.2660065
(.. ..)
           0.0037351          96.9850006
*END
```

Appendix E: LS-DYNA Keyword for UNIAXIAL Tensile Simulation

```
$# LS-DYNA Keyword file created by LS-PREPOST 2.2 -
20Mar2008(16:12)
$# Created on Jul-17-2008 (18:49:30)
*KEYWORD
*TITLE
$# title
LS-DYNA keyword deck by LS-Prepost
*CONTROL_TERMINATION
$#  endtim    endcyc     dtmin    endeng    endmas
  0.100000
*DATABASE_ELOUT
$#      dt    binary      lcur     ioopt
 1.0000E-4         1
*DATABASE_NODFOR
$#      dt    binary      lcur     ioopt
 1.0000E-4         1
*DATABASE_NODOUT
$#      dt    binary      lcur     ioopt      dthf     binhf
 1.0000E-4         1
*DATABASE_BINARY_D3PLOT
$#      dt      lcdt      beam     npltc
 1.0000E-4
$#   ioopt
         0
*DATABASE_EXTENT_BINARY
$#   neiph     neips    maxint    strflg    sigflg    epsflg
rltflg    engflg
         0         0         3         1         1         1
1         1
$#  cmpflg    ieverp    beamip     dcomp      shge     stssz
n3thdt   ialemat
         0         0         0         1         1         1
2         1
$# nintsld   pkp_sen      sclp    unused     msscl     therm
         0         0  1.000000
*DATABASE_NODAL_FORCE_GROUP
$#    nsid       cid
         3
*DATABASE_HISTORY_NODE
$#     id1       id2       id3       id4       id5       id6
id7       id8
       758
*DATABASE_HISTORY_SHELL_ID
$#     id1
heading
      6847
$#     id1
heading
      7096
(.. ..)
*BOUNDARY_PRESCRIBED_MOTION_SET
$#    nsid       dof       vad      lcid        sf       vid
death     birth
```

```
         2         1         0         7  1.000000
01.0000E+28
*BOUNDARY_SPC_SET
$#    nsid       cid      dofx      dofy      dofz     dofrx
dofry     dofrz
         1         0         1         1         1         1
1         1
*SET_NODE_LIST_TITLE
NODESET(SPC) 1
$#     sid       da1       da2       da3       da4
         1
$#    nid1      nid2      nid3      nid4      nid5      nid6
nid7      nid8
         1         2         3         4         5         6
7
(.. ..)
9887
*PART
$# title
C008V000
$#     pid     secid       mid     eosid      hgid      grav
adpopt      tmid
         1         1         4
*SECTION_SHELL_TITLE
test piece
$#   secid    elform      shrf       nip     propt   qr/irid
icomp     setyp
         1         2  1.000000         5         1         0
0         1
$#      t1        t2        t3        t4      nloc     marea
idof    edgset
  4.000000  4.000000  4.000000  4.000000
*MAT_PIECEWISE_LINEAR_PLASTICITY
$480P16 23C LS-Dyna MAT24 LCSS Material Card
$HMNAME MATS       1DYLARK480P16
$#     mid        ro         e        pr      sigy      etan
fail      tdel
         4 1.1800E-9 5117.0000  0.279000     0.000     0.000
0.005000
$#       c         p      lcss      lcsr        vp
     0.000     0.000         1
$#    eps1      eps2      eps3      eps4      eps5      eps6
eps7      eps8
     0.000     0.000     0.000     0.000     0.000     0.000
0.000     0.000
$#     es1       es2       es3       es4       es5       es6
es7       es8
     0.000     0.000     0.000     0.000     0.000     0.000
0.000     0.000
*DEFINE_TABLE_TITLE
LCSS Table
$#    tbid
         1
$$ HM Entries in number of values =         5
$#             value      lcid
           0.0100000         2
(.. ..)
         100.0000000         6
```

```
*DEFINE_CURVE
$HMNAME CURVES       2480P16_SR0.01
$HMCOLOR CURVES       2       1
$HMCURVE     2    2 LoadCurve1
$#    lcid      sidr       sfa       sfo      offa      offo
dattyp
         2         0  1.000000  1.000000
$#               a1                  o1
               0.000          26.3675995
(.. ..)
            0.0051000          59.2760010
*DEFINE_CURVE
$HMNAME CURVES       3480P16_SR0.1
$HMCOLOR CURVES       3       1
$HMCURVE     3    3 LoadCurve2
$#    lcid      sidr       sfa       sfo      offa      offo
dattyp
         3         0  1.000000  1.000000
$#               a1                  o1
               0.000          29.4930992
(.. ..)
            0.0053000          67.4855957
*DEFINE_CURVE
$HMNAME CURVES       4480P16_SR1.0
$HMCOLOR CURVES       4       1
$HMCURVE     1    1 LoadCurve3
$#    lcid      sidr       sfa       sfo      offa      offo
dattyp
         4         0  1.000000  1.000000
$#               a1                  o1
               0.000          37.5430031
(.. ..)
            0.0047000          69.6080017
*DEFINE_CURVE
$HMNAME CURVES       5480P16_SR10
$HMCOLOR CURVES       5       1
$HMCURVE     2    2 LoadCurve4
$#    lcid      sidr       sfa       sfo      offa      offo
dattyp
         5         0  1.000000  1.000000
$#               a1                  o1
               0.000          47.2814980
(.. ..)
            0.0033930          77.0909958
*DEFINE_CURVE
$HMNAME CURVES       6480P16_SR100
$HMCOLOR CURVES       6       1
$HMCURVE     3    3 LoadCurve5
$#    lcid      sidr       sfa       sfo      offa      offo
dattyp
         6         0  1.000000  1.000000
$#               a1                  o1
               0.000          91.2660065
(.. ..)
            0.0037351          96.9850006
```

```
*DEFINE_CURVE_TITLE
test velocity
$#    lcid      sidr       sfa       sfo      offa      offo
dattyp
         7         0  1.000000  1.000000
$#              a1                  o1
              0.000               0.000
     5.0000002e-004         500.0000000
          0.0100000         500.0000000
*SET_NODE_LIST_TITLE
NODESET(SPC) 2
$#     sid       da1       da2       da3       da4
         2
$#    nid1      nid2      nid3      nid4      nid5      nid6
nid7      nid8
       287       288       289       290       291       292
293
(.. ..)
9880
      9881      9882      9883
*SET_NODE_LIST
$#     sid       da1       da2       da3       da4
         3
$#    nid1      nid2      nid3      nid4      nid5      nid6
nid7      nid8
       287       288       289       290       291       292
293       294
*SET_NODE_LIST_TITLE
rigid node set 4
$#     sid       da1       da2       da3       da4
         4
$#    nid1      nid2      nid3      nid4      nid5      nid6
nid7      nid8
      7589      6923      7590
*CONSTRAINED_NODAL_RIGID_BODY
$#     pid       cid      nsid     pnode      iprt    drflag
rrflag
         1         0         4      7589         1
*ELEMENT_SHELL
$#   eid     pid      n1      n2      n3      n4      n5      n6
n7      n8
       1       1       1       2     771     770
       2       1     730     731     732     772
 (.. ..)
    9518       1    9664    9660    9815    9817
*NODE
$#   nid               x               y               z      tc
rc
       1           0.000      20.0000000       4.0000000
(.. ..)
    9887      27.9090786       9.9135313       4.0000000
*END
```

Appendix F: LS-DYNA Keyword for Drop Weight Impact Simulation

```
$# LS-DYNA Keyword file created by LS-PREPOST 2.2 - 7Nov2007(09:44)
$# Created on May-09-2008 (00:44:58)
*KEYWORD
*TITLE
$# title
LS-DYNA keyword deck by LS-PRE
*CONTROL_TERMINATION
$#  endtim    endcyc     dtmin    endeng    endmas
  0.005000
*DATABASE_NODOUT
$#      dt    binary      lcur     ioopt      dthf     binhf
 1.0000E-4         1
*DATABASE_BINARY_D3PLOT
$#      dt      lcdt      beam     npltc
 1.0000E-5
$#   ioopt
         0
*DATABASE_HISTORY_NODE
$#     id1       id2       id3       id4       id5       id6
id7       id8
       557
*BOUNDARY_SPC_NODE
$#     nid       cid      dofx      dofy      dofz     dofrx
dofry     dofrz
      1429         0         1         1         1         1
1         1
      1430         0         1         1         1         1
1         1
(...)
     1577         0         1         1         1         1
1         1
      1578         0         1         1         1         1
1         1
*CONTACT_AUTOMATIC_NODES_TO_SURFACE_ID
$#     cid
title
         1
$#    ssid      msid     sstyp     mstyp    sboxid    mboxid
spr       mpr
         2         1         2         2
$#      fs        fd        dc        vc       vdc    penchk
bt        dt
     0.000     0.000     0.000     0.000     0.000         0
0.0001.0000E+20
$#     sfs       sfm       sst       mst      sfst      sfmt
fsf       vsf
  1.000000  1.000000     0.000     0.000  1.000000  1.000000
1.000000  1.00000
*SET_PART_LIST_TITLE
slave
$#     sid       da1       da2       da3       da4
         2
```

```
$#    pid1      pid2      pid3      pid4      pid5      pid6
pid7      pid8
         2
*SET_PART_LIST_TITLE
master
$#     sid       da1       da2       da3       da4
         1
$#    pid1      pid2      pid3      pid4      pid5      pid6
pid7      pid8
         1
*PART
$# title
C008V000
$#     pid     secid       mid     eosid      hgid      grav
adpopt      tmid
         1         1         5
*SECTION_SHELL_TITLE
impactor
$#   secid    elform      shrf       nip     propt   qr/irid
icomp     setyp
         1         2  1.000000         2         1         0
0         1
$#      t1        t2        t3        t4      nloc     marea
idof    edgset
  1.000000  1.000000  1.000000  1.000000
*MAT_RIGID
$#     mid        ro         e        pr         n    couple
m     alias
         5 5.6100E-6 2.1000E+5  0.300000     0.000     0.000
0.000
$#     cmo      con1      con2
  1.000000         6         7
$#lco or a1       a2        a3        v1        v2        v3
     0.000     0.000     0.000     0.000     0.000     0.000
*PART
$# title
plaque
$#     pid     secid       mid     eosid      hgid      grav
adpopt      tmid
         2         2         4
*SECTION_SHELL_TITLE
plaque
$#   secid    elform      shrf       nip     propt   qr/irid
icomp     setyp
         2         2  1.000000         5         1         0
0         1
$#      t1        t2        t3        t4      nloc     marea
idof    edgset
  2.500000  2.500000  2.500000  2.500000
*MAT_PIECEWISE_LINEAR_PLASTICITY
$HMNAME MATS       1DYLARK480P16
$#     mid        ro         e        pr      sigy      etan
fail      tdel
         4 1.1800E-9 5117.0000  0.279000
$#       c         p      lcss      lcsr        vp
     0.000     0.000         1
$#    eps1      eps2      eps3      eps4      eps5      eps6
eps7      eps8
```

```
     0.000     0.000     0.000     0.000     0.000     0.000
0.000     0.000
$#     es1       es2       es3       es4       es5       es6
es7       es8
     0.000     0.000     0.000     0.000     0.000     0.000
0.000     0.000
*INITIAL_VELOCITY_NODE
$#     nid        vx        vy        vz       vxr       vyr
vzr
         1     0.000-6700.0000
         2     0.000-6700.0000
     (...)
     1427     0.000-6700.0000
      1428     0.000-6700.0000
*DEFINE_TABLE_TITLE
LCSS Table
$#    tbid
         1
$$ HM Entries in number of values =         5
$#             value      lcid
          0.0100000         2
         (...)
         100.0000000         6
*DEFINE_CURVE
$HMNAME CURVES       2480P16_SR0.01
$HMCOLOR CURVES       2       1
$HMCURVE     2    2 LoadCurve1
$#    lcid      sidr       sfa       sfo      offa      offo
dattyp
         2         0  1.000000  1.000000
$#               a1                  o1
              0.000          26.3675995
           (...)
           0.0051000          59.2760010
*DEFINE_CURVE
$HMNAME CURVES       3480P16_SR0.1
$HMCOLOR CURVES       3       1
$HMCURVE     3    3 LoadCurve2
$#    lcid      sidr       sfa       sfo      offa      offo
dattyp
         3         0  1.000000  1.000000
$#               a1                  o1
              0.000          29.4930992
           (...)
           0.0053000          67.4855957

*DEFINE_CURVE
$HMNAME CURVES       4480P16_SR1.0
$HMCOLOR CURVES       4       1
$HMCURVE     1    1 LoadCurve3
$#    lcid      sidr       sfa       sfo      offa      offo
dattyp
         4         0  1.000000  1.000000
$#               a1                  o1
              0.000          37.5430031
           (...)
           0.0047000          69.6080017
```

```
*DEFINE_CURVE
$HMNAME CURVES       5480P16_SR10
$HMCOLOR CURVES       5       1
$HMCURVE     2    2 LoadCurve4
$#    lcid      sidr       sfa       sfo      offa      offo
dattyp
         5         0  1.000000  1.000000
$#               a1                  o1
              0.000          47.2814980
           (...)
           0.0033930          77.0909958
*DEFINE_CURVE
$HMNAME CURVES       6480P16_SR100
$HMCOLOR CURVES       6       1
$HMCURVE     3    3 LoadCurve5
$#    lcid      sidr       sfa       sfo      offa      offo
dattyp
         6         0  1.000000  1.000000
$#               a1                  o1
              0.000          91.2660065
           (...)
           0.0037351          96.9850006
*ELEMENT_SHELL
$#   eid     pid      n1      n2      n3      n4      n5      n6
n7      n8
       1       1     144     462      65      65
    (...)
    2678       2    1536    1594    1595    1537
*ELEMENT_SEATBELT_ACCELEROMETER
$#  sbacid      nid1      nid2      nid3     igrav    intopt
         1       557       545       546
*NODE
$#   nid               x               y               z      tc
rc
       1 -4.7683716e-007      12.6129808      -6.3499999
    (...)
    2623      13.3484240      -8.0000000     -11.2972984
*END
```

Appendix G: Simulation based on Approximated Stress-Strain Curves at 85°C

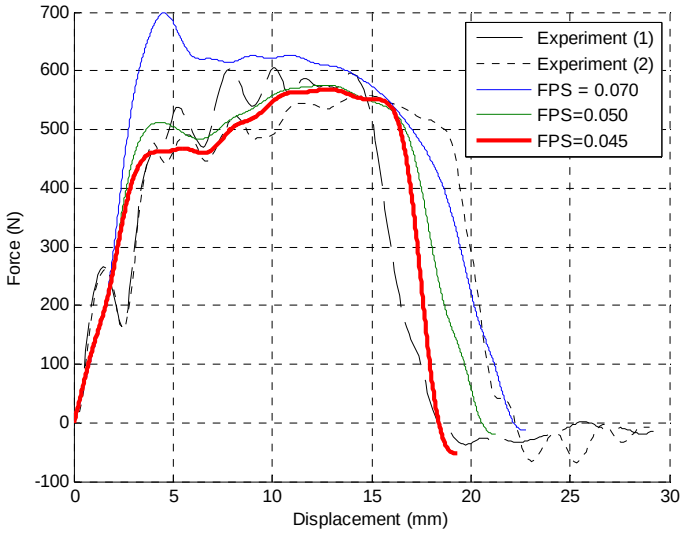

Figure G.1 Force Vs Displacement plots for DYLARK 480P16 at 85°C with FPS variation (Approximated Stress-Strain Curves)

Table G.1 Experimental and Simulation results comparison for basic correlation parameters for 85°C (Approximated Stress-Strain Curves)

	Parameter	Experimental (Test 1/Test 2)	Simulation	Modified Curves
1	Peak Load (N)	605.40/558.00	526.40	568.5
2	Displacement @Peak Load (mm)	10.14/14.89	10.52	12.90
3	Final Displacement @Zero Load (mm)	18.55/22.24	19.45	18.40

Appendix H: SR Set Without SR = 100/s & 10/s

Step 1: FPS Iteration

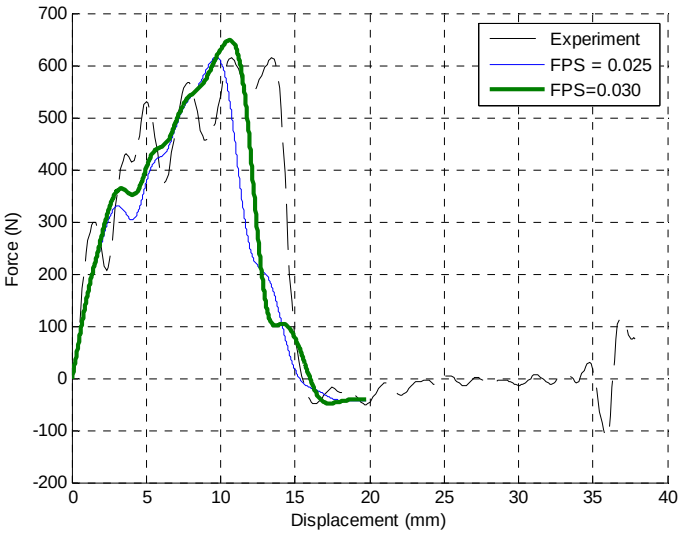

Figure H.1 Force Vs Displacement plots for DYLARK 480P16 at -40°C with FPS variation (Without SR = 100 & 10)

Step 2: Modulus of Elasticity for DYLARK 480P16 at -40°C

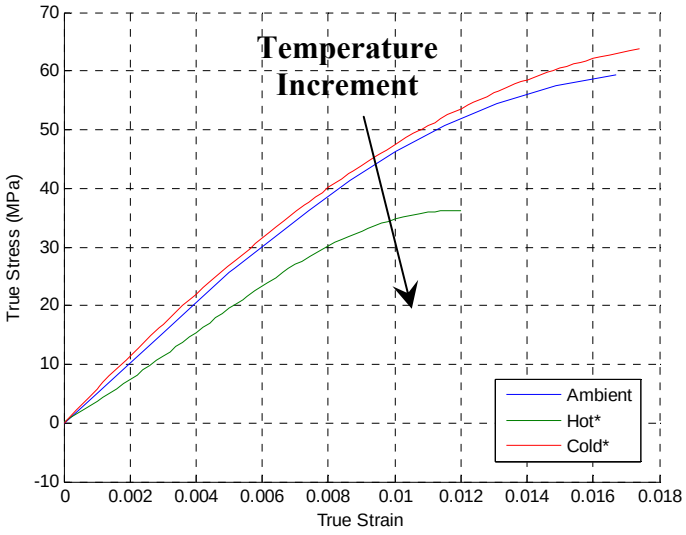

Figure H.2 True Stress-True Strain curve for DYLARK 480P16 at different temperatures (SR = 0.01)

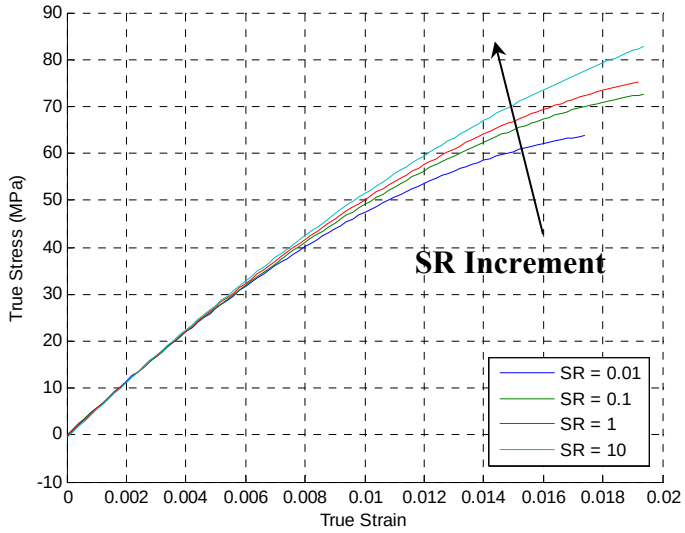

Figure H.3 True Stress-True Strain curve for DYLARK 480P16 with various strain rates at -40°C

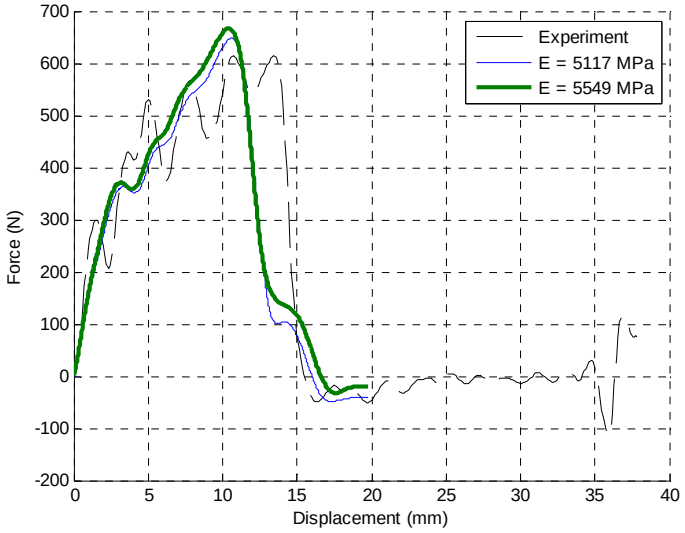

Figure H.4 Force Vs Displacement plot comparison for DYLARK 480P16 at -40°C with different Modulus of Elasticity (FPS = 0.030, SC = 1.07)

Step 3: Curve Shape Correlation

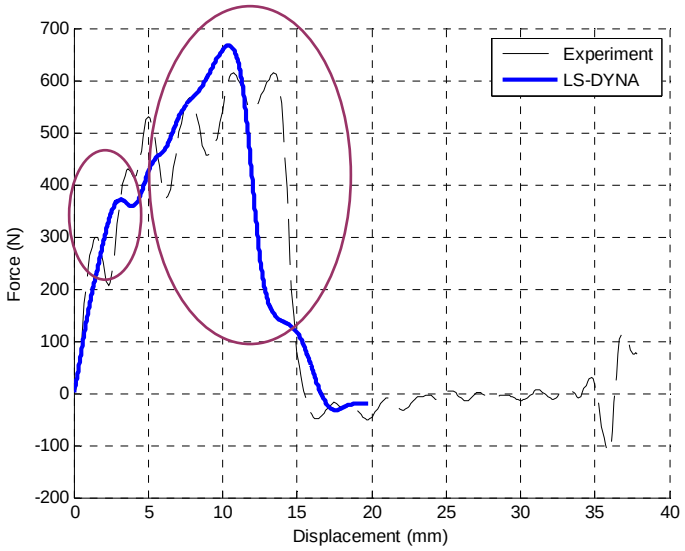

Figure H.5 Force Vs Displacement plot comparison for DYLARK 480P16 at -40°C indicating shape correlation region (FPS = 0.030, SC = 1.07, E=5549 MPa)

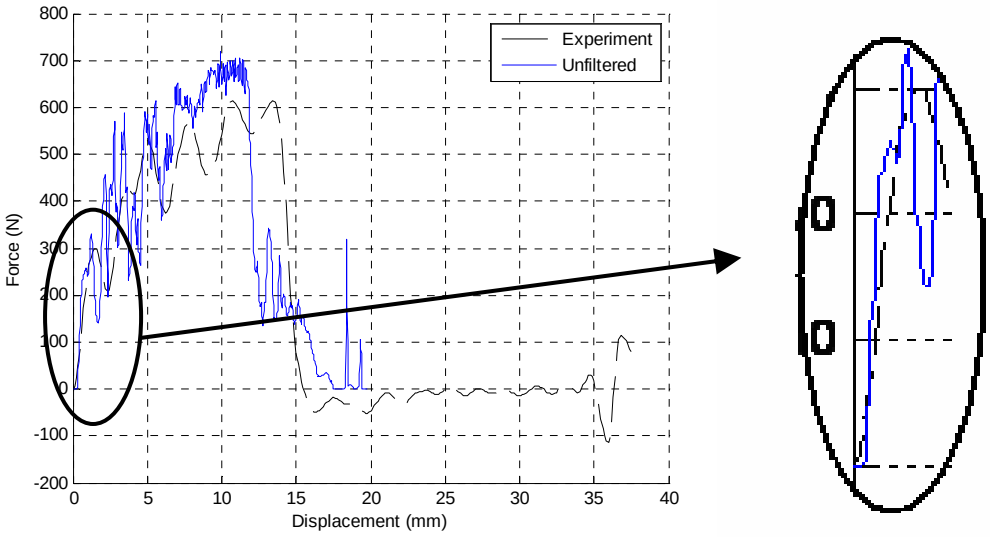

Figure H.6 Force Vs Displacement plot comparison for DYLARK 480P16 at -40°C indicating shape correlation region (Unfiltered Simulation Data - FPS = 0.030, SC = 1.07, E=5549 MPa)

Element Formulation Variation (Without SR = 100 & 10)

To check on the reliability of the results produced using the default ELFORM, the simulation model was simulated again using the FISE formulation. The simulated force-displacement plots for various ELFORM are shown in Figure H.7.

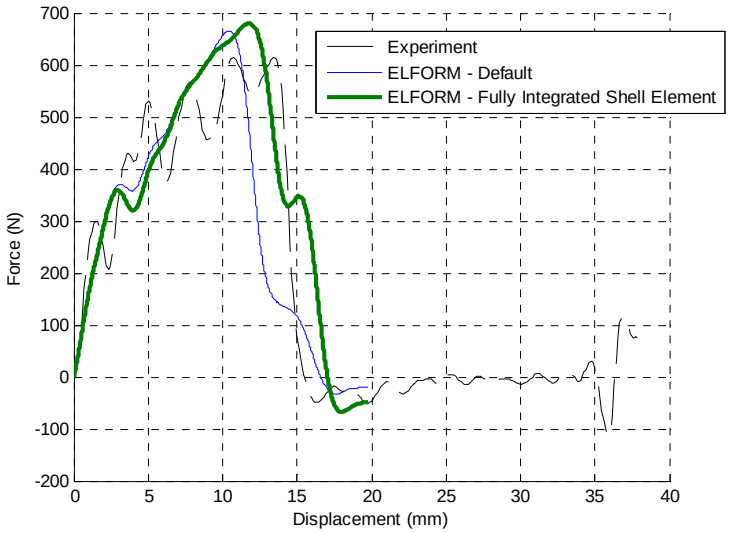

Figure H.7 Force Vs Displacement plot comparison for DYLARK 480P16 at -40^{o}C with ELFORM variation (FPS = 0.030, SC = 1.07, E = 5549MPa)

It can be seen in Figure H.7 that the force-displacement curve simulated using FISE formulation showed an obvious deviation from the result produced using the default ELFORM. However, by running a few simulations by varying the FPS values for the FISE formulation model, it was chosen that a nearer correlation to the default formulation can be achieved by using FPS = 0.025.

The force-displacement curve for FISE formulation using FPS = 0.025 is compared to the one of the default formulation in Figure H.9. The iteration study results are shown in Figure H.8. The numerical comparison between the various ELFORM is presented in Table H.1.

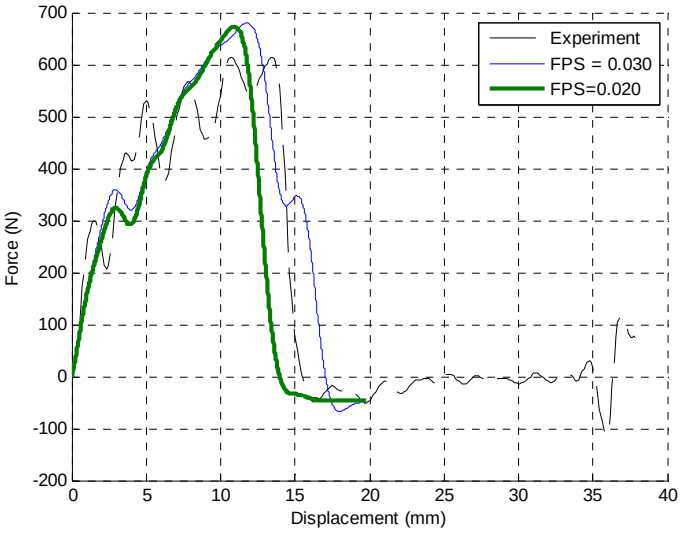

Figure H.8 Force Vs Displacement plot comparison for DYLARK 480P16 at -40°C with various FPS (ELFORM = FISE, without SR = 100/s and 10/s)

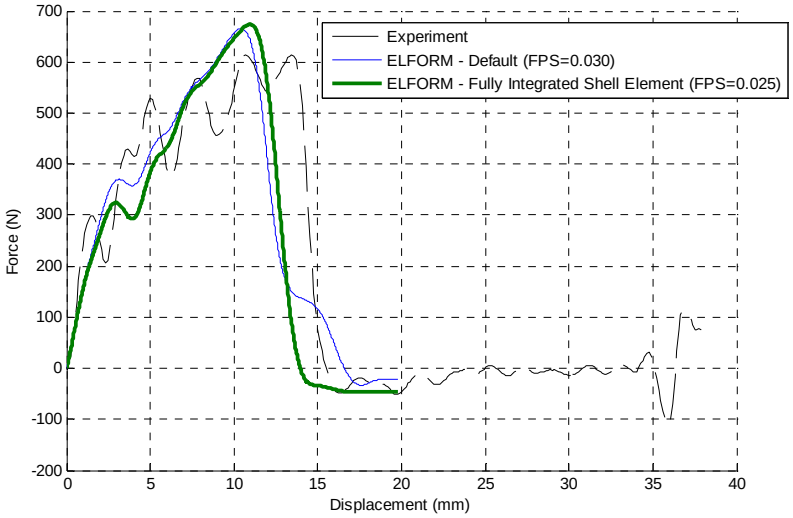

Figure H.9 Force Vs Displacement plot comparison for DYLARK 480P16 at -40°C with ELFORM variation (SC = 1.07, E = 5549MPa)

Table H.1 Experimental and Simulation results comparison for basic correlation parameters at -40°C (Various ELFORM)

	Parameter	Experimental	Default	FISE
1	Peak Load (N)	614.2	666.70	673.60
2	Displacement @Peak Load (mm)	10.69	10.43	10.97
3	Final Displacement @Zero Load (mm)	15.48	16.61	13.97

Appendix I: SR Set Without SR = 100/s

Step 1: FPS Iteration

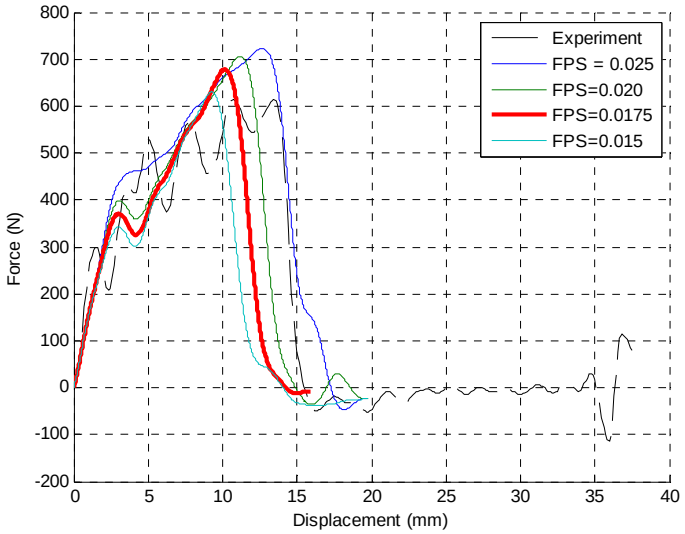

Figure I.1 Force Vs Displacement plots for DYLARK 480P16 at -40°C with FPS variation (Without SR = 100)

Step 2: Modulus of Elasticity of DYLARK 480P16 at -40°C

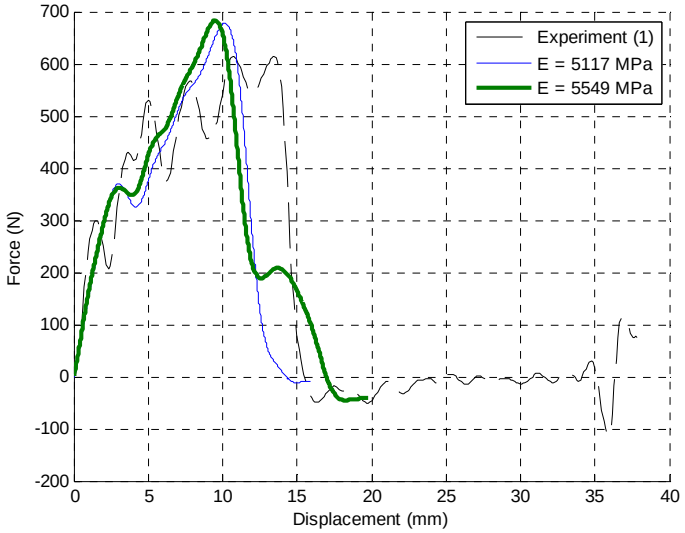

Figure I.2 Force Vs Displacement plots for DYLARK 480P16 at -40°C with (Without SR = 100)

Step 3: Curve Shape Correlation

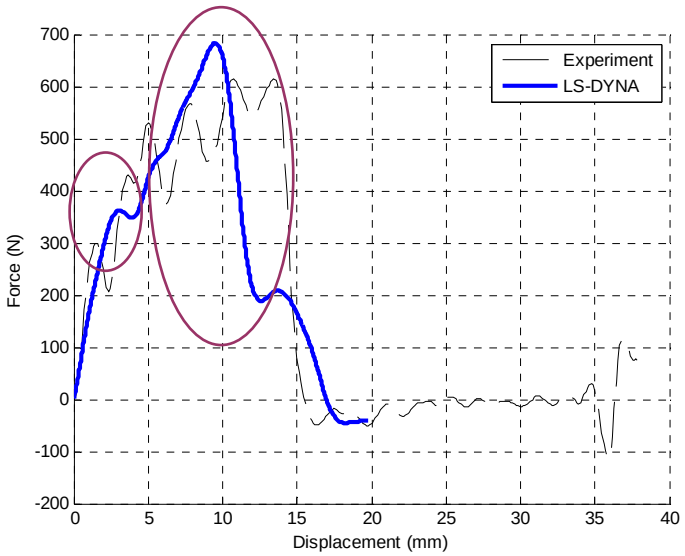

Figure I.3 Force Vs Displacement plot comparison for DYLARK 480P16 at -40°C indicating shape correlation region (FPS = 0.0175, SC = 1.07, E=5549 MPa)

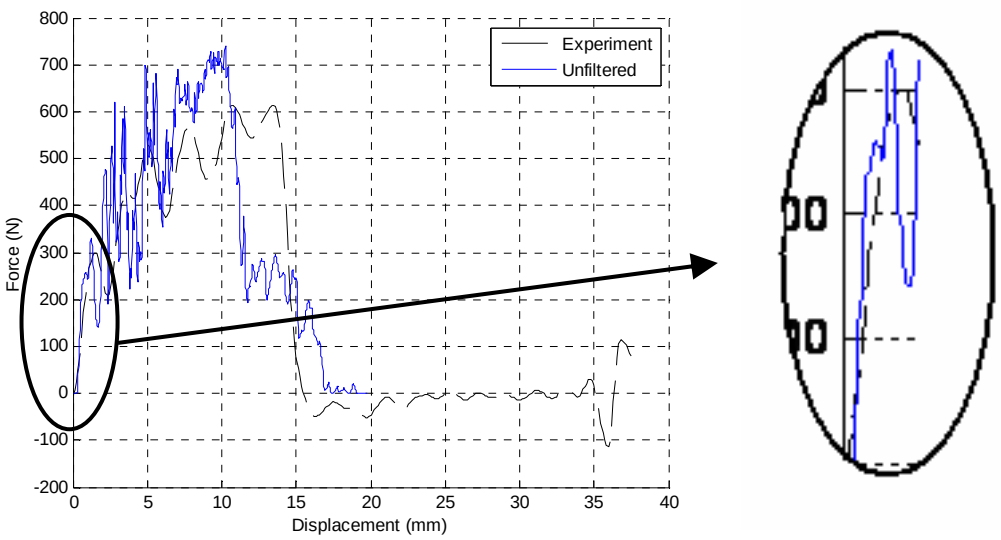

Figure I.4 Force Vs Displacement plot comparison for DYLARK 480P16 at -40°C indicating shape correlation region (Unfiltered Simulation Data - FPS = 0.0175, SC = 1.07, E=5549 MPa

Element Formulation Variation (Without SR = 100)

For the simulation model without SR = 100, the ELFORM of the simulation model was also checked for its reliability. The simulated force-displacement curves using various ELFORM are compared in Figure I.5.

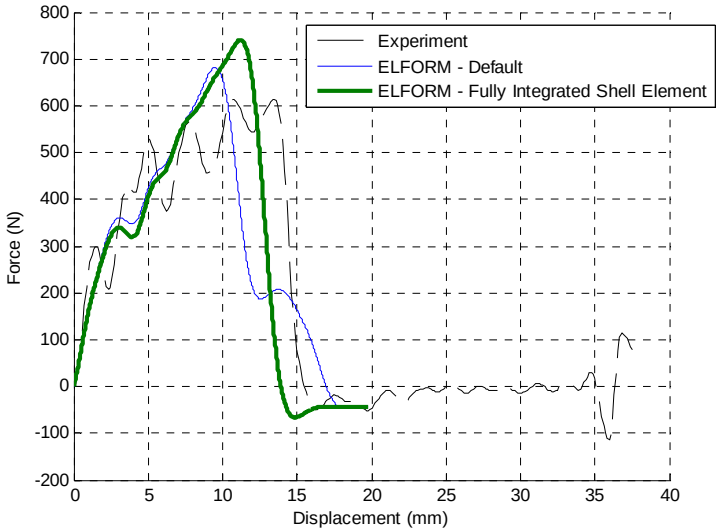

Figure I.5 Force Vs Displacement plot comparison for DYLARK 480P16 at -40^{o}C with ELFORM variation (FPS = 0.0175, SC = 1.07, E = 5549MPa)

An obvious deviation of force-displacement curve can be observed in Figure I.5 when the ELFORM was changed from the default to FISE formulation. However, by running iterative simulations on the FPS values as was done for the model without SR = 100/s and 10/s, the result produced using the FISE formulation can be as close to the one produced using the default formulation. The comparison is shown in Figure I.7. The iterative study plots are attached as Figure I.6. The numerical comparison of this simple study is tabulated in Table I.1.

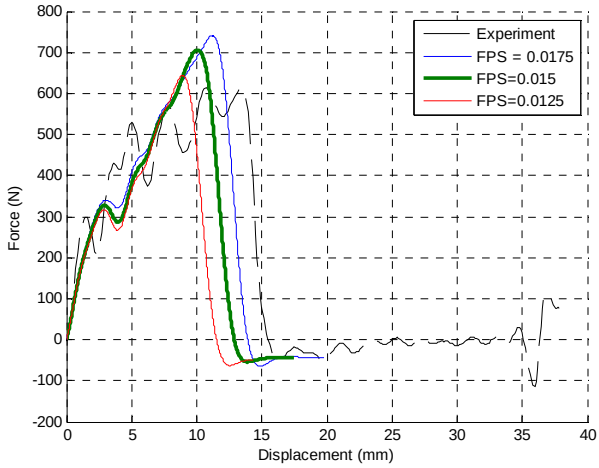

Figure I.6 Force Vs Displacement plot comparison for DYLARK 480P16 at -40°C with various FPS (ELFORM = FISE, without SR = 100)

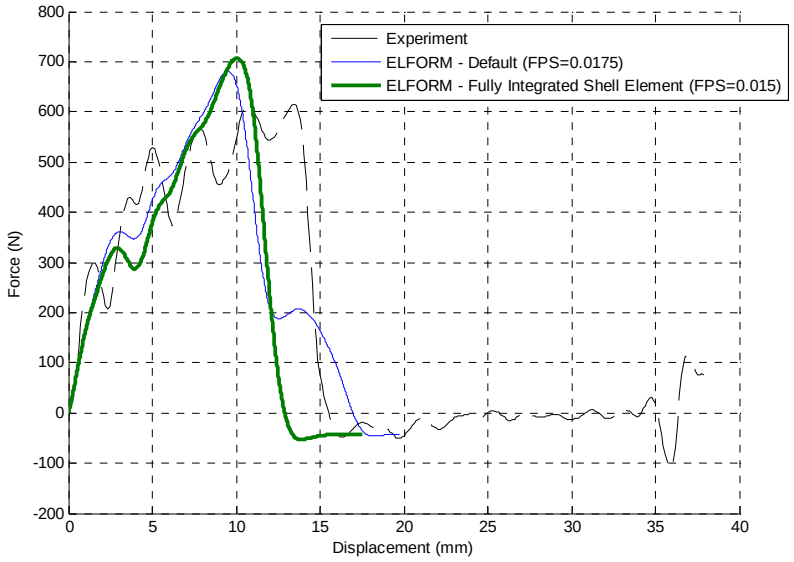

Figure I.7 Force Vs Displacement plot comparison for DYLARK 480P16 at -40°C with ELFORM variation (SC = 1.07, E = 5549MPa)

Table I.1 Experimental and Simulation results comparison for basic correlation parameters at -40°C (Various ELFORM)

	Parameter	Experimental	Default	FISE
1	Peak Load (N)	614.2	682.1	706.0
2	Displacement @Peak Load (mm)	10.69	9.53	10.10
3	Final Displacement @Zero Load (mm)	15.48	16.95	12.90

Appendix J: Simulation based on Approx. Stress-Strain Curves at -40°C

SR sets without SR = 100/s and 10/s

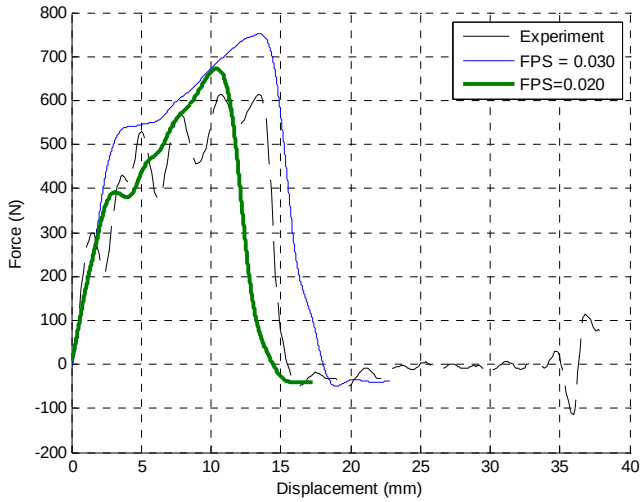

Figure J.1 Force Vs Displacement plots for DYLARK 480P16 at -40°C with FPS variation without SR = 100/s and 10/s (Approximated Stress-Strain Curves)

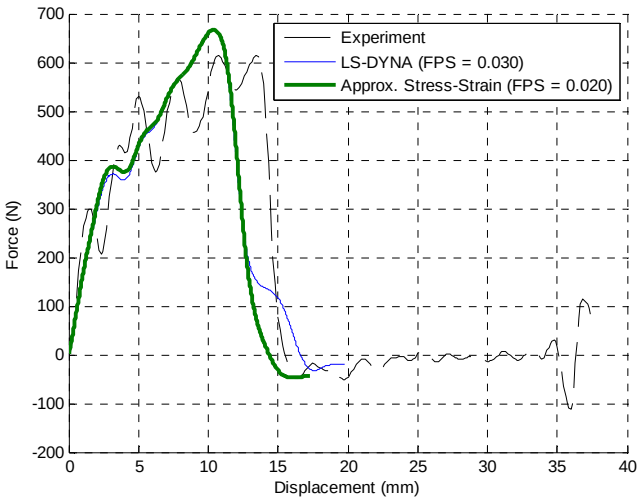

Figure J.2 Force Vs Displacement plots for DYLARK 480P16 at -40°C without SR = 100/s and 10/s (Approximated Stress-Strain Curves)

Table J.1 Experimental and Simulation results comparison for basic correlation parameters without SR = 100/s and 10/s for -40°C (Approximated Stress-Strain Curves)

	Parameter	Experimental	LS-DYNA	Modified Curves
1	Peak Load (N)	614.2	666.70	666.99
2	Displacement @Peak Load (mm)	10.69	10.43	10.42
3	Final Displacement @Zero Load (mm)	15.48	16.61	14.35

SR sets without SR = 100/s

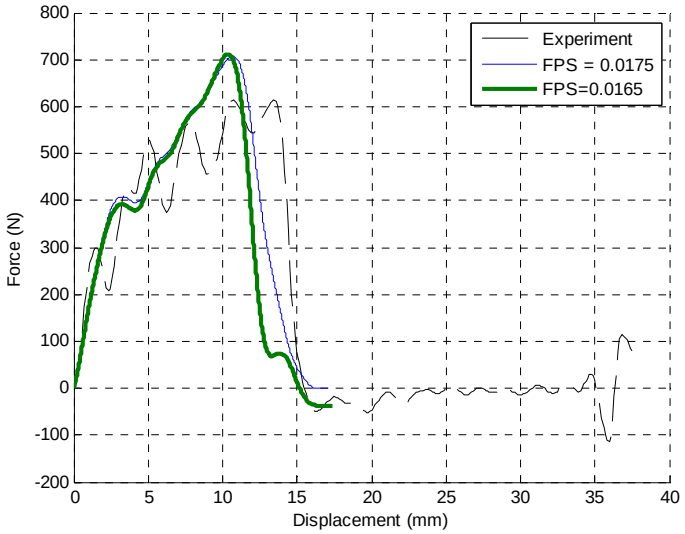

Figure J.3 Force Vs Displacement plots for DYLARK 480P16 at -40°C with FPS variation without SR = 100/s (Approximated Stress-Strain Curves)

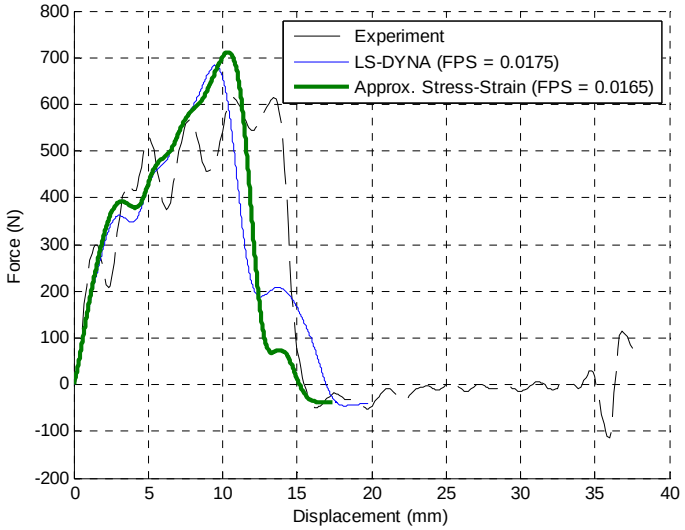

Figure J.4 Force Vs Displacement plots for DYLARK 480P16 at -40°C without SR = 100/s (Approximated Stress-Strain Curves)

Table J.2 Experimental and Simulation results comparison for basic correlation parameters without SR = 100/s for -40°C (Approximated Stress-Strain Curves)

	Parameter	Experimental	LS-DYNA	Modified Curves
1	Peak Load (N)	614.2	682.1	711.6
2	Displacement @Peak Load (mm)	10.69	9.53	10.35
3	Final Displacement @Zero Load (mm)	15.48	16.95	15.16